Recombinant IgG expression in mammalian cells

Von der Fakultät für Lebenswissenschaften
der Technischen Universität Carolo-Wilhelmina
zu Braunschweig

zur Erlangung des Grades
eines Doktors der Naturwissenschaften
(Dr. rer. nat.)

genehmigte
D i s s e r t a t i o n

von Jiandong Li
aus Hebei, VR China

1. Referent: Prof. Dr. Stefan Dübel

2. Referent: Prof. Dr. Jürgen Bode

eingereicht am: 04.05.2006

mündliche Prüfung (Disputation) am: 26.07.2006

Druckjahr: 2006

Name: Jiandong Li

Anschrift: Emsstr. 2a, 38120 Braunschweig

Ich erkläre hiermit an Eides Statt, dass ich

1. die vorliegende Dissertation mit dem Thema

   selbständig verfasst,

   noch nicht veröffentlicht

   nicht als Diplomarbeit oder ähnliche prüfungsarbeit verwendet

   und die benutzten Hilfsmittel vollständig angegeben,

2. früher ein Promotionsgesuch noch nicht eingereicht habe

Datum:.....

.....

(Unterschrift)

Im Zusammenhang mit der Thematik der vorliegenden Dissertation wurden bzw. werden folgende Publikationen erstellt:

Publications (in process):

Jiandong Li, Christian Menzel, Doris Meier, Congcong Zhang, Stefan Dübel, Thomas Jostock. A comparative study of different vector designs for the mammalian expression of recombinant IgG antibodies.

Jiandong Li, Congcong Zhang, Christian Menzel, Stefan Dübel, Thomas Jostock. The impact of the relative ratio of heavy and light chain expression on IgG production in mammalian cells.

Posters presented on international congress:

Jiandong Li, Doris Meier, Stefan Dübel and Thomas Jostock. (2005) A comparative study of different vector designs for mammalian expression of recombinant IgG antibodies. 4th International Congress on Recombinant Antibodies, Hilton Berlin, Germany.

Lars Toleikis, Jiandong Li, Doris Meier, Thomas Jostock and Stefan Dübel. (2005) A human antibody for targeting adenocarcinomas. 4th International Congress on Recombinant Antibodies, Hilton Berlin, Germany.

Content

Recombinant IgG expression in mammalian cells ····· i
1 Summary ····· 1
2 Introduction ····· 3
2.1 Immunoglobulins ····· 3
2.2 Recombinant antibodies ····· 4
2.3 IgG expression in mammalian cells ····· 5
2.4 Eukaryotic gene expression ····· 6
2.5 Protein translation in eukaryotic cells ····· 8
2.6 Internal ribosomal entry site (IRES) mediated cap-independent translation ····· 9
2.7 EMCV IRES ····· 10
2.8 Scaffolds/matrix attached region (S/MAR) ····· 12
2.9 Recombinase mediated cassette exchange (RMCE) ····· 13
2.10 Breast Cancer ····· 15
2.11 Mucin 1 (MUC1) ····· 15
2.11.1 Molecular character ····· 15
2.11.2 Physiological function of MUC1 ····· 17
2.11.3 MUC1 induced immune response ····· 17
2.11.4 The human anti-MUC1 antibody IIB6 ····· 18
2.12 Purpose of this study ····· 18
3 Results ····· 20
3.1 Vector construction and elements ····· 20
3.2 The impact of cistron arrangement on IRES mediated bicistronic gene expression ····· 23
3.3 Transient antibody expression in 293T and CHO-K1 cells ····· 26
3.4 IgG1 expression in stably transfected CHO-K1 clones ····· 27
3.5 The impact of scaffold matrix attached region (S/MAR) elements on IgG expression ····· 31
3.6 The impact of the H chain to L chain ratio on IgG production ····· 36
3.7 IgG purification ····· 37
3.8 Analytical gel-filtration ····· 38
3.9 Characterization of human anti-MUC1 IgG ····· 39
3.9.1 Peptide ELISA ····· 39
3.9.2 Western-blot on cell lysates ····· 40
3.9.3 Flow cytometry analysis of binding to living cells ····· 41
3.9.4 Surface plasmon resonance (SPR) analysis ····· 42
4 Discussion ····· 45
4.1 The impact of H and L chain on the reporter gene expression ····· 46
4.2 The impact of different vectors designs on recombinant IgG expression. ····· 47
4.3 The impact of the relative ratio of H and L chain on IgG transient expression ····· 50
4.4 The impact of S/MAR elements on IgG expression ····· 51

4.5 The human anti-MUC1 IgG 53
4.6 Outlook 55
5 Materials and methods 59
5.1 Materials 59
5.1.1 E.coli strain 59
5.1.2 Eukaryotic cells 59
5.1.3 Chemicals, solvents and enzymes 59
5.1.4 Materials for electrophoresis 60
5.1.5 Materials for cell culture and storage 60
5.1.6 Equipments 60
5.1.7 Kits for DNA purification and transfection 61
5.1.8 Buffer and solutions 62
5.1.9 Protease inhibitors 63
5.1.10 Oligo-nucleotide primers 63
5.1.11 Plasmids 64
5.2 Methods 64
5.2.1 Sterilization 64
5.2.2 Cell culture and storage 65
5.2.2.1 E. *coli* culture and storage 65
5.2.2.2 Mammalian cell culture and storage 65
5.2.3 DNA cloning 65
5.2.3.1 Plasmid DNA preparation from E. coli cells 65
5.2.3.2 DNA electrophoresis 65
5.2.3.3 Digestion of DNA by restriction endonucleases 66
5.2.3.4 PCR 66
5.2.3.5 DNA isolation from agarose gels 66
5.2.3.6 Precipitation of DNA 66
5.2.3.7 Dephosphorylation of digested DNA 67
5.2.3.8 DNA ligation 67
5.2.3.9 Transformation of E. coli 67
5.2.4 Plasmid construction 67
5.2.5 Genomic DNA preparation from mammalian cells 68
5.2.6 Protein samples analysis 69
5.2.6.1 SDS-Polyacrylamide gel electrophoresis (SDS-PAGE) 69
5.2.6.2 Coomassie blue staining 69
5.2.6.3 Preparation of Cell extracts 69
5.2.6.4 Western-blot 70
5.2.6.5 Sample preparation for protein N-terminal sequencing 70
5.2.7 Transient transfection 70
5.2.8 Establishment of stable cell lines 71
5.2.8.1 Titrating G418 (Kill Curves) 71
5.2.8.2 Cell counting using Hemacytometer 71
5.2.8.3 Screening of stably transfected CHO-K1 clone 71
5.2.9 Analysis of the expression levels of YFP reporter gene 72
5.2.9.1 Measurement of fluorescence expression using the TECAN GENios 72
5.2.9.2 Flow cytometry 72
5.2.10 Affinity chromatography purification of IgG1 72
5.2.11 Determination of protein concentration 73
5.2.11.1 Human IgG capture sandwich ELISA 73
5.2.11.2 Bradford Assay 73
5.2.12 Analytical gel filtration 73
5.2.13 IgG characterization 74
5.2.13.1 Peptide ELISA 74

5.2.13.2 FACS analysis of IIB6 IgG binding to cells 74
5.2.13.3 Surface plasmon resonance 74
6 Abbreviations 76
6.1 General abbreviations 76
6.2 Amino acid 79
7 Literature 80
8 Acknowledgements 93
9 Curriculum Vitae 95

1 Summary

IgG are heterotetrameric proteins with two identical heavy (H) and two identical light (L) chain, which are now one of the largest categories of biopharmaceutical products in development. Mammalian cells are the dominant system for the production of recombinant proteins for clinical applications. The volumetric productivity of mammalian cells cultivated in bioreactors increased significantly over the past 20 years because of improvements in media composition and process control. However, there are only few ideas to predict what kind of vector design is optimal for stable or transient production of recombinant IgG. In this study, a series of mammalian expression vectors for the production of recombinant human or chimeric IgG antibodies with different expression cassette designs were constructed. The impact of promoters, the effects of the ratio of heavy chain to light chain for efficient IgG folding and assembly, the difference between monocistronic and policistronic mammalian expression as well as the impact of bicistronic expression vector on the stability of long term recombinant IgG expression were systematically analyzed.

The impact of cistron arrangement of H and L chain in polycistronic vectors was firstly evaluated in transfected cells using yellow fluorescence protein as reporter. No apparent affection was detected from the cistron arrangements of H and L chain in transiently transfected HEK 293T cells. However, in stably transfected CHO-K1 cells, the downstream cistron of H chain exerted more negative affection to cap-dependent translation of upstream cistron than L chain did. Promoters effect IgG expression levels significantly in transiently transfected cells, the EF1-α promoter was more efficient than the human CMV-IE promoter for recombinant IgG expression. The Encephalomyocarditis virus (EMCV) IRES mediated bicistronic expression constructs could yield IgG expression levels in the same range as monocistronic expression in transiently transfected cells, and it could keep long-term stability in CHO-K1 cell lines.

To investigate the optimal range of the H and L chain intracellular expression levels for IgG folding and assembly, a series of EMCV IRES variants with different translation efficiencies was used to mediate H chain translation in the bicistronic setup L-IRES-H with IgG L chain as first cistron. It provides a novel method for the investigation of oligomeric protein mammalian expression. It seems that the optimal expression level was obtained when the IRES mediated translation efficiency was about 0,5 compared to cap-dependent translation.

To enhance the stability of IgG expression in stably transfected CHO cells, a 2,2 Kb

scaffold/matrix attached region (S/MAR) from human beta-interferon gene was used to modify the bicistronic IgG expression plasmid. It was shown that the S/MAR could apparently increase the prevalence of positive clones when it was placed flanking the bicistronic expression cassette. The effect on the expression levels from single clones needs to be studied further.

Finally, a human anti-MUC1 scFv was transformed into IgG and produced in CHO cells. Expression levels were evaluated in transiently and stably transfected cells.

2 Introduction

2.1 Immunoglobulins

Immunoglobulins are heterotetrameric proteins with two identical heavy (H) and two identical light (L) polypeptide chains. H chains are of five different classes: μ, γ, δ, α, or ε, with four subclasses of γ and two of α in humans. The L chains come with two different constant regions, κ and λ. In humans, there is one κ gene and four highly similar functional λ genes.

Table 1 Immunoglobulin type and structure

Type	IgM	IgD	IgG	IgA	IgE
H Chain	μ	δ	γ	α	ε
Structure	$(\mu_2L^+_2)_5J^\#$	δ_2L_2	γ_2L_2	$(\alpha_2L_2)_2J$	ε_2L_2

$^+$ Light chain is composed of κ and λ subclass. $^\#$J is a joining protein in IgM and IgA. All other Igs exist as tetramer.

The ratio of the two types of L chains present in the serum varies from species to species. In mice, the κ:λ ratio is 20:1, in human it is 2:1 and in cattle it is 1:20. Each chain folds into globular, β barrel structures. The isotype of the L chain can influence the kinetics of Ig intracellular folding and assembly (Montano and Morrison 2002). The type and function of immunoglobulins are determined by the heavy chain (Tab 1). IgM is the first Ig to be made by the fetus and the first Ig to be made by a B cells when it is stimulated by antigen, and is the third most common serum Ig. IgM normally exists as a pentamer but it can also exist as a monomer. IgA is the second most common serum Ig and is the major class of Ig in secretions - tears, saliva, colostrum, mucus. Serum IgA is a monomer but IgA found in secretions is a dimer. IgD is found in low levels in serum and its role in serum is uncertain. IgD exists only as a monomer. IgE is the least common serum Ig, it binds very tightly to Fc receptors on basophils and mast cells even before interacting with antigen, which is involved in allergic reactions. IgE exists as a monomer and has an extra domain in the constant region. The IgG class is the predominant antibody isotype in the blood and interstitial fluids, which is composed of 4 subclasses, IgG1, IgG2, IgG3 and IgG4. IgG posses the central ability to activate complement, binding to effector cells, which leads to destruction of invading cells, but not all subclasses work equally well. IgG4 does not fix complement, and IgG2 and IgG4 do not bind to Fc receptors. All IgG's are monomers of heterotetrameric proteins; the main differences between each subclass are the number of disulfide bonds and length of the hinge region (Fig. 1). The IgG molecule is divided into three functional domains, two

antigen-binding (Fab) regions with identical antigen specificity connected by a highly flexible hinge region to the Fc (effector) portion (Fig. 2). The antigen-binding regions of the Ab are located at the "upper" tips of the Y-shaped IgG molecule. Each binding site of the IgG is composed of the two variable regions of the heavy and light chain, which include 6 hypervariable loops (CDRs). These CDR-loops create most of the antigen-binding surface of the molecule. The effector functions of IgG such as activation of the complement cascade, induction of immune phagocytosis and Ab-dependent cell cytotoxicity are mediated by the Fc portion of the molecule. Within the Fc, many of the structural motifs responsible for the recognition of effector elements have been identified.

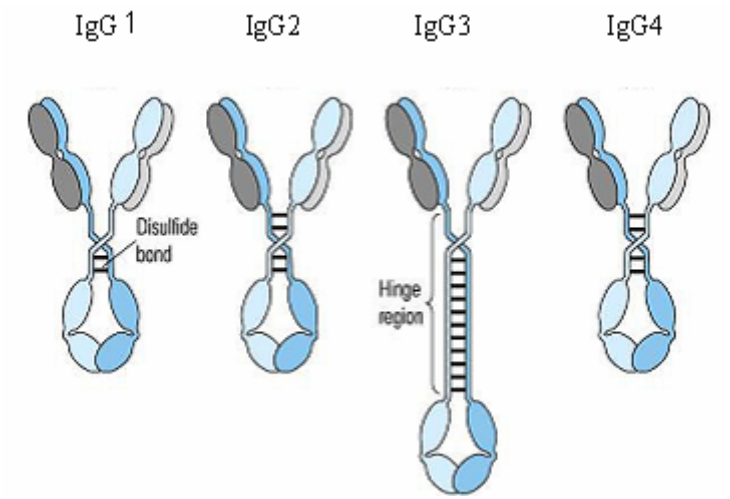

Figure 1 Schematic drawings of IgG subclasses. (The drawing was originally designed by Mike Clark)

2.2 Recombinant antibodies

One of the main obstacles to effective antibody therapy is the immunogenicity of xenogeneic antibodies. The genetic engineering technology opened a new era for the generation of antibodies, which makes it possible to isolate fully human antibodies. Many different methods have been developed for the selection of antigen binding Ab fragments scFv or Fab (Fig. 2), including phage, yeast, bacterial or ribosomal display. Among these, the antibody phage display has developed into the most robust, versatile and widely used selection method during the past decade (Hust and Dübel 2004). It has proven its capability to supply human antibody fragments, binders to toxic or non-immunogenic substances and even fragile conformational variants. This technology is continuing to be optimized and improved (Kirsch, Zaman et al. 2005). Antibody display leads to the isolation of Ab fragments, which can be produced in *E.coli*. If entire antibodies like IgG are desired, the antibody variable (V) genes have to be transformed into related

eukaryotic expression systems containing the constant region of the antibody gene.

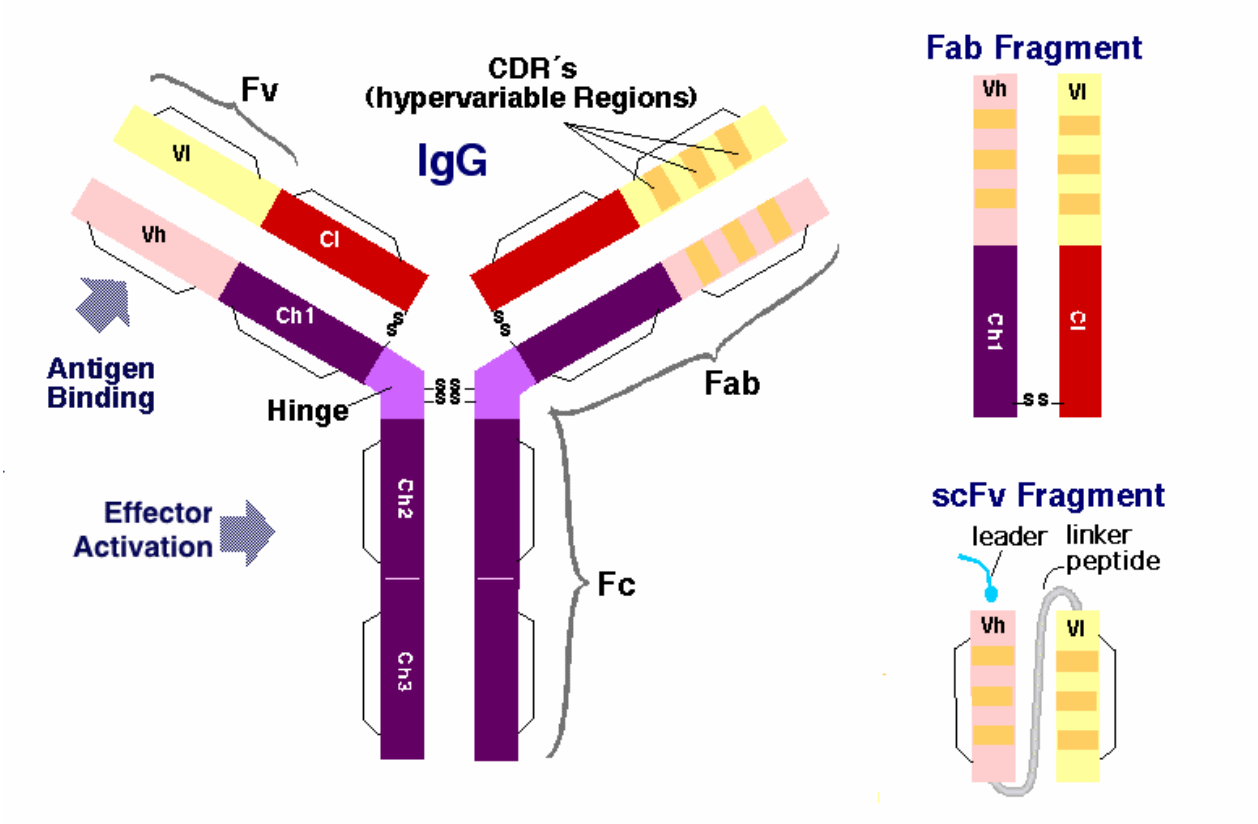

Figure 2 Schematic drawings of IgG, Fab and scFv antibodies. (The drawing was derived from http://rzv054.rz.tu-bs.de/Biotech/SD/IgG_Fv.gif)

2.3 IgG expression in mammalian cells

During the production of IgG in mammalian cells, the antibodies have to travel along the cellular secretory pathway to reach the final destination outside of the host cells. The H and L chains first enter the endoplasmic reticulum as unfolded polypeptides, which are modified there to reach their final three-dimensional structure. Attributes such as conformation, structure of attached carbohydrates, and oligomeric state does not only control the functional properties but also are critical for intracellular transport. Newly synthesized polypeptides are retarded in exiting the ER before they acquire a so-called export-competent conformation (Hurtley, Bole et al. 1989; Hammond and Helenius 1995). Free H chains are not exported (Morrison and Scharff 1975), unless assembled with L chains into antibody molecules (Sonenshein, Siekevitz et al. 1978; Leitzgen, Knittler et al. 1997), while most L chains can be secreted as free molecules, such as monomer or dimer (Shapiro, Scharff et al. 1966; Skvortsov and Gurvich 1968; Hannam-Harris and Smith 1981; Hopper and Papagiannes 1986; Dul, Aviel et al. 1996). However, some Ig L

chains depend on Ig H chain association to be secreted (Oi, Morrison et al. 1983).

The L chain plays an important role in IgG folding. L chains possess five cysteine residues, four of them are involved in two disulfide bonds that stabilize the variable (V) and constant (C) domains respectively, and a carboxyl terminal cysteine that is responsible for the intermolecular disulfide bond to the Ig H chain. The thiol group of the carboxyl-terminal cysteine of unassembled L chains causes a delay in secretion and the secreted L chains usually no longer possess unpaired cysteines, which is either covalently linked to a second L chain (or to H chain) or paired with a free cysteine (Knittler, Dirks et al. 1995; Reddy, Sparvoli et al. 1996). The removal of unpaired cysteines can result in a significant increase in antigen-binding activity and increased product yields (Schmiedl, Breitling et al. 2000). Export-incompetent Ig L chains may covalently interact with ER matrix proteins or noncovalently bind to BiP, an ER-resident molecular chaperone (Knittler and Haas 1992). In some cases, a single amino acid substitution in the light chain resulted in a loss of secretion competence (Wu, Hozumi et al. 1983, Dul and Argon 1990)). In the two classes of L chain, the assembling of λ light chain with IgG1, IgG2, and IgG4 H chain are more slowly than their κ counterparts (Montano and Morrison 2002).

For the H chain, the correct assembly of H and L chains require the interaction of BiP with incompletely folded CH1 domains (Kaloff and Haas 1995). In the kinetic model for the folding of a Fab fragment, Pro159 within the Fd region is involved in the rate-limiting folding reaction (Lilie, Rudolph et al. 1995). Somatic mutations in CDR2 of the H chain can influence the intracellular half-lives of H and L chains (Martin, Wiens et al. 1998). In addition, the H chain is synthesized slower than L chain (Bergman, Harris et al. 1981; Schlatter, Stansfield et al. 2005).

These molecular characteristics of IgG make it difficult to set a general profiling for all recombinant antibody mammalian production.

2.4 Eukaryotic gene expression

In eukaryotes, each cell packages its genome into a unique pattern of heterochromatin and euchromatin and this pattern is maintained after cell division. The chromatin structure plays a pivotal role in regulating gene transcription by marshalling access of the transcriptional apparatus to genes (Narlikar, Fan et al. 2002). The pattern of packaging into different chromatin states determines which genes will be active in a newly divided cell (Orphanides and Reinberg 2002). It is also referred to “position effect” for recombinant protein expression in stably transfected mammalian cells, where the genomic integration site has a dominant impact on the expression levels. Therefore, to achieve recombinant protein high-level expression mammalian cell lines,

high numbers of clones have to be screened to find a highly active position. This is a low efficiency and time consuming process. With the improvement of gene transfer methods and site-specific integration procedures, the expenditure clone screening may be reduced. Gene expression, from the activation of transcriptional regulators to the synthesis of a functional protein, is a multi-step process, starting in the cell nucleus with the synthesis of the primary transcripts that undergo several modifications including capping, splicing and polyadenylation, leading to the export of the mature mRNAs into the cytoplasm for translation into proteins. The multi-step gene expression is a continuous process, with each phase physically and functionally connected to the following one (Figure 3) (Orphanides and Reinberg 2002). The transcriptional apparatus plays an active role in recruiting the machinery that caps and processes the nascent RNA transcript (Proudfoot, Furger et al. 2002), the pre-mRNA splicing promotes transcription elongation in reverse (Fong and Zhou 2001). The mRNA exportation into the cytoplasm occurs even as the transcription is ongoing and is enhanced by the splicing (Reed and Hurt 2002).

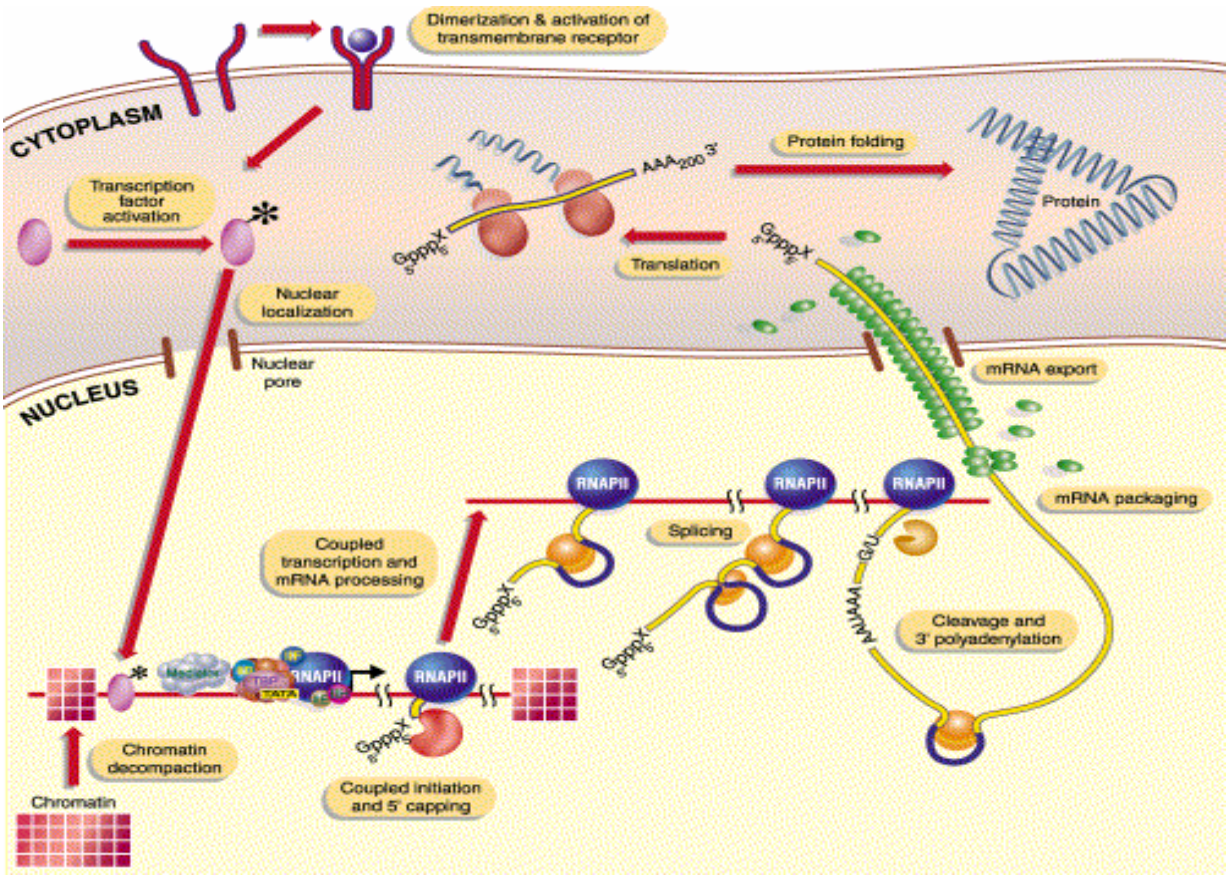

Figure 3 A Contemporary View of Gene Expression. Reproduced from literature (Orphanides and Reinberg 2002).

Gene expression is regulated at multiple levels in a coordinated fashion. The promoter identity

not only regulates transcription, but also can impact pre-mRNA processing (Auboeuf, Dowhan et al. 2005). Transcription factors play an important role on the regulation of the gene expression by binding to DNA regulatory sequences. The activities of these factors are controlled by a diverse array of regulatory pathways. Regulating a rate-limiting step is an efficient way to control the overall rate of a multi-step process. However, there is a limit to the level of regulation that was achieved by controlling a single step if another soon becomes rate limiting. Different DNA sequences present in promoter regions, including untranslated and translated sequences, affect the rate of transcription, pre-mRNA processing, mRNA exportation and protein synthesis. There are additional sequences that govern the localization and stability of mRNAs and proteins (Orphanides and Reinberg 2002). The identification of these DNA sequence elements will enhance the understanding of the mechanism of gene expression and the possibility to regulate gene expression.

2.5 Protein translation in eukaryotic cells

Translation of mRNA in the eukaryotic cell is an extremely competitive process, the recruitment of the 40S ribosomal subunit onto the mRNA is believed to be the rate-limiting step of mRNA translation (Mathews, Sonenberg et al. 2000.). The translation initiation of eukaryotic mRNAs was supposed to use a scanning mode (Kozak 1980), which suggests that the 40S ribosomal subunit first recognizes the 5' terminus of the mRNA, in a process which is strongly stimulated by the presence of a cap structure, then migrates and stops at the first AUG codon in a favorable context for initiating translation. Recognition of the initiator AUG is followed by 60S ribosomal subunit joining to produce the translation-competent ribosome. The first-AUG rule is not absolute, subsequent revisions to the scanning model included the reinitiation and context-dependent leaky scanning mechanisms (Kozak 1989; Kozak 2002). They were used to explain the bypassing of upstream AUG codons for initiation because of unfavourable local sequences, or the affection of RNA secondary structure upstream or downstream of the initiation codon. By using point mutation analysis of the base around the AUG initiation codon, the optimal sequence for translation initiation by eukaryotic ribosomes was identified to be (GCC)GCCRCCaugG (R = purine) (Kozak 1986; Kozak 1987). Mutations within that sequence affected the yield over a 20-fold range and it was showed that A or G in position -3 (3 nt upstream from the AUG codon, which is numbered +1 to +3) and G in position +4 make the strongest contributions (Kozak 1997). In the absence of -3R and +4G, mutations in positions -1 and -2 score strongly (Kozak and Neufeld 2003). Recognition of an AUG initiator codon in a suboptimal context was improved when a modest amount of secondary structure is introduced near the beginning of the protein-coding sequence (Kozak 1990). The 3’ UTR and poly(A) also exert an important role on

many mRNAs translation (Gray and Wickens 1998).

2.6 Internal ribosomal entry site (IRES) mediated cap-independent translation

The IRES-driven translation initiation was first demonstrated for picornavirus (Jang, Krausslich et al. 1988), which can recruit ribosomes directly to initiate translation using a 5'-end independent method, without a previous scanning of untranslated region of mRNA. IRESs are commonly used to direct the expression of the downstream cistrons of bicistronic or oligocistronic mRNAs. The translation initiation directed by an IRES requires IRES-specific trans-acting factors as well as the same set of initiation proteins necessary for cap–dependent mRNA translation initiation. The main difference compared to cap-dependent translation initiation was believed to be eIF4G. The C-terminal part of eIF4G contains binding sites for eIF3 and eIF4A, stimulates IRES-mediated translation (Ohlmann, Rau et al. 1995). The 40S ribosomal subunit is recruited to the IRES through interaction with eIF3 bound to the C-terminal domain of eIF4G. Binding of eIF4G to the mRNA does not occur through eIF4E because the mRNAs are not capped. eIF4G may bind to the IRES either directly or through a "linker" protein (Fig 4). Several cellular proteins have been shown to participate in IRES directed translation. Human La autoantigen, which is involved in regulating the initiation and termination of transcription by RNA polymerase III, stimulates IRES-dependent translation of PV mRNA (Meerovitch, Svitkin et al. 1993; Craig, Svitkin et al. 1997; Izumi, Das et al. 2004). Polypyrimidine tract binding protein (PTB), a cellular RNA-binding protein (57 kDa) that binds to the 5' region of EMCV IRES, is required for the polio virus (PV) and EMCV IRES elements mediated translation (Hellen, Pestova et al. 1994; Kaminski, Hunt et al. 1995; Kolupaeva, Hellen et al. 1996; Kaminski and Jackson 1998; Hunt and Jackson 1999; Gosert, Chang et al. 2000; Back, Kim et al. 2002). Poly(rC)-binding protein 2 (PCBP-2) and a heterogeneous nuclear ribonucleoprotein E2 (hnRNP E2) bind at multiple sites within the poliovirus IRES and abolish binding of poly r(C)–binding proteins causing a decreased translation in vitro (Blyn, Swiderek et al. 1996). And some other RNA-binding proteins, such as those upstream of N-ras (unr), heterogeneous nuclear ribonucleoprotein C (hnRNP C) and heterogeneous nuclear ribonucleoprotein L (hnRNP L) also modulate IRES-dependent translation (Hahm, Kim et al. 1998; Hunt, Hsuan et al. 1999; Boussadia, Niepmann et al. 2003; Kim, Paek et al. 2003). However, there was no single protein been identified that is essential for the function of every IRES. It was supposed that certain types of IRES have different requirements for cellular proteins.

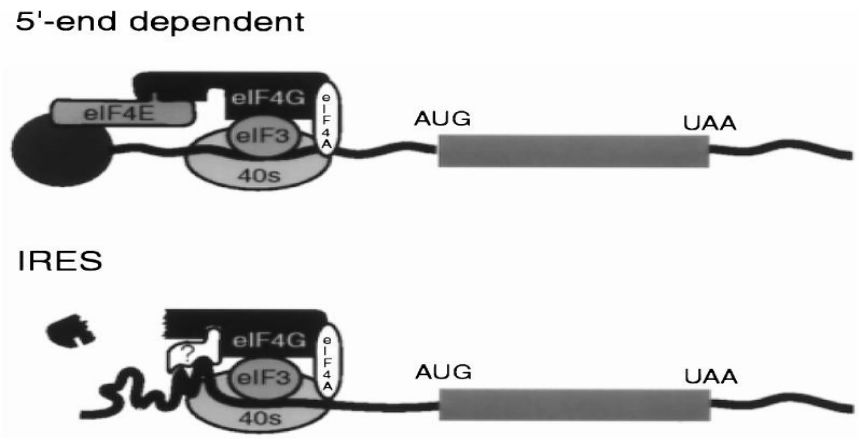

Figure 4 Models for protein translation initiation complex formation. In 5´ cap–dependent initiation, the 40S subunit is recruited to the mRNA through its interaction with eIF3, which binds eIF4G. The latter initiation factor is part of eIF4F, which also contains eIF4A and eIF4E. Binding of eIF4E to the cap thus positions eIF4E at the 5´-end and positions the 40S subunit on the mRNA. In IRES-dependent translation, a 5´-end is not required. The eIF3–40S complex is believed to be recruited to the RNA by the interaction of eIF4G with cellular IRES-binding proteins, marked by "?" Reproduced from literature (Racaniello 2001).

2.7 EMCV IRES

Encephalomyocarditis virus (EMCV) is a member of the cardiovirus genus of the positive-sense picornaviruses. The picornavirus genomes RNA contain a highly structured IRES element in 5' the untranslated region (5' UTR) (Fig. 5). Picornaviral IRES elements have been classified into three groups by sequence and structural similarities. Type I IRES elements include those of enteroviruses and rhinoviruses, such as poliovirus (PV) and human rhinovirus (HRV). Type II IRES elements include IRES elements from cardioviruses and aphthoviruses, such as encephalomyocarditis virus (EMCV) and foot-and-mouth disease virus (FMDV). The Hepatitis A virus (HAV) IRES element belongs to type III IRES.

The EMCV IRES element is least affected by the flanked coding sequence, and the mediated translation is accurate and the most efficient in reticulocyte lysate translation extracts and culture cells among picornavirus IRES elements, which makes it attractive for driving heterologous gene expression (Borman, Deliat et al. 1994; Borman, Bailly et al. 1995; Borman, Le Mercier et al. 1997; Hennecke, Kwissa et al. 2001). In the first description of EMCV IRES, the sequence between nucleotides 260 and 484 in the 5'UTR of encephalomyocarditis RNA was found to play a critical role in the efficient translation in both mono- and dicistronic mRNAs (Jang, et al. 1988).

Regions and particularly loops playing an essential role in EMCV IRES function have been identified subsequently. The 5´ border of the EMCV IRES has been mapped by deletion analysis to base 387 of the genome, a region near stem-loop G. The H segment facilitates translation initiation by stabilizing the IRES overall structure and aiding general protein binding (Hoffman and Palmenberg 1995). Stems J and K are important for IRES function, some of the single point mutants are highly defective, which is believed to be associated with the binding of translation factors (Duke, Hoffman et al. 1992; Hoffman and Palmenberg 1995; Houdebine and Attal 1999; Witwer, Rauscher et al. 2001; Clark, Robertson et al. 2003). So far, two conserved structure were identified to be essential for IRES function, include a conserved GNRA sequence (N, any nucleotide; R, purine) in stem-loop I of the EMCV IRES and a conserved Yn-Xm-AUG motif, in which Yn is a pyrimidine-rich region and Xm is a 15- to 25-nucleotide spacer followed by the initiator AUG codon. It was also reported that some point mutations could enhance IRES mediated translation initiation 1,5-5-fold time more active (Martinez-Salas, Saiz et al. 1993).

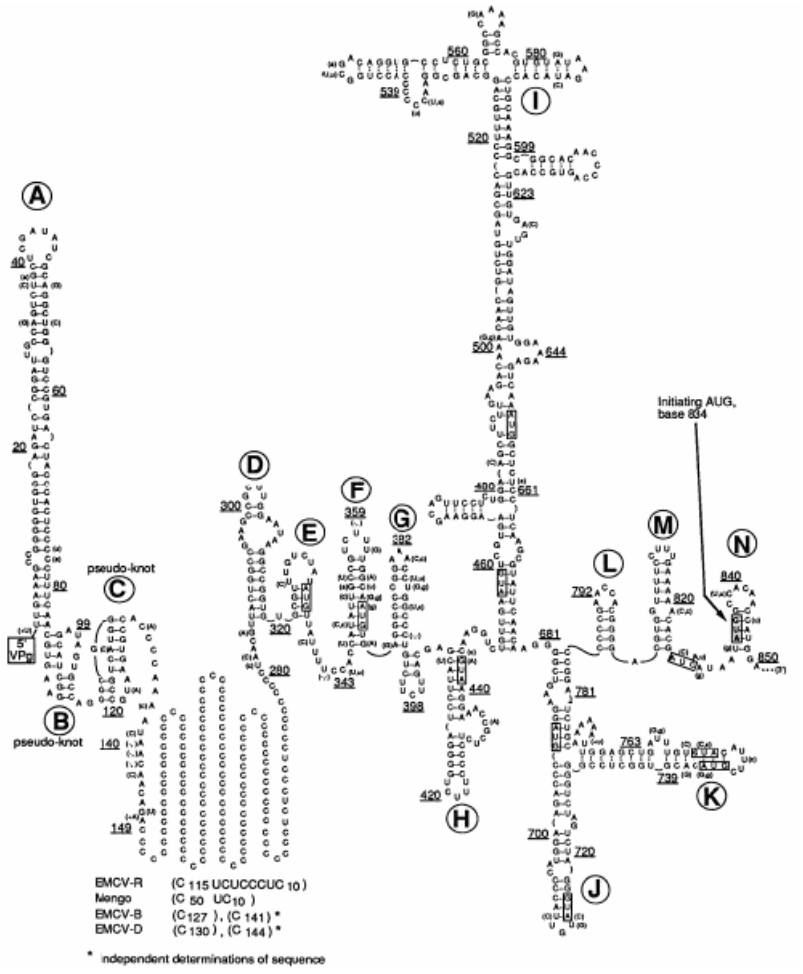

Figure 5 Consensus secondary structure of 5' UTRs of four related cardioviruses. The sequence shown is for EMCV-R. Changes in mengovirus and other EMCV strains (EMCV-B and EMCV-D) are given parenthetically as capital and lowercase letters, respectively. Stem-loop features are lettered consecutively, and AUG sequences (EMCV-R) are boxed. Reproduced from literature (Duke, Hoffman et al. 1992).

2.8 Scaffolds/matrix attached region (S/MAR)

The architecture of the nucleus includes chromatin and a nuclear matrix. Periodic and specific attachments of chromatin fibers to the nuclear matrix create the chromatin loop domains (Nickerson 2001), through which the eukaryotic genomes are organized into domains containing individual genes and gene clusters that have distinct patterns of expression during development (West, Gaszner et al. 2002). The loops are essential for DNA replication, transcription and chromosomal packaging (Jackson 1997). The formation of each loop is dependent on specific chromatin segments that function as an anchor to the nuclear matrix, which have been termed either `SARs' or `MARs' (collectively termed S/MARs) (Hart and Laemmli 1998). S/MAR anchors are necessary but not sufficient for chromatin loops to form, they work in a selective and dynamic fashion (Fig. 6) (Heng, Goetze et al. 2004). It was supposed that there are two types of S/MARs. Functional S/MARs serve as mediators to bring genes onto the nuclear matrix. Structural S/MARs serve as anchors, which are less dynamic compared with functional S/MARs. There is increasing evidence that S/MARs have both boundary and transcription regulation functions, which can dampen positional effects in eukaryotic cells as the insulating boundary elements and augment transcriptional levels by a enhancer-independent mechanism, and in some systems enhancers are fully active only when associated with S/MAR elements (Bode, Schlake et al. 1995; Bode, Stengert-Iber et al. 1996; Bode, Benham et al. 2000). "Insulators" regulate gene expression through establishing and maintaining the organization of the chromatin fiber within the nucleus by tethering the DNA to the nuclear matrix and creating chromatin loops (Byrd and Corces 2003). However, S/MAR sequences were required for the establishment but not for the maintenance of chromosomal insulation (Namciu and Fournier 2004).

It was hypothesized that S/MARs reversibly associate with protein factors through a mechanism called "mass binding phenomenon" (according to which, low-affinity binding of many individual protein molecules to S/MAR results in strong and specific interactions and that can serve specific regulatory roles) to functionally compartmentalize eukaryotic genomes into chromatin domains (Bode, Goetze et al. 2003). Many protein factors were identified that interact with S/MARs. The nuclear lamina, scaffold-attachment factor A (SAF-A), scaffold attachment factor B1 (SAFB1) and SATB2 were relatively well studied. They are involved in chromatin remodeling and numerous

genes regulation.

The 2.2 kb S/MAR element used in this study was the fragment released via EcoRI from the 14 kb domain of the human interferon gene, which locates at upstream of well-characterized beta-interferon gene (Mielke, Kohwi et al. 1990).

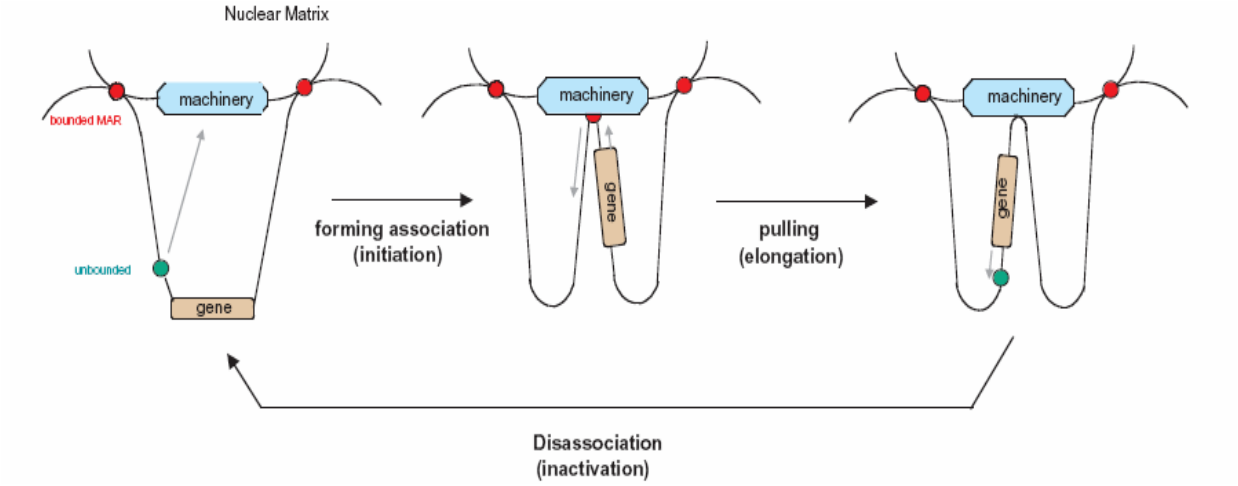

Figure 6 A proposed model for the S/MAR function in transcription/replication regulation. The left panel shows a gene located on the loop with a S/MAR in close proximity. When functional demands require the specific association of this gene with the transcriptional machinery located on the nuclear matrix, the S/MAR moves the gene to the nuclear matrix, thereby initiating gene expression (center). Following initiation, the gene is pulled in through the transcriptional machinery, thus completing the process (right). (Reproduced from Heng, et al. 2004).

2.9 Recombinase mediated cassette exchange (RMCE)

The first described site-specific recombinases, Cre from P1 phage and Flp from yeast, catalyze recombination between two 34-base pair recognition sites, lox and FRT, respectively, resulting in excision, inversion, or translocation of DNA sequences depending upon the location and the orientation of the recognition sites (O´Gorman, Fox et al. 1991; Fukushige and Sauer 1992). The integration reaction is often limited with wild-type recombinase recognition sites due to the re-excision of the recombined product. Therefore mutant target sites were developed to increase the efficiency of Cre/Flp-mediated insertion or replacement reactions. The recombinase mediated cassette exchange (RMCE) strategy was developed using heterospecific sites, such as combination of the LE/RE mutant and lox2272 for Cre (Araki, Araki et al. 2002) or F and F3 for Flp (Seibler, Schubeler et al. 1998). RMCE has been successfully used to achieve predictable gene expression in cell culture and for the systematic creation of transgenic animals (Baer and

Bode 2001). The improved RMCE methods permit expression in the absence of any co-expressed selection marker gene in ES cells (Seibler, Schubeler et al. 1998; Feng, Seibler et al. 1999).

The Flip mediated RMCE method tested in this work was developed by Seibler et al. (Seibler, Schubeler et al. 1998). Flp-RMCE utilizes a set of two 48 bp Flp target sites, wild-type F and mutant F3, which was mutated in the 8 bp spacer localized between the Flp binding elements (Schlake and Bode 1994). Flp can mediate recombination between the F3/F3 with the same efficiency as between the wild-type sites (F/F), but it does not catalyze recombination between the F/F3 sites (Seibler and Bode 1997). For enhancing the system, a hygromycin phosphotransferrase and thymidine kinase (hygtk) positive/negative fusion selection marker was inserted between the heterospecific tags, and the construct was integrated into the genome of embryonic stem (ES) cells. The successful Flp-mediated replacement of the hygtk cassette is enriched by ganciclovir (GANC) selection for cells that lack the encoded fusion protein (Fig. 7). Using this method, after positive plus negative double selection, the targeting efficiency was about 54% to 100% at different gene loci in murine ES cells. The stably transfected CHO-K1 cell line used in this study was with a single copy integration tag cassette, which was established by Dr. Alexandra Baer (in her Ph.D. work at GBF). Here the insertion “hygtk” fusion selection marker between F/F3 tags was further modified to hygromycin-thymidine kinase-enhanced green fluorescence protein (hygtkgfp) and was flanked by two S/MAR elements.

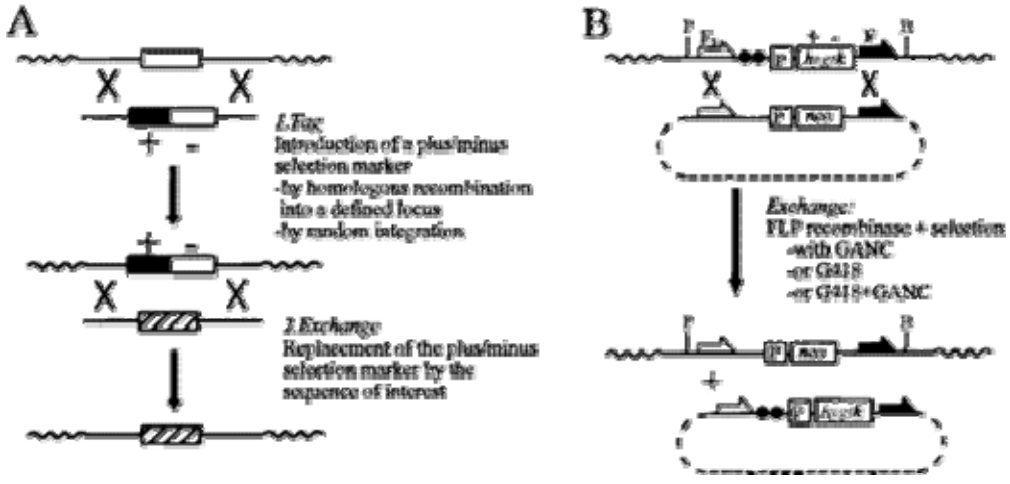

Figure 7 Schematic representation of recombinase mediated cassatte exchange (RMCE). (A) Outline of a tag-and exchange experiment. (B) Use of the Flp-RMCE to exchange a genomically anchored plus/minus selection marker (hygtk) for an expression cassette. Half arrows mark the positions of heterospecific FRT-sites (solid, wild type; light, mutant F3). Reproduced from literature (Seibler, Schubeler et al. 1998).

2.10 Breast Cancer

Not like other disease, the incidence of breast cancer is increasing (Harris, Lippman et al. 1992; Clarke, Glaser et al. 2002). By far, it is the most frequent cancer of women (23% of all cancers), with an estimated 1.15 million new cases in 2002 worldwide, ranking second overall when both sexes are considered together. More than half of the cases are in industrialized countries—about 361,000 in Europe (27.3% of cancers in women) and 230,000 in North America (31.3%) (Parkin, Bray et al. 2005). In part, the high incidence in the more affluent world areas is likely because of the presence of screening programs that detect early invasive cancers, some of which in developing areas would otherwise have been diagnosed later or not at all (Parkin, Bray et al. 2005). About 5% of breast cancer is attributable to rare high-penetrance mutations in a small number of specific genes (eg, BRCA1, BRCA2, ATM, PTEN, and TP53); mutations in BRCA1 and BRCA2 account for up to 50% of hereditary and familial breast cancer. Each gene shows some differences in the familial pattern of cancer: BRCA1 is more strongly associated with ovarian cancer, BRCA2 with male breast cancer, ATM with radiosensitivity, PTEN with Cowden's syndrome (including hamartomas of the skin and other organs), and p53 with Li-Fraumeni syndrome (including sarcomas and a variety of other tumors) (Rahman and Stratton 1998; Chen and Hunter 2005). However, etiological factors of most breast cancer cases remain unclear. It was estimated after epidemiological survey of population-attributable risks that at least 45% to 55% of breast cancer cases in the United States might be explained by later age at first birth, nulliparity, family history of breast cancer, higher socioeconomic status, earlier age at menarche, and prior benign breast disease (Madigan, Ziegler et al. 1995). But it is difficult to find substantial evidence to support a major role of environmental risk factors in the etiology of breast cancer (Laden and Hunter 1998). Early detection and early treatment of breast cancer at a stage when it is potentially curable have reduced the mortality of breast cancer during the past decade (Peto, Boreham et al. 2000). Now, recombinant IgG has been used as an adjuvant therapy to standard treatments of breast cancer. It has shown significant efficacy in the treatment (Mehren, Adams et al. 2003).

2.11 Mucin 1 (MUC1)

2.11.1 Molecular character

MUC1 is a member of the mucins family, which was the first defined tumor associate antigen in 1980s. It is a type I transmembrane molecule, which consists of a small transmembrane and intracellular tail and an extracellular domain consisting of a variable number (30–100) of tandem repeats (VNTR) segments of 20 amino acids (Fig. 8). Mucins are large glycoproteins that are

heterogeneously expressed by a wide variety of epithelial cells. Mucin proteins are characterized by the presence of VNTR amino acid sequences (depending on mucin type and also subject to allelic polymorphism between individuals). Serine and threonine residues constitute a large proportion of mucin VNTR sequences, giving rise to numerous potential O-glycosylation sites. Carbohydrate constitutes the major portion of the mature mucin molecule (Gendler and Spicer 1995).

The peptide core is densely coated with oligosaccharides, conferring a rigid rod-like structure, which can extend several hundred nanometers from the apical cell surface into the lumen of ducts and glands (Gendler and Spicer 1995; Brayman, Thathiah et al. 2004). Cancer-associated MUC1 is aberrantly overexpressed (10–40 fold) in a variety of cancers and incompletely glycosylated. As a result internal sugar units and naked peptide sequences are exposed, which are cryptic in the normal mucin molecule. It makes them useful targets for antibodies and cellular immunity. MUC1 glycoprotein is often found in circulation in late-stage breast and lung cancer. It has been used as a tumour marker (CA15.3) in the follow-up of breast cancer patients (Berruti, Tampellini et al. 1994).

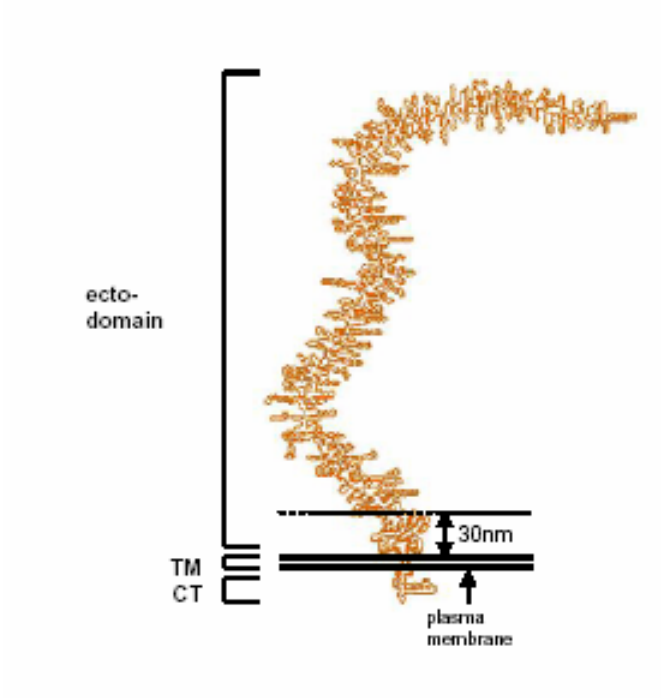

Figure 8 Schematic diagram of the size and structure of the full length MUC1 protein relative to the plasma membrane. The horizontal bar indicates the distance that most cell surface proteins extend into the pericellular space. The three major domains of MUC1 are indicated to the left: an N-terminal, extracellular domain (ECTO); a single, membrane spanning domain (TM) and a C-terminal cytoplasmic domain (CT).

Reproduced from literature (Brayman, Thathiah et al. 2004).

2.11.2 Physiological function of MUC1

The high degree of glycosylation is believed to provide lubrication, prevent dehydration, and offer protection from proteolysis, but the knockout mice, lacking MUC1, had no alteration in their development and in their glandular morphology (Spicer, Rowse et al. 1995). The huge extracellular domain protects against attack by sterically inhibiting microbial access to the cell surface (Vimal, Khullar et al. 2000; Lillehoj, Kim et al. 2002), which is a process that normally protects against infection. In addition, MUC1 modulates cell-cell and cell-extracellular matrix (ECM) interactions by steric hindrance of the extracellular domain (Wesseling, van der Valk et al. 1996; Komatsu, Carraway et al. 1997).

MUC1 seems to be involved in signal transduction through its cytoplasmic tail, which was shown to be associated with β-catenin (Yamamoto, Bharti et al. 1997), as well as Grb2/Sos (Pandey, Kharbanda et al. 1995). MUC1 could down-regulate the activities of other molecules such as catenins, cadherins or integrins via signal transduction events (Agrawal and Longenecker 2005). Activation of erbB1 with EGF induces tyrosine phosphorylation of the MUC1 cytoplasmic tail (Li, Kuwahara et al. 2001) and activation of ERK 1/2 (Schroeder, Thompson et al. 2001). Moreover, EGF mediated activation of ERK 1/2 was drastically enhanced in the presence of high levels of MUC1 in the mouse mammary gland (Schroeder, Thompson et al. 2001). The MUC1-induced signal transduction could also be involved in a Src family kinase, phosphoinositol 3-kinase, phospholipase C and lipid rafts. The tumor cells metastasis may be related to the functions of MUC1 involved a calcium-based pro-migratory signal transduction (Rahn, Shen et al. 2004). The MUC1 VNTRs are necessary for an ordered tertiary structure and also important for intercellular adhesion molecule-1 (ICAM-1) recognition, which are involved in the regulation of T cell responses (Agrawal, Krantz et al. 1998; Kam, Regimbald et al. 1998; Agrawal and Longenecker 2005).

2.11.3 MUC1 induced immune response

It was confirmed that immunisation with MUC1 antigenic epitopes can induce T-cell proliferative responses as well as MHC-restricted cytotoxic T-cells. A specific T proliferative response directed against an epitope of the human MUC1 tandem repeat domain was found in 1990's (Spicer, Rowse et al. 1995), however the MUC-1-directed immune response is not limited to the extracellular tandem repeat domain (Brossart, Heinrich et al. 1999). Murine experiments have shown that immunization with MUC1 polypeptides without tandem repeats is effective in inducing

a tumor rejecting anti-MUC1 immune response (Taylor-Papadimitriou, Burchell et al. 2002). In addition to the T-cell response, a predominant antibody response was documented following serial vaccinations with a peptide-mannan fusion protein (Apostolopoulos, Osinski et al. 1998). In some studies, only antibody but not T-cell responses to MUC1 was observed in MUC1 transgenic mice immunized with vaccinia-MUC1-IL-2 (Acres, Apostolopoulos et al. 1999). It was found in clinical epidemiological follow-up studies that elevated natural antibodies to MUC1 in early-stage breast cancer patients could benefit long term survival, which was attributed to the controlling of tumor cells dissemination and outgrowth by aiding the destruction of circulating or seeded MUC1-expressing tumor cells (von Mensdorff-Pouilly, Verstraeten et al. 2000).

2.11.4 The human anti-MUC1 antibody IIB6

Monoclonal antibody therapy has emerged as an important therapeutic modality for cancer. Most of the MAb employed in early clinical trials were derived from mice. Patients exposed to them developed human anti-mouse antibody (HAMA) responses, which limited the number of treatments patients could safely receive. The possibility to create fully human immunoglobulins limited the capacity to induce HAMA. Recently, a human anti-breast cancer MUC1 antibody scFv fragment was developed using phage display technology (by Dr. Lars Toleiks, a former Ph.D student of Professor Dr. Stefan Dübel). A patient suffering from breast cancer was immunized with synthesized glycopeptide of the tumor associated MUC1 VNTR region. Then a human recombinant antibody phagemid library was established based on the peripheral lymphocytes donated by the immunized patient. Panning was performed on tumor associated MUC1 peptide and one specific antibody was isolated. The VH gene belongs to the VH1 subfamily and the VL gene belongs to the Vλ3 subfamily. The binding epitope is “XRPAP”, a linear epitope in the MUC1 VNTR region. The isolated human anti-MUC1 scFv antibody was expressed in *E.coli* and characterized using FACS on different breast cancer cell lines. Further, the binding kinetics parameter was measured using the surface plasmon resonance (SPR) technology. It was confirmed that the IIB6 scFv could specifically bind on tumor associated MUC1 antigen and breast cancer derived cell lines. The binding affinity on the synthesized MUC1 16-mer biotin conjugated glycopeptide is KD (M) 2,28x10e-7.

2.12 Purpose of this study

Cultivated mammalian cells are the dominant system for the production of recombinant proteins for clinical applications because of their capacity for proper protein folding, assembly and post-translational modification (Wurm 2004). The productivity of mammalian cells cultivated in bioreactors has increased remarkably over the last two decades, the increasing in volumetric

productivity resulted mainly from improvements in media composition and process control (Wurm 2004). Current strategies to improve expression systems comprise: enhancement of gene expression rates, enhancement of secretion, enhancement of polypeptide folding and assembly, prevention of premature product degradation, simplification of the procedure of high producer screening, host cells modification and optimization of subsequent feeding.

In this study, a comparative analysis of different vector designs of monocistronic and bicistronic constructs with different promoter and cistron arrangement should be made in transiently transfected HEK 293T and CHO-K1 cells. Stable transfected CHO cell lines should be established to compare the affection of different version of vectors on stable mammalian IgG expression. The affection of cistron arrangement and the impact of H and L chain on bicistronic IgG expression should be analyzed. Methods should be explored to investigate the optimal ratio of HC:LC intracellular expression levels for efficient IgG folding and assembly.

Skeleton or matrix attached regions (S/MAR) are genomic elements that were found to be able to augment gene expression and orchestrate the local chromosome structure (Agarwal, Austin et al. 1998; Bode, Benham et al. 2000; Kurre, Morris et al. 2003). In this study, the impact of S/MAR element on recombinant mammalian IgG expression, including the stability and expression levels should be investigated and the possibility of developing an alternative strategy using nonviral episomes for recombinant IgG production should be explored.

Finally, a human anti-MUC1 antibody should be transformed from the scFv to the IgG format and produced in mammalian cells for characterazation. The character of the mammalian produced IgG from different cell lines would be evaluated.

3 Results

3.1 Vector construction and elements

In eukaryotic cells, gene expression is a multi-step interconnected process. To develop vectors for IgG expression in mammalian cells, the elements involved in gene expression were chosen as candidates for vector variation and a comparative analysis. The cytomegalovirus immediately early promoter and the cellular EF1-α promoter were used to drive the transcription of the gene of interest. The optimal Kozak sequence 5'-GCCACCATGG-3' was arranged as the cap-dependent translation initiation, in the polycistronic vectors the EMCV IRES was used to mediate internal protein translation initiation. The human antibody Vκ3 (hVκ3S) subfamily signal sequence and the mouse antibody heavy chain VH3 (mVH3S) subfamily signal sequence containing a synthetic intron were used for secretory IgG expression. The BGH polyadenylation sequence was used to mediate transcription termination and polyadenylation. A series of monocistronic and bicistronic vectors were constructed. The pre-mRNA transcript from a monocistronic and a bicistronic construct is depicted in figure 9. To speed up the analysis, a variant of the yellow fluorescence protein (YFP) gene, Venus (Nagai, Ibata et al. 2002), was used as a reporter in the bicistronic constructs to determine translation efficiencies. The construction of plasmids are depicted in figure 10 A and B

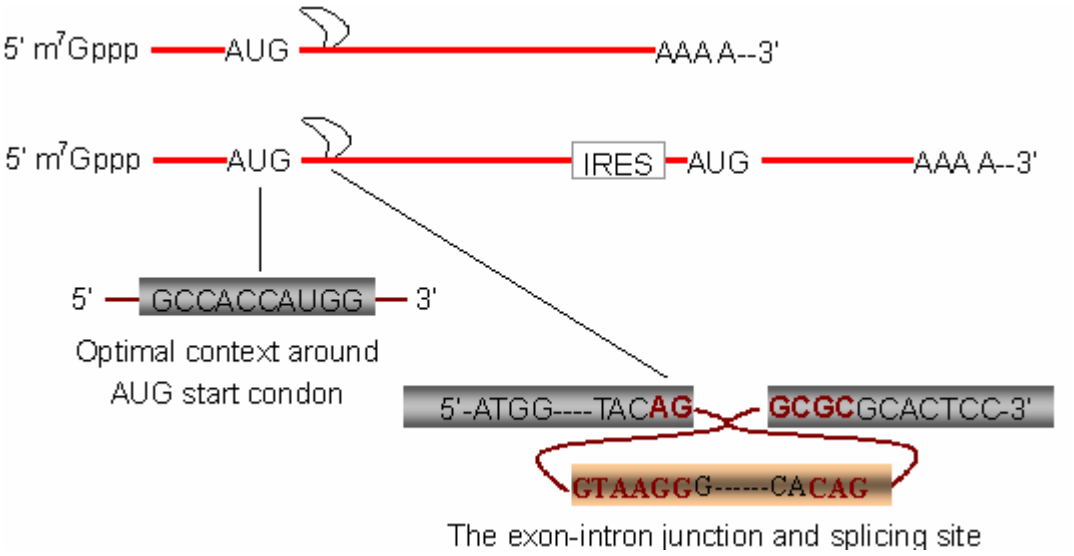

Figure 9 Schematic representation of a monocistronic and a biscistronic transcript. Insertion elements are not drawn to scale.

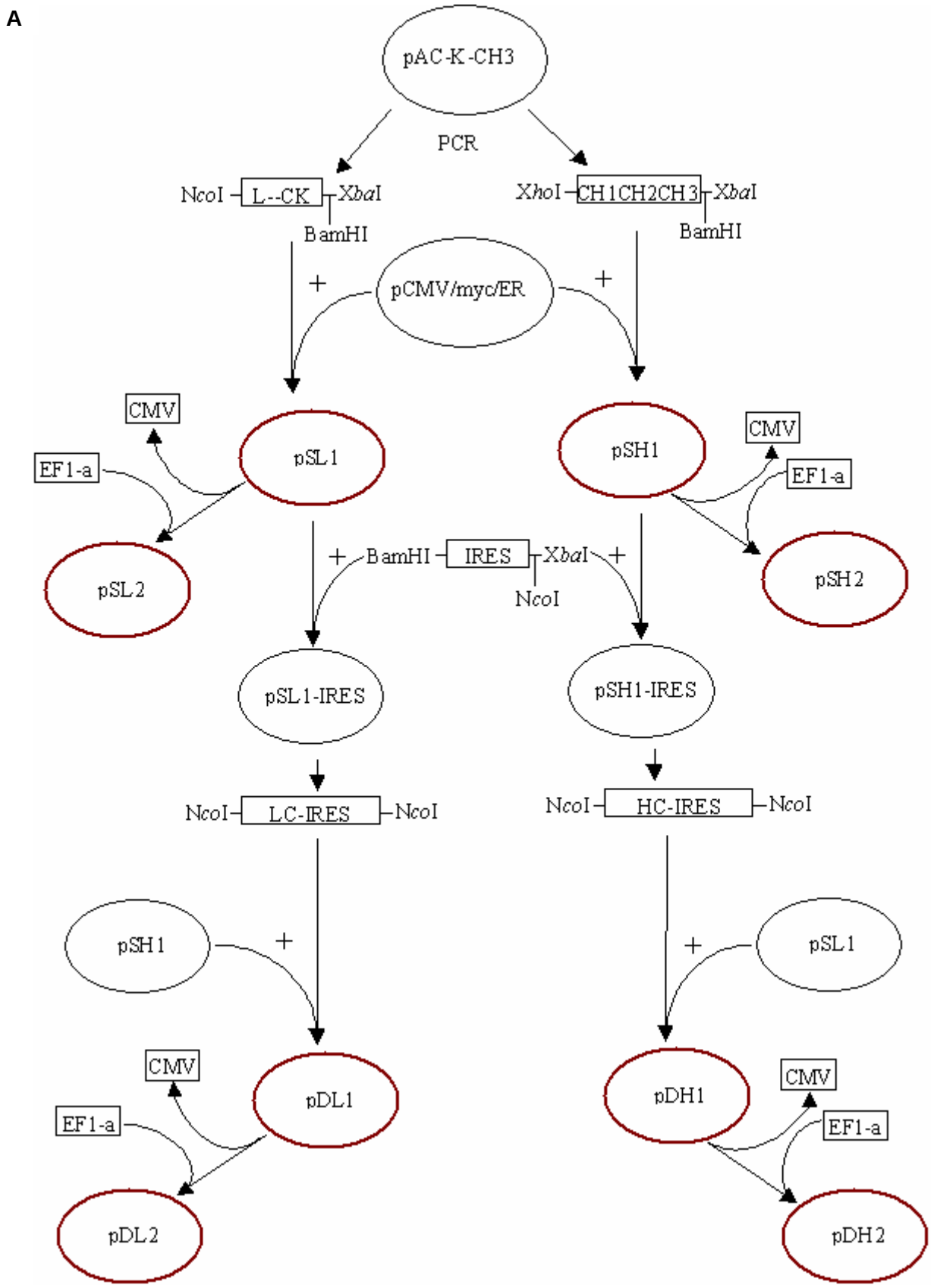
A
pAC-K-CH3
PCR
NcoI
L--CK
XbaI
BamHI
XhoI
CH1CH2CH3
XbaI
BamHI
pCMV/myc/ER
CMV
EF1-a
pSL1
pSL2
pSH1
CMV
EF1-a
pSH2
BamHI
IRES
XbaI
NcoI
pSL1-IRES
pSH1-IRES
NcoI
LC-IRES
NcoI
NcoI
HC-IRES
NcoI
pSH1
pSL1
CMV
EF1-a
pDL1
pDL2
pDH1
CMV
EF1-a
pDH2

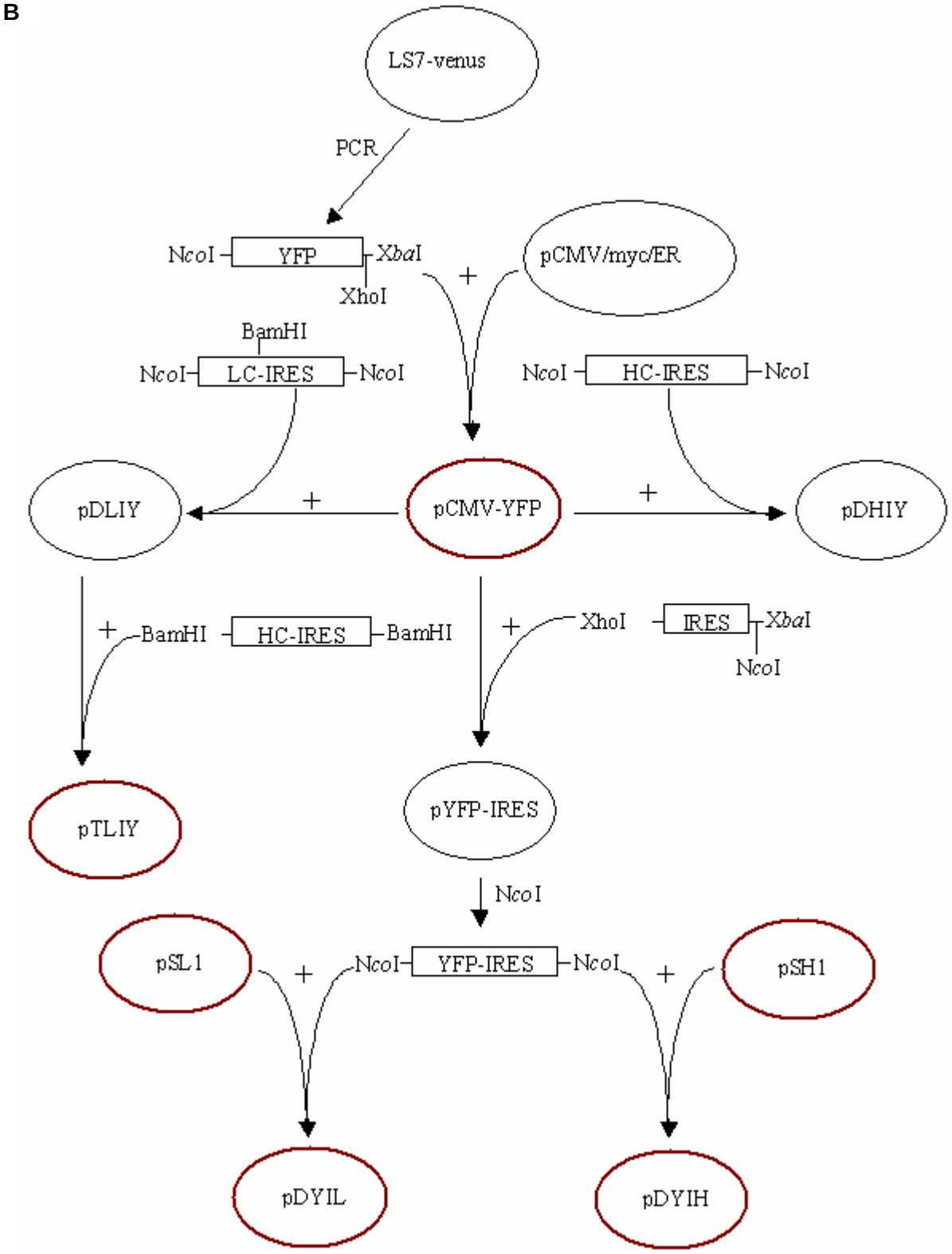

Figure 10 Flow chart of the construction of IgG expression plasmids (A) and polycistronic plasmids with YFP gene as reporter (B). The elements are not drawn to scale. Detail descriptions of indicated cloning steps refer to chapter 5.2.4.

3.2 The impact of cistron arrangement on IRES mediated bicistronic gene expression

To analyze of the impact of cistron arrangement and the affection of H and L chain on IgG expression, a series of bicistronic and tricistronic plasmids using an YFP variant (Venus) as reporter gene were constructed (Fig. 11). A comparative analysis of the cap-dependent and the IRES-mediated cap-independent translation efficiency was performed in 293T and CHO-K1 cells. In all the constructs, the IRES element used was an EMCV IRES variant with one C deletion between base 270 and 280, and an A345G mutation. Transiently transfected cells samples were harvested and analyzed by flow cytometry (FACSCalibur with CellQuest software).

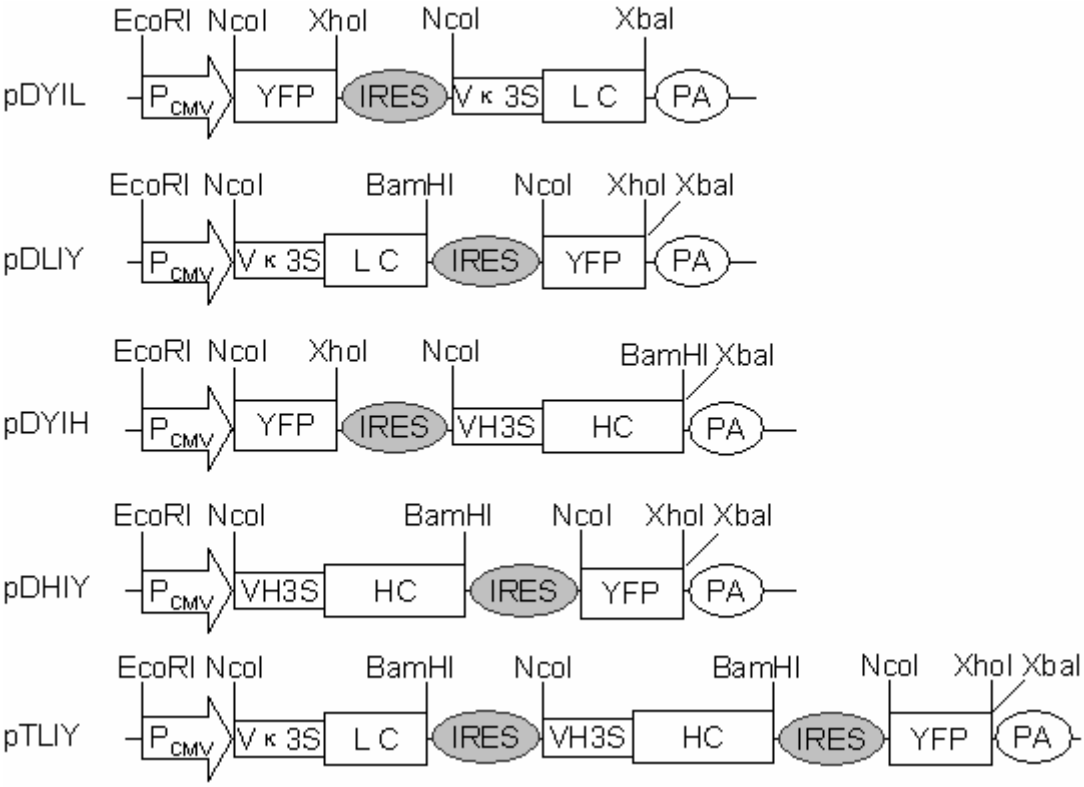

Figure 11 Schematic representations of the vectors for the expression of the mouse/human chimeric IgG and yellow fluorescence protein genes. CMV: CMV immediately early promoter, YFP: a variant of yellow fluorescence protein gene (Venus), IRES: internal ribosome entry site fragment (a variant of EMCV 5' UTR nt260 to 848), Vκ3S: human antibody Vκ3 subfamily signal sequence, LC: IgG light chain gene, PA: BGH polyadenylation sequence, VH3S: Mouse antibody heavy chain VH3 subfamily signal sequence, HC: IgG1 heavy chain gene. The elements are not drawn to scale.

After collecting 10000 to 50000 events, living cell subsets were gated within the total forward-side scatter dot plots based on mock-transfected control cells. The quadrant was set to define the positive cells as those falling in the upper-left. The mean fluorescence intensity (MFI) for the YFP (FL1) was determined on the events falling within the upper-left of the quadrant (Fig. 12A). Three independent transfection experiments were performed using the five different constructs in transiently transfected 293T cells (Fig. 12B). When YFP was positioned as the first cistron

expressed by cap-dependent translation initiation, pDYIH and pDYIL gave nearly equal fluorescence signals; when YFP was positioned as the second cistron at downstream of IRES element, the pDHIY and pDLIY expressed the YFP gene almost equal to each other, but 2-4 fold lower than from 5' cap-dependent translation (pDYIH and pDYIL). The reporter gene transient expression levels were not significantly affected by the other cistron being L or H chain.

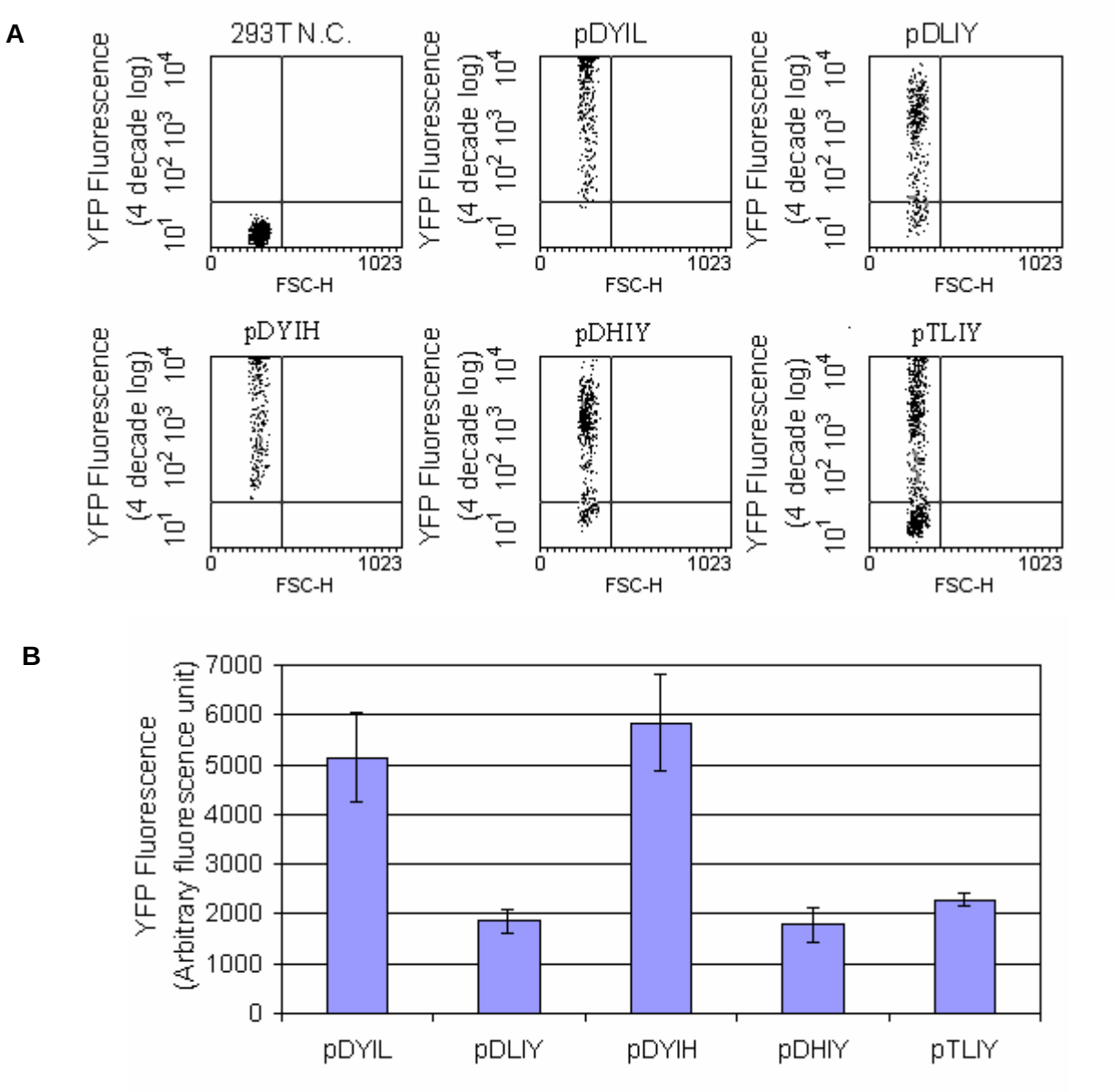

Figure 12 Comparison of cap-dependent and IRES mediated cap-independent YFP expression in transiently transfected 293T cells. (A) Fluorescence distribution after flow cytometry of transiently transfected 293T cells. 48 hours after transfection, cells were harvested and analyzed by flow cytometry. Fluorescence emission (FL1) was analyzed for yellow fluorescence. Forward and side scatter was used to establish a collection gate through which dead cells and debris were excluded. (B) Quantitation of YFP fluorescence intensity of transient transfected HEK 293T cells measured by flow cytometry 48 hours after transfection. Standard error variance were from three independent experiments

Interestingly, in pooled stably transfected CHO-K1 cell lines, pDYIL gave a 2-fold higher fluorescence signal compared to pDYIH (Fig.13A). The prevalence of the positive cells in pools of cells transfected with pDYIL transfected was also about 2-fold higher than cells transfected with pDYIH.

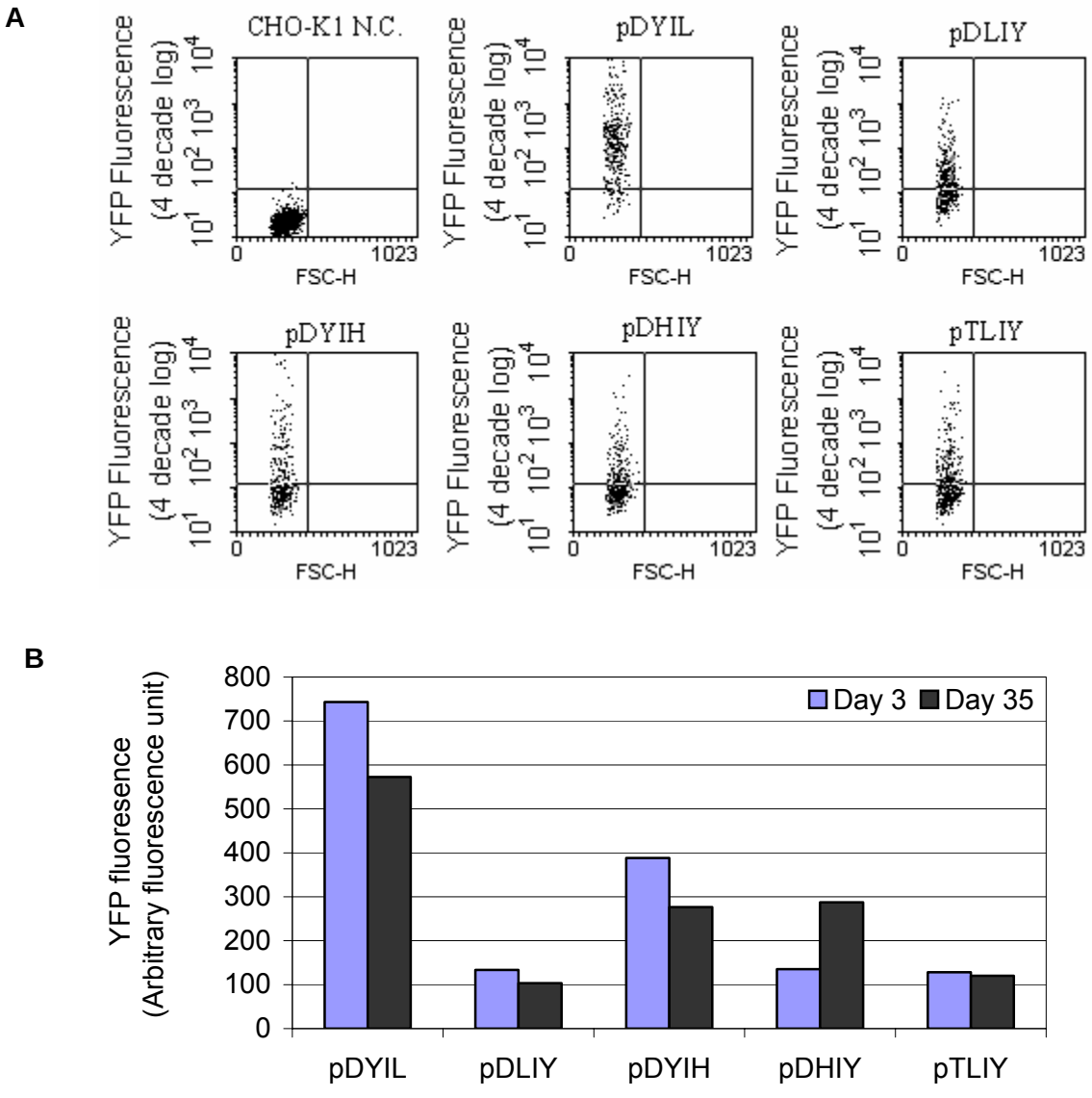

Figure 13 Comparison of reporter YFP gene expression by cap-dependent and IRES mediated cap-independent way in stably transfected CHO-K1 cells. (A) Fluorescence distribution of pooled stably transfected CHO-K1 clones measured by flow cytometry after two weeks selection with 500 µg/ml G418. (B) Quantitation of mean fluorescence intensities of pooled stably transfected CHO-K1 cells cultured for 3 days and 35 days in absence of selection pressure.

Here, the IgG H or L chain positioned as the downstream cistron obviously affected on cap-dependent translation initiation of the upstream cistron (Fig. 13B). Repeated experiments showed the same result. For YFP being placed at second or third cistron, the IRES mediated YFP

expression 3 days after selection gave signals at the same level (Fig.13). 35 days after selection, reporter gene expression from the construct pDHIY is about 2-fold higher than pDLIY and in the same range of the expression levels from pDYIH. The prevalence of positive among the gated cells, pDHIY was about 8,88%, pDLIY was about 14,19%, pDYIH was about 6,86% and pDYIL was about 14,03% (data not shown in the figure). This indicates that constructs with the same elements have a similar prevalence of detectable YFP positive cells one month after selection. The bicistronic construct with H chain as first cistron seems to be beneficial for stable protein expression. IRES mediated YFP expression appeared to be about 3-5 folds lower than cap-dependent translation in CHO-K1 cells. In the tricistronic construct, where the YFP gene was positioned as the third cistron, the YFP expression was found to be not reduced compared to bicistronic constructs in both transiently transfected 293T and stably transfected CHO-K1 cells, which is consistent with a previous report (Zhu, Musco et al. 1999). These results indicted that the cistrons following IRES in combination with antibody genes in the context of our vectors are translated efficiently, however not as efficient as cap-dependent translation of the first cistron.

3.3 Transient antibody expression in 293T and CHO-K1 cells

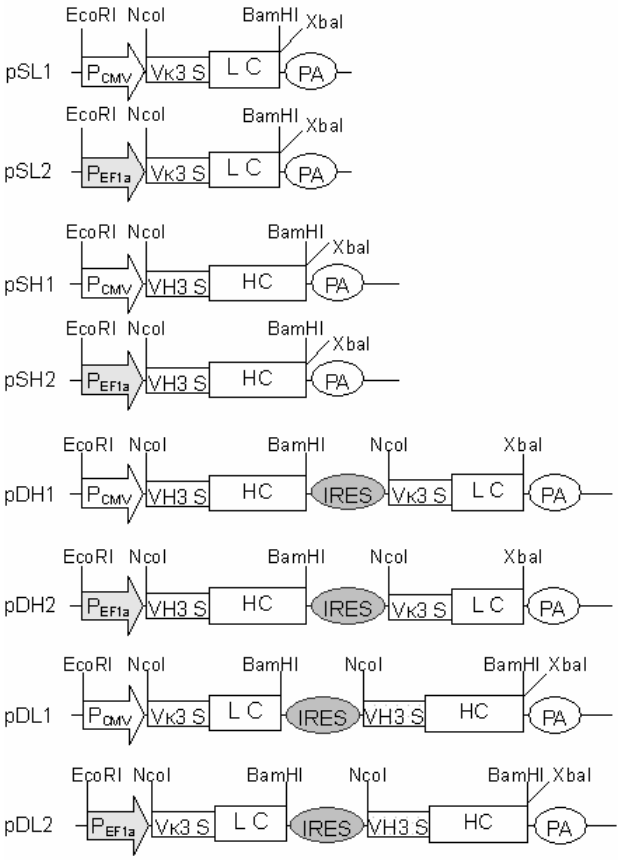

Figure 14 Schematic representations of the vectors for the IgG expression in mammalian cells. For abbreviations see Figure 11. The elements are not drawn to scale.

To assess the antibody expression capabilities of the constructed vectors, we transfected HEK 293T and CHO-K1 cells with monocistronic and bicistronic vectors with two different promoters and cistron arrangements (Fig. 14). 48 hours after transfection, the IgG expression levels in the supernatant were measured by sandwich ELISA. Since free IgG H chains are not secreted (Morrison and Scharff 1975), detection of the γ heavy chain in the supernatant should represent the expression levels of entire IgG molecules. Different combinations of monocistronic expression constructs gave different expression levels (Fig. 15). The combination of monocistronic L and H chain expression constructs driven by EF1-α promoter gave the highest yield. For bicistronic expression, the EF1-α promoter driven bicistronic expression construct with L-IRES-H arrangement in 293T cells gave an about 2-fold higher IgG expression than all other bicistronic expression constructs. The optimal EF1-α driven bicistronic expression construct and the cotransfected EF1-α promoter driven two monocistronic ones show a similar IgG expression levels (Fig. 15).

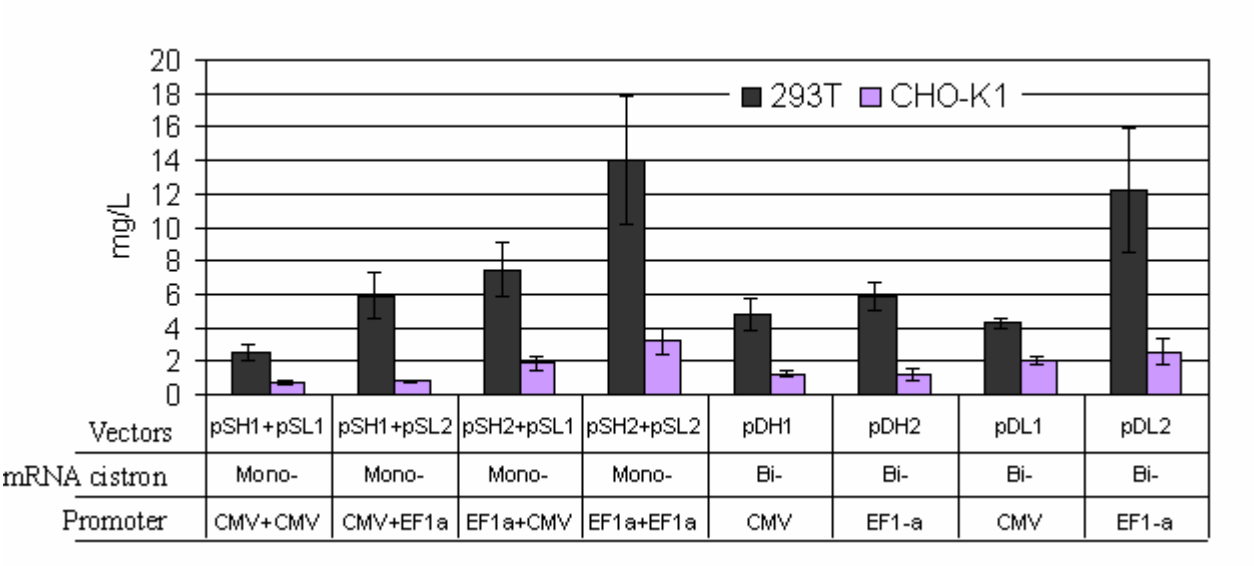

Figure 15 Comparison of the mouse/human chimeric IgG1 transient expression levels from different constructs in 293T and CHO-K1 cells. 293T and CHO-K1 cells were seeded in 24-well plate the day before transfection in 1mL appropriate medium and transfected with monocistronic and bicistronic plasmid, 48 hours after transfection, IgG concentration in the supernatant was determined by ELISA. Standard error variance was from three independent experiments.

3.4 IgG1 expression in stably transfected CHO-K1 clones

Based on the transient expression data, the bicistronic expression plasmids pDH1-215 and pDL1-215 and a combination of the two-monocistronic expression plasmids pSH2-215 and pSL2-215 were used to transfect into CHO-K1 cells to compare the expression levels of stable cell lines. After two weeks of selection with 500 μg/ml G418, 15 clones were randomly picked

from each transfection and the antibody expression levels were measured by ELISA. 6-8 clones per transfection expressed detectable levels of antibody. The 15 random clones from the cotransfection of two-monocistronic plasmids resulted in an expression patterns equal to the one from bicistronic expression constructs (Fig. 16). In transient expression, the combination of two EF1-α promoter driven monocistronic plasmids gave a higher yield than the combination of CMV promoter driven monocistronic plasmids and the bicistronic plasmids pDH1-215 and pDL1-215. This may suggest that for stable expression, the site of integration has a dominant impact. The bicistronic vectors allow stable expression with yield comparable to the monocistronic vectors.

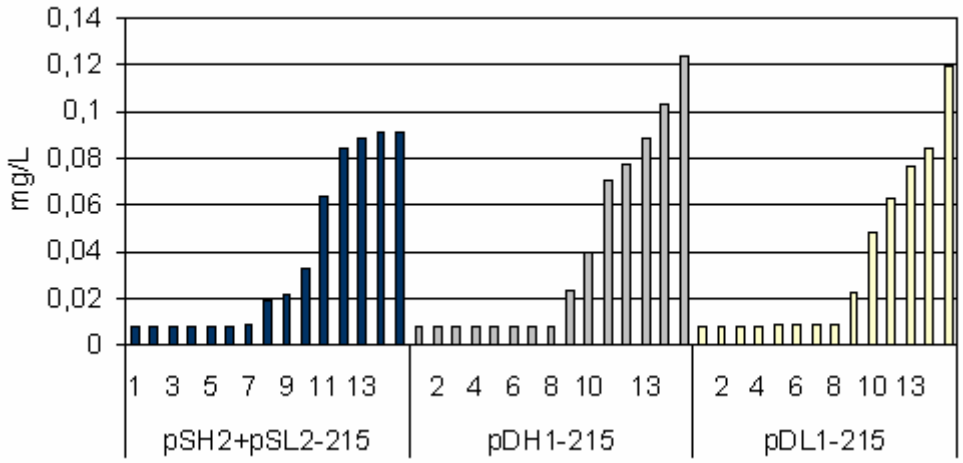

Figure 16 IgG expressions of randomly selected stable CHO-K1 clones. Human/mouse chimeric IgG 215 expression levels for clones obtained by either cotransfection with two monocistronic vectors pSH2-215 and pSL2-215, or a bicistronic vector pDH1-215, pDL1-215 respectively. The IgG concentration in the supernatant was determined by ELISA. It is shown of 15 clones ranked from lowest to highest expression levels.

To evaluate the long-term stability of EMCV IRES mediated bicistronic antibody expression, CHO-K1 cells were transfected with the bicistronic human IgG1 expression plasmid pDH1-IIB6 and selected with G418. Of 51 clones tested after selection, 23 clones, about 45% expressed detectable levels of antibody (Fig. 21A). The highest expressing clone (Lj98-1-13) was scaled up to 6-well plate, cultured with medium without selection pressure and evaluated for antibody expression for a period of 300 days (Fig. 17). After 100 days of culture in absence of G418 selection, the expression level reduced to 50% relative to the start level. After 300 days, the tested clone still expressed detectable levels of antibody, about 10% relative to the start levels. The stability of this clone was at least equivalent to previously reported for the recombinant protein production in CHO cells (Barnes, Bentley et al. 2003). This indicates that EMCV IRES mediated bicistronic expression does not affect the stability of protein expression and can be used to generate highly expressing stable clones.

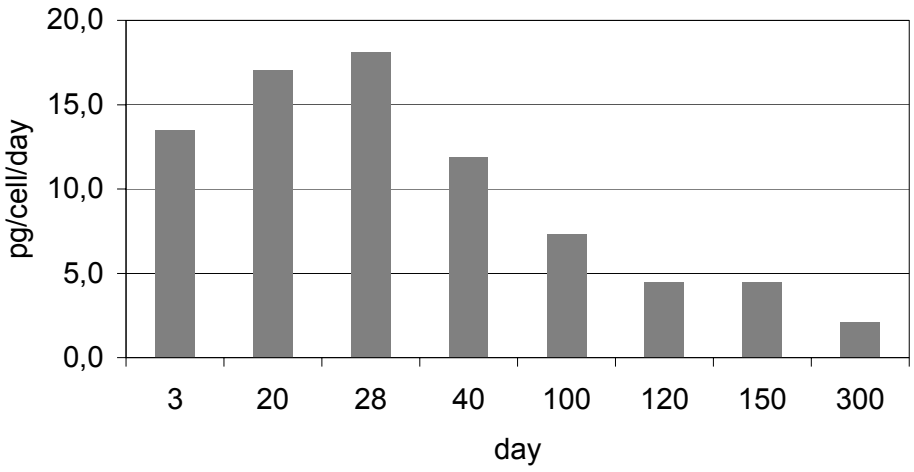

Figure 17 Evaluation of the stability of IgG expressions using EMCV mediated bicistronic vector in CHO-K1 cells. A stable CHO-K1 clone expressing human IgG was isolated and kept culture over 300 days. Culture medium supernatant was harvested at different period of time, centrifuged at 12000rpm for 5min to get rid of cell debris, was quickly frozen the in liquid nitrogen and stored at –80°C. IgG concentration in the supernatant was determined by ELISA in one experiment.

The causes of the loss of productivity in absence of G418 were studied by subcloning analysis of this clone over a period of 5, 35 and 300days respectively. Among the randomly picked clones, 100% of the cells from cultured in absence of G418 selection over 5 and 35 days gave detectable IgG in the supernatant, the expression levels from different clone were nearly in the same level, which indicted the unity of the selected monoclonal cell lines. The IgG expression levels from the cells cultured over 35 days were slightly down regulated compared the cells cultured over a period of 5 days in absence of selection (Fig. 18A, B). The subcloning analysis of the cells cultured in absence of selection over a period of 300 days showed only about 10% of the picked 200 clones expressed detectable IgG in the supernatant and the expression levels were also apparently down regulated (Fig. 18C). 24 clones were further selected from the subcloning of the cells cultured in absence of selection over a period of 300 days and cultured in 24-well plate, and reselect with G418 (500 µg/mL) for 2 weeks. All the cells kept living under selection pressure, the IgG expression levels in the supernatant were slightly increased compared to the expression levels before selection, but the down regulated cells did not recover to the original expression levels (Fig. 19). This might indicate that the loss of productivity was not likely due to the loss of the genes of interest.

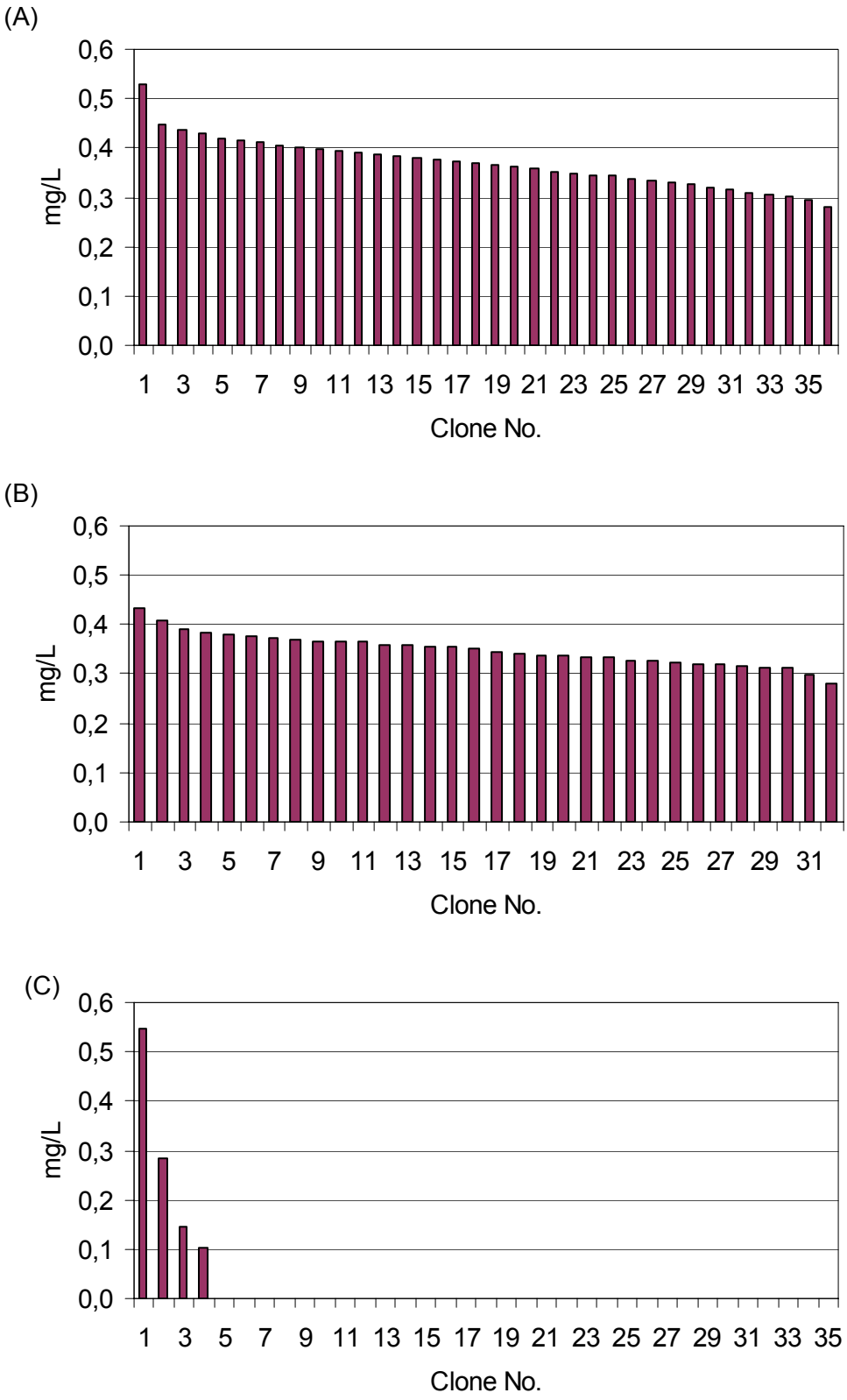

Figure 18 Subcloning analysis of the human IgG expression in absence of G418 selection over a different period. Human IgG expression in the supernatant for subclones obtained from the stable clone cultured over a period of: (A) 5 days, (B) 35 days and (C) 300 days in absence of selection, here is shown randomly selected clones, ranked from highest to lowest expression level. Antibody concentration in the supernatant was determined by using ELISA.

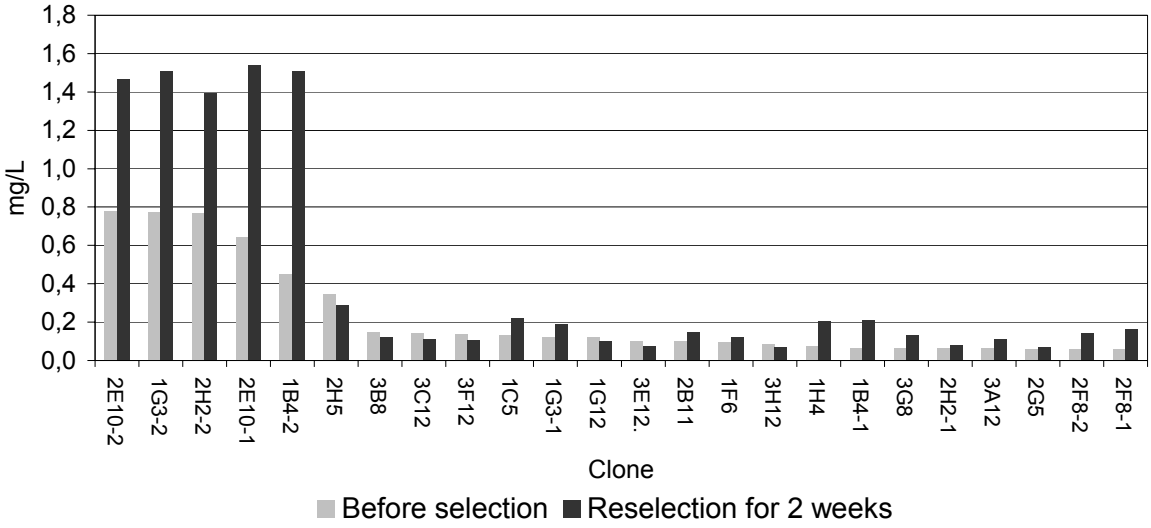

Figure 19 IgG expression levels from subclones of the clone culture over a period of 300 days in absence of selection. 24 clones were randomly picked, culture in 24-well plate with 1 mL medium, the cells were selected under G418 (500 µg/mL) for 2 weeks. IgG expression levels in the supernatnant were determined by ELISA when the cells reach mono-layer confluent before and after selection.

3.5 The impact of scaffold matrix attached region (S/MAR) elements on IgG expression

S/MARs are DNA sequences that bind isolated nuclear scaffolds or nuclear matrices in vitro with high affinity (Hart and Laemmli 1998). The human interferon beta domain S/MAR element was shown to confer position-independent gene expression and augment gene transcription increasing the gene expression levels (Bode, Benham et al. 2000). To apply these findings in the IgG expression vectors, the 2,2kb S/MAR element from the human beta interferon gene was cloned into a bicistronic human anti-MUC1 IgG expression construct upstream or upstream and downstream of the expression cassette (Fig. 20). The impact on IgG expression levels was analyzed.

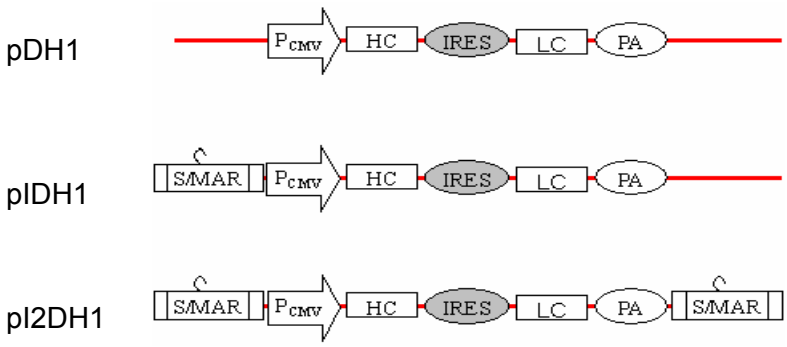

Figure 20 Schematic representation of the bicistronic vectors with or without S/MAR, pDH1

bearing no S/MAR element, pIDH1 bearing one S/MAR element at upstream of CMV promoter, pI2DH1 bearing two S/MAR element flanking the bicistronic expression cassette. Elements are not drawn to scale.

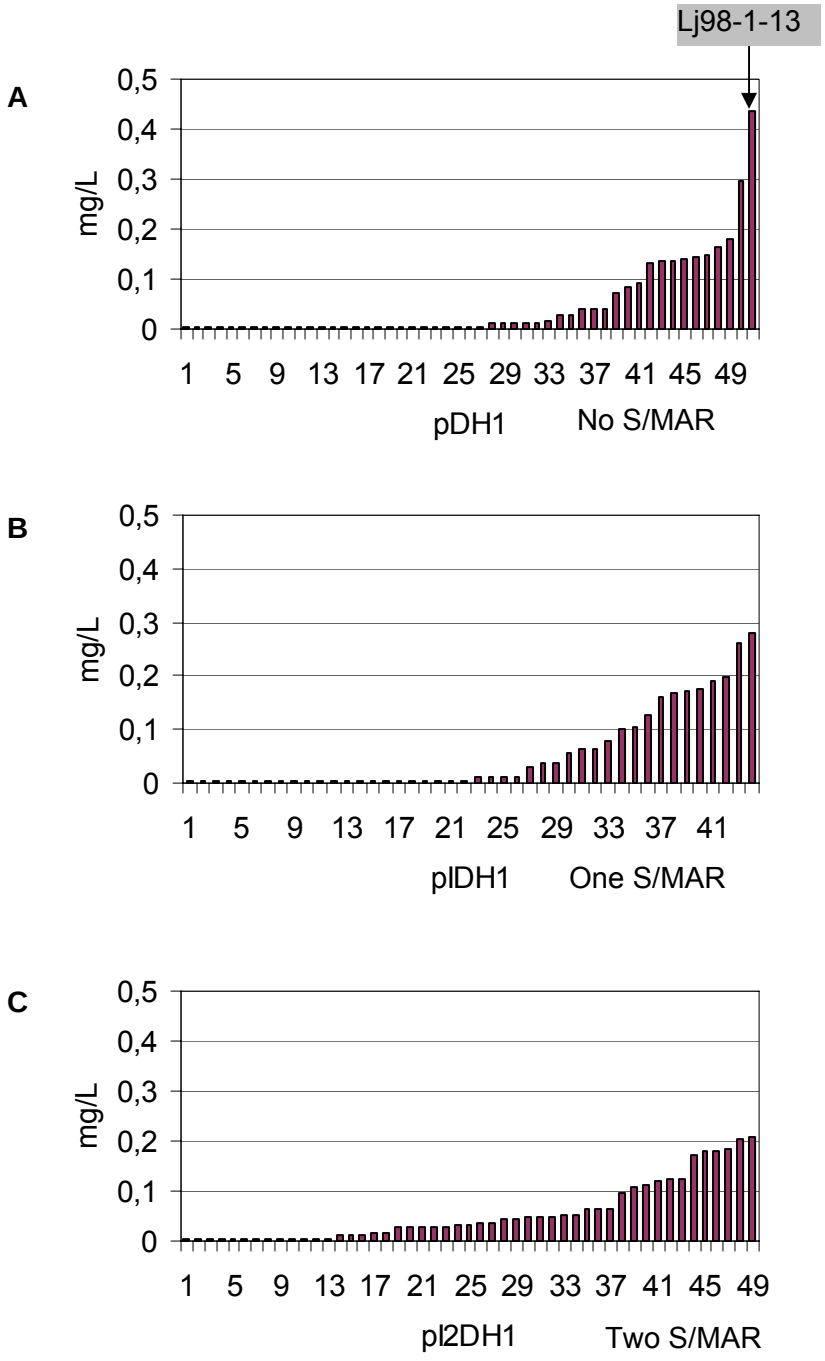

Figure 21 The impact of S/MAR on IgG1 expression in stable CHO-K1 clones. The antibody concentration in the supernatant is shown for randomly selected clones ranked from lowest to highest expression level. (A) Transfected with pDH1 bearing no S/MAR element; (B) transfected with pIDH1 bearing one S/MAR element at upstream of CMV promoter; (C) transfected with pI2DH1 bearing two S/MAR elements flanking the bicistronic expression cassette.

In stably transfected CHO-K1 cells, the percentage of randomly selected stable CHO-K1 clones

expressing detectable IgG levels, for pDH1 without S/MAR was about 47% (24/51), for pIDH1 with one S/MAR was 50% (22/44) and for pI2DH1 with two S/MAR was 75% (37/49) (Fig. 21 A, B, C). It seems that S/MAR elements could increase the prevalence of positive clones when two S/MAR elements are flanking the expression cassette. However, among the defined amount of screened clones, the highest producing clone was isolated from the vector without S/MAR element. To compare the antibody expression levels from single clones, the two highest expression clones were selected from each transfection and cultured in 6-well plates. Antibody yields in the supernatant was determined by ELISA. The highest expressing clone from pDH1, gave about 5-8 times higher IgG yields than the others (Fig. 22). That result is partially inconsistant with a previous report that a chicken lysozyme 5' MAR element could significantly increase the prevalence of positive clones and the expression levels of single clones (Zahn-Zabal, Kobr et al. 2001).

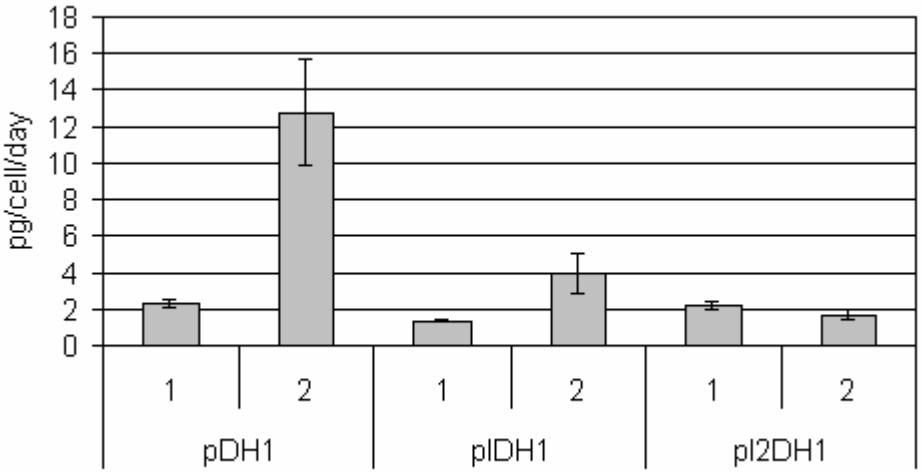

Figure 22 Anti-MUC1 IgG1 expression levels of stably transfected CHO-K1 clones from constructs with or without S/MAR elements. 3 days after selection, 10^6 cells were counted and culture in 3mL medium for 24 hours in triplicate, antibody concentration in the supernatant was determined by using IgG capture ELISA.

It was shown that the S/MAR element when linked directly to an upstream transcription unit can mediate episomal replication of circular DNA and keep mitotic stability in mammalian cells in the absence of selection (Jenke, Stehle et al. 2004). From this, the idea of designing nonviral episomal vectors for IgG expression was accrued. To make a comparative analysis of the ability of the S/MAR element mediated episome on IgG expression, the 2,2kb human beta interferon gene S/MAR element was cloned into a tricistronic IgG expression vector pTLIY (Fig. 23).

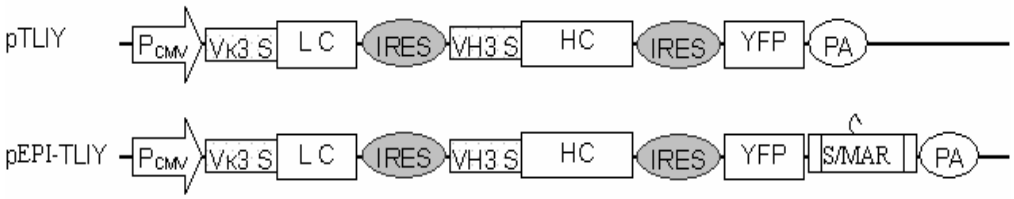

Figure 23. Schematic representation of episomal vector pEPI-TLIY and reference vector pTLIY. The gene elements are not drawn to scale.

The transient expression of the reporter gene YFP from the S/MAR containing vector pEPI-TLIY was found to be lower than from pTLIY in transiently transfected CHO-K1 cells (Fig 24). Pools of stably transfected CHO-K1 cells obtained by selection with G418 (500µg/mL for 2-3 weeks) were analyzed and sorted by FACS. And it was compared with cells obtained without selection from the same transfection (Tab. 2 and Fig. 23).

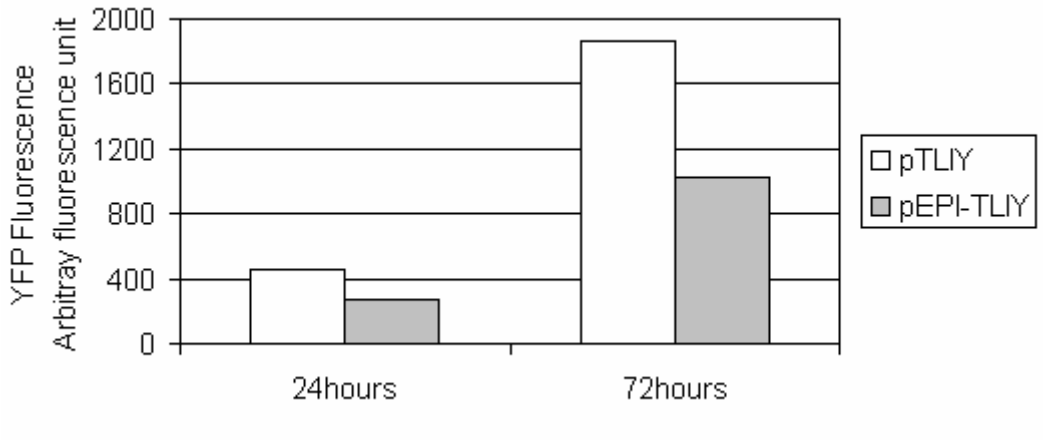

Figure 24 Reporter gene YFP expression levels in transiently transfected CHO-K1 cells from tricistronic pTLIY and pEPI-TLIY. YFP fluorescence intensity was measured using a TECAN GENios, cells transfected with only transfection reagents was set as background control.

Table 2 Flow cytometry analysis of pools of stably transfected CHO-K1 cell with or without selection

	Selected with 500µg/ml G418		No selcetion	
	Positive(%)	Sorting(%)	Positive(%)	Sorting(%)
CHO-K1	-	-	-	-
pTLIY	33%	20%	1,9%	1%
PEPI-TLIY	28%	18%	0,47	0,20%

The cells transfected with pEPI-TLIY expressed slightly lower levels of YFP than the control cells transfected with pTLIY (Table 2). In pools of transfected cells cultured for one month without any selection, YFP expression from pEPI-TLIY transfected cells was about 3-5 times less than from pTLIY transfected cells. This result showed that when a 2,2 kb S/MAR fragment was directly

placed at downstream of a polycistronic transcription unit and upstream of the polyA signal, the stability of the foreign gene expression was not increased but the expression levels of the reporter gene YFP were decreased. To test the expression levels from single clones, 20 clones expressing detectable levels of YFP were isolated by FACS sorting, cultured in 24-well tissue culture plates and IgG concentration in the supernatant was determined by ELISA (Fig. 25). The average expression levels from the selected pEPI-TLIY single clones were lower than from the reference clones (pTLIY). Therefore, it might be argued that the expression levels from pEPI-TLIY are generally lower than from pTLIY.

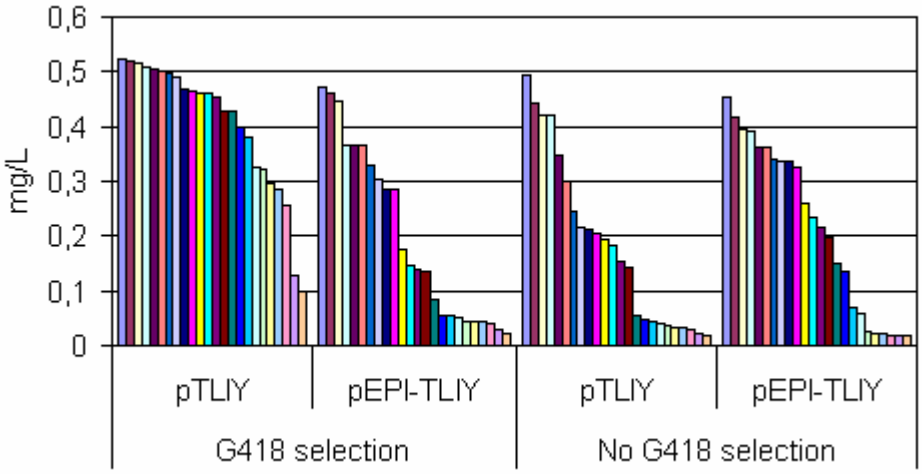

Figure 25 Mouse/human IgG expression levels from randomly selected clones. Antibody concentration in the supernatant was determined by ELSIA, here is shown for the randomly selected clones ranked from highest to lowest expression level.

To test if the plasmid DNA was integrated into genome of the host cells or replicated as an episome, six clones were randomly picked and cultured in 6-well tissue culture plates. A plasmid rescue experiment was performed, but no relevant plasmid could be rescued from stable clones, in contrast, plasmids were successfully rescued from transiently transfected controls. PCR amplification of the IgG heavy chain constant region was performed to test for integration using genomic DNA as template. A band of about 1-kb was found from most of the clones (5/6) in the pEPI-TLIY transfected cells with or without selection (Fig. 26). This demonstrated that when the S/MAR element is directly linked to one polycistronic transcription unit, the plasmid rather integrates into chromosome than replicates as an episome, although, further evidence needs to be collected.

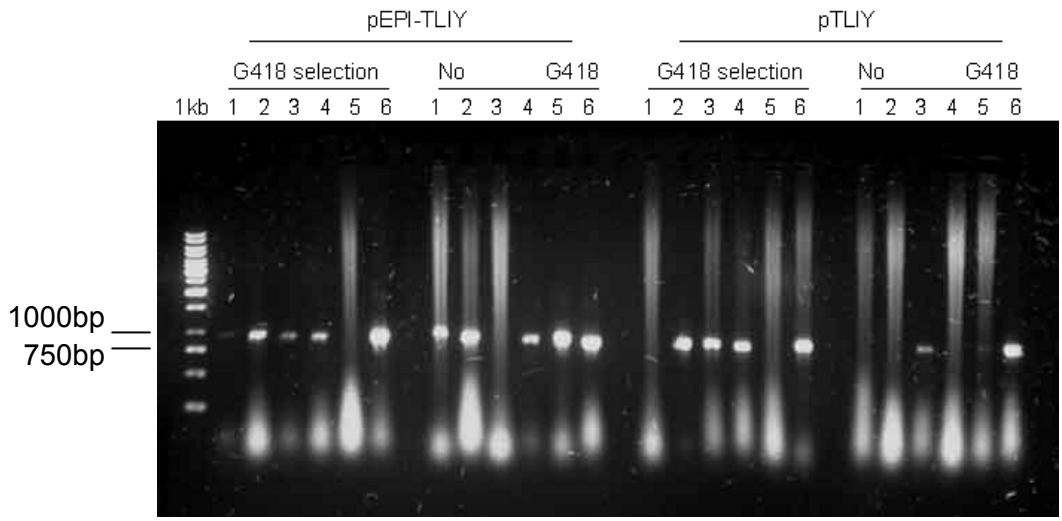

Figure 26 PCR amplification of IgG constant region using genomic DNA as template. GeneRuler 1kb DNA ladder was used as fragment sizes reference, the genomic DNA was isolated from 6 randomly selected clones in each experimental group and was identified by PCR amplification of the H chain constant region. The clones with positive integration should have a band around 1kb.

3.6 The impact of the H chain to L chain ratio on IgG production

It is a crucial step for IgG production in mammalian cells that the H chain and L chain polypeptides in the endoplasmic reticulum yields properly folded and assembled structures with full biological activity. When folding promotion is not sufficient, proteins are retained in the ER and eventually retranslocated to the cytosol for degradation by the ubiquity proteasome pathway. The folding and assembly of H chain and L chain relies on the chaperone system in the ER and the HC:LC ratio could influence assembly time (Gonzalez, Andrews et al. 2002). To investigate the optimal ratio of intracellular H chain and L chain expression levels for IgG production, a series of EMCV IRES variants with different translation efficiencies were used (Chongchong Zhang's master thesis). The translation efficiency of the different IRES variants were compared to cap-dependent translation, by using bicistronic constructs with inverse cistron arrangement. The translation efficiency of the IRES variants ranged from 0,03 to 0,6 compared to cap-dependent translation. The L chain expression levels were set as constant obtained by positioning the L chain gene as the first cistron in a bicistronic construct. The H chain expression levels were set as variate obtained by using EMCV IRES variants with different translation efficiency. Thus, it was supposed that the IgG expression levels depend on the H chain expression levels, since the cap-independent translation efficiency is lower than cap-dependent translation efficiency. The L chain and H chain were translated from the same mRNA, the IgG expression levels may reflect the impact of H and L chains ratio on IgG folding and assembly. The IgG expression data collected from different bicistronic constructs showed that when the relative translation efficiency

of the IRES variant is higher than 0,4, IgG production levels increased rapidly. When the relative translation efficiency reaches to 0,5, IgG expression levels are nearly in the optimal status (Fig. 27). The expression levels obtained were not increased, in the contrary, slightly reduced when using a more efficient IRES variant leading to a higher HC:LC ratio.

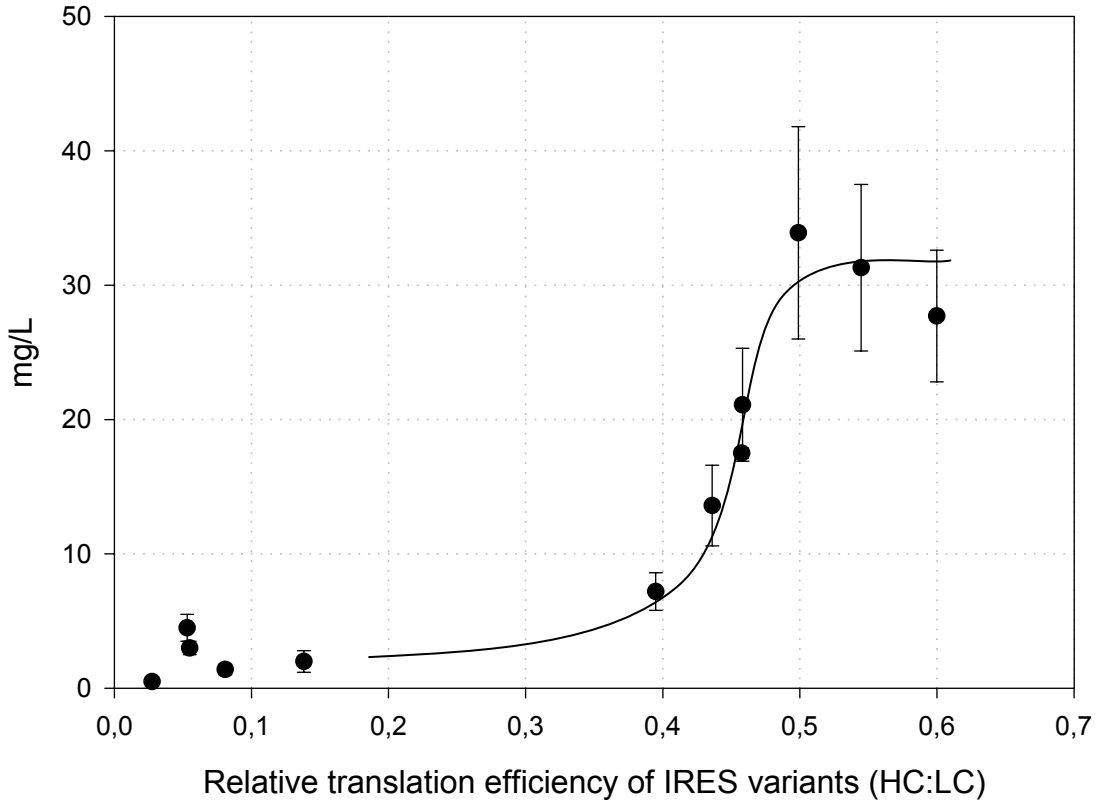

Figure 27 Effect of the ratio of translation efficiency of HC:LC on IgG production. The IgG was transiently expressed in HEK 293T cell with bicistronic vectors, the IgG concentration in the supernatant was determined by ELISA. The L chain was positioned as first cistron and translated under a cap-dependent mechanism; the H chain was positioned as second cistron and translated under IRES-driven internal initiation mechanism. The IRES mediated relative translation efficiency was determined in bicistronic constructs, which encodes the IgG L chain and an YFP reporter gene respectively in inverse cistron arrangement. The YFP fluorescence was analysed using flow cytometry. The relative translation efficiency of HC:LC ratio was derived from the relative translation efficiency of IRES variants compared to cap-dependent translation efficiency (I am very grateful to Congcong Zhang, for his help on acquiring of the raw data during his master thesis work)

3.7 IgG purification

Having validated a bicistronic expression system on the production levels, it had to be confirmed that the produced material is fully functional IgG. Supernatant from a CHO-K1 cell clone stably transfected with pDH1-IIB6 or from transiently transfected 293T cells was subjected to affinity

chromatography on protein A. The purified IgG antibody was analyzed by SDS-PAGE under reducing and non-reducing conditions (Fig. 28). Under reducing conditions, the about 50 kD heavy chain and the about 25 kD light chains appear close to the theoretical size of the chains based on its DNA sequence. Under non-reducing conditions, a higher molecular weight band with an apparent molecular mass higher than 250 kD is stained. Free light or heavy chain could not be detected. This indicates that the antibody chains are assembled into whole IgG molecule.

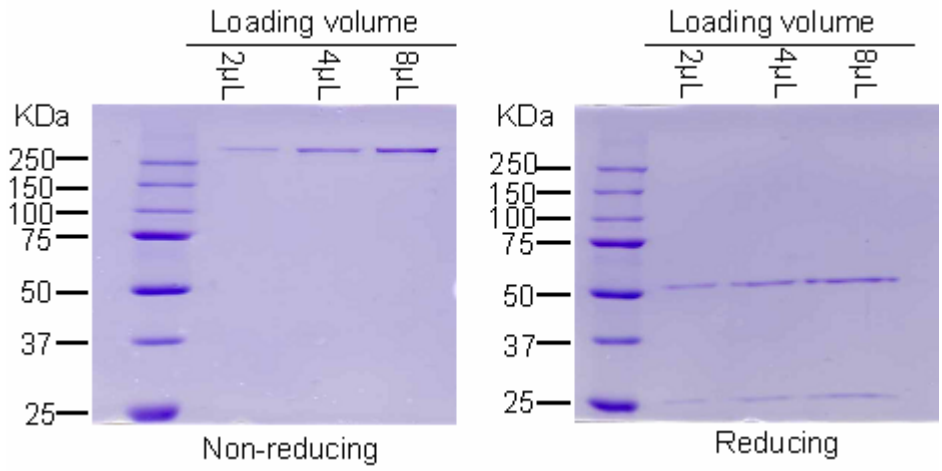

Figure 28 SDS-PAGE and Coomassie staining of the purified human anti-MUC1 IgG. The IgG was produced from a stably transfected CHO-K1 clone with the pDH1 bicistronic vector, purified using affinity chromatography on protein A column. The antibody concentration was about 0,3 mg/L determined by Bradford assay.

3.8 Analytical gel-filtration

Analytical gel-filtration of purified IgG1 from transiently transfected HEK293T and stably transfected CHO-K1 cells were performed on a superdex-200 column. It showed that the IgG molecules from transiently transfected HEK293T cells were presented as IgG monomers, no aggregates were detected, however the IgG molecules from stably transfected CHO-K1 cells were present mainly as IgG monomer, some IgG dimers aggregates were formed (Fig. 29). This might reflect the subtle difference of protein intracellular modification and maturation in different host cells. The difference between the protein sample migrations on the non-reducing SDS-PAGE and size exclution gel filtration could be attributed to IgG being highly structured heterotetramers under non-reducing conditions, which may impact the migration rate compared to the denatured polypeptide. In addition, N-terminal sequencing of the purified IgG1 H chain and lambda L chain confirmed that the antibody expressed from the EMCV-IRES mediated bicistronic vector was processed accurately by correct cleavage of both heavy and light chain signal peptide.

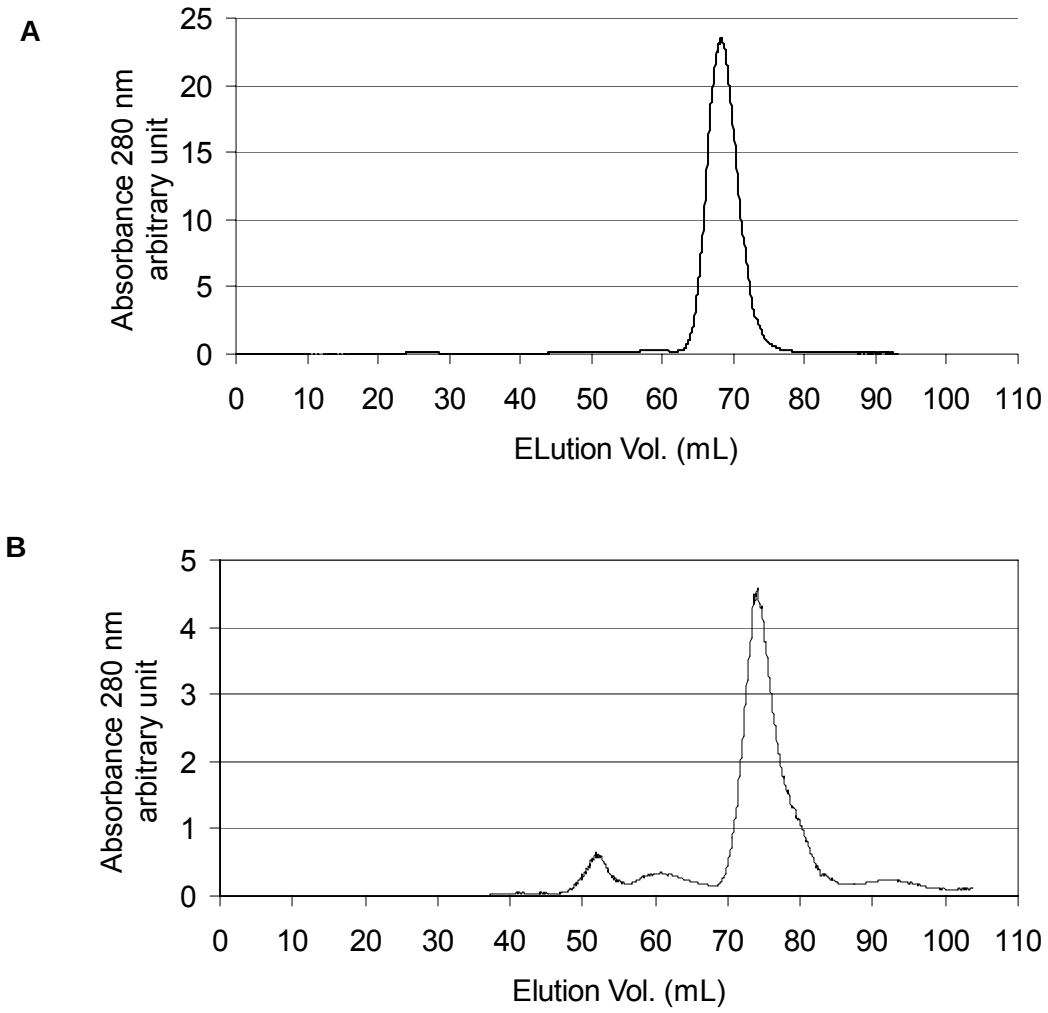

Figure 29 Analytical gel-filtration of the human IgG produced from the pDH1 bicistronic vector on a superdex-200 column. A, the purified IgG produced from transiently transfected HEK293T cells with a concentration of about 1mg/ml. B, the purified IgG produced from stably transfected CHO-K1 cells with a concentration of about 0,3mg/L. For both, a 0,5 mL sample was injected.

3.9 Characterization of human anti-MUC1 IgG

3.9.1 Peptide ELISA

To test the human anti-MUC1 IgG binding specificity, a peptide ELISA was performed on a 16-mer MUC1 peptide antigen, a synthesized STAT3 peptide and BSA were used as control. The purified IgG and scFv both bind specifically to the MUC1 peptide; no unspecific binding to the control STAT3 peptide antigen and BSA was detected. However the binding activity of the IgG to the MUC1 peptide is about 20-30 times lower than of the scFv, which was derived from. The OD450 nm of 300 nM IgG corresponds to 9,4 nM scFv (Fig. 30).

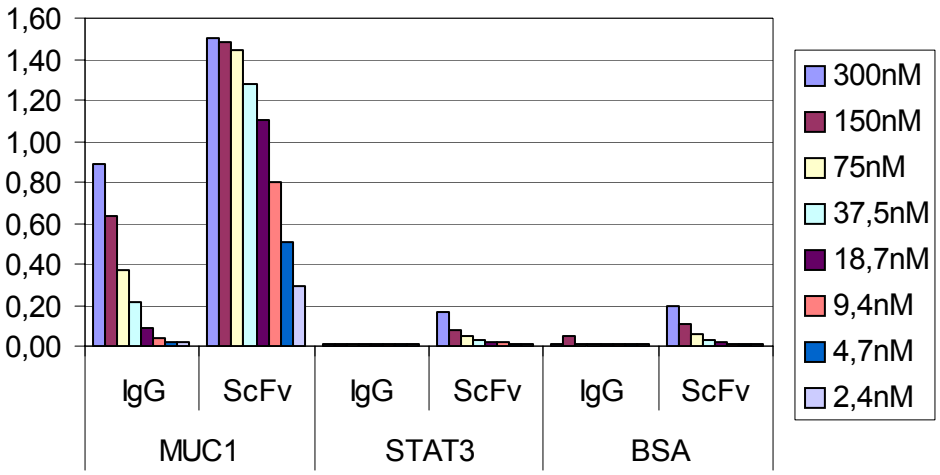

Figure 30 Specificity test of human anti-MUC1 IgG and scFv using peptide ELISA. 1µg/well peptide antigen and BSA control were coated on Nunc Max 96-well microtiter plate at 4°C overnight, the purified IgG and scFv with different dilution were loaded and incubated at RT for 1-2 hours, mouse anti-human or mouse anti-pentahis were added as secondary antibody with appropreate dilution and detected with POD conjugated anti-mouse antibody.

3.9.2 Western-blot on cell lysates

A human breast cancer derived T47D cell line was lysed and subjected to 6% SDS-PAGE, Jurkat lymphoma T cells lysates served as negative control. The seperated samples were transferred to a PVDF membrane, and the purified scFv and IgG were used to stain the MUC1 antigen respectively. MUC1 is a large, transmembrane glycoprotein, expressed at the apical surface of a variety of reproductive tract epithelia with a variable number of tandem repeat of 20 amino acids in its extracellular domain (Fig. 8). The binding signal of both IgG and scFv to cell lysates of T47D cells appeared to be a characteristic smear of high molecular weight bands as previously reported (Walsh, Luckie et al. 2000; Toleiks 2003), which was not found on Jurkat cell lysates (Fig. 31). The IgG gave a stronger binding signal than the scFv when an equal amount of antibodies was used to stain the PVDF membrane.

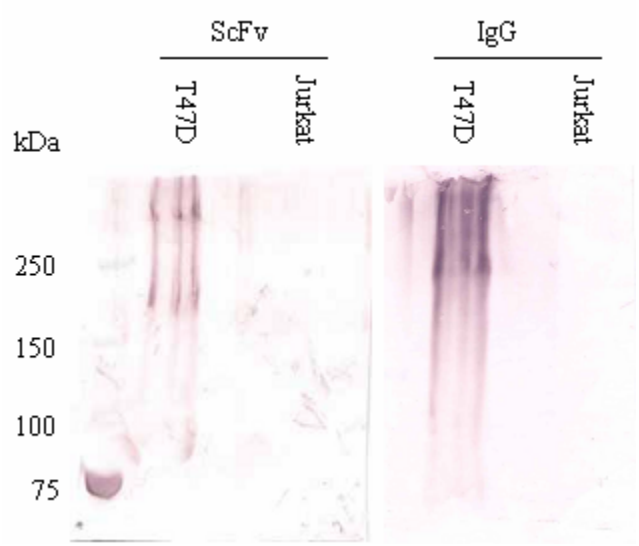

Figure 31 Western-blot analysis anti-MUC1 antibodies on cell lysate of T47D and Jurkat cells. 10^7 T47D and Jurkat cells were lysed in 200µL lysis buffer, 10µL of the cell lysates were mixed with 5 x Laemmli sample buffer and denatured at 95°C for 10min and subjected to 6% SDS-PAGE. The separated protein samples were blotted on a PVDF membrane, stained with purified anti-MUC1 scFv and IgG and detected with alkaline phosphotase conjugated antibodies. The membrane was developed using NBT/BICP substrate.

3.9.3 Flow cytometry analysis of binding to living cells

FACS analysis of the binding specificity to living cells was performed using T47D and jurkat cells. Following incubation of the cells with 5, 25, 50 and 100 µg IgG, or 5 and 10 µg scFv antibodies respectively, a mouse anti-human and a mouse anti-penta-his monoclonal antibodies were used as secondary antibody respectively, and the cells were detected with FITC conjugated goat anti-mouse polyclonal antibody. Samples were analyzed by flow cytometry (FACSCalibur with CellQuest pro software). 30000 to 50000 total events were collected. Data was analyzed using the software WinMDI 2.8. The living cell subset was gated within the total forward-side scatter dot plots. Both IgG and scFv bound specially to T47D cells but not to Jurkat cells (Fig. 32 A). For the IgG, the median of the fluorescence intensity was increased with the increasing amounts of antibody up to 100 µg for staining of 10^6 T47D cells (Fig. 32 B). When an equal molar amount of anti-MUC1 antibodies was used to stain the cells, the IgG gave a higher fluorescence intensity signal than the scFv (Fig. 32 B).

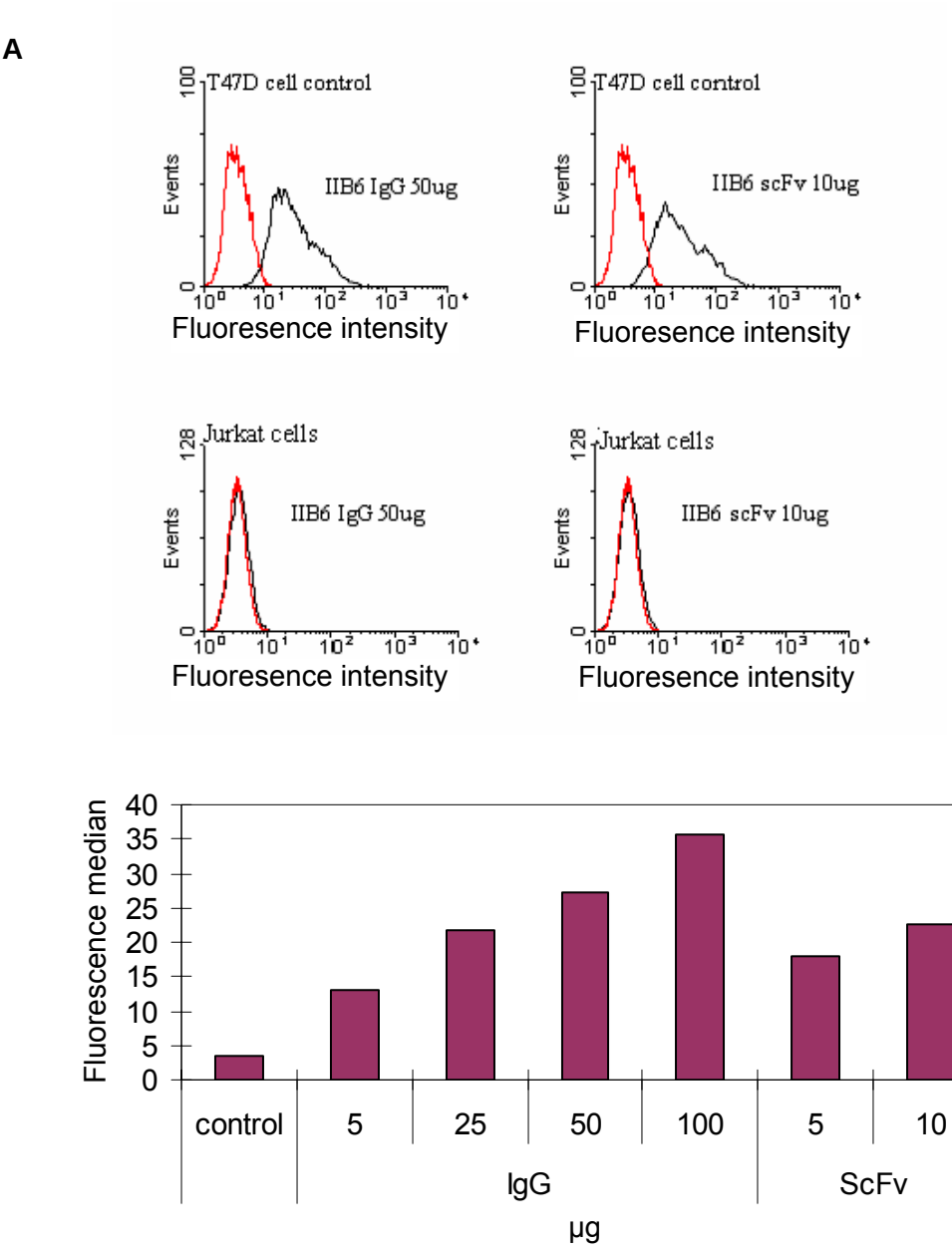

Figure 32 Flow cytometry analysis of the anti-MUC1 antibodies binding to T47D and jurkat cells. (A) Similar molar amounts of purified human anti-MUC1 scFv (10 µg) and IgG (50 µg) were used to stain T47D and Jurkat cells, positive binding to cells were detected by FITC conjugated antibodies. Data was collected by flow cytometry, diagram was obtained by using WinMDI 2.8 software. (B) The median of the fluorescence intensity of the anti-MUC1 IgG and scFv stained T47D cells. T47D cells were stained with different amounts of the human anti-MUC1 IgG and scFv and the binding to cells was detected by FITC conjugated antibodies. Data was collected by flow cytometry, Median of the gated cells fluorescence was obtained by using WinMDI 2.8 software.

3.9.4 Surface plasmon resonance (SPR) analysis

To determine the affinity of the IgG antibody to the synthesized MUC1 peptide, SPR analysis with a Biacore X was used to analyze the antibody-peptide interaction. The binding curves obtained

using concentrations of purified IgG from 6nM to 6µM (Fig 33A) were analyzed assuming a one to one interaction influenced by baseline drifting and bivalent analyte. The bivalent analyte model could be appropreate since the IgG is a bivalent analyte, although the coupled MUC1 peptide antigen "454* NH2-APDT(GalNAC)RPAPGSTAPPAC-COOH" glycopeptide offers only one binding site "XRPAP". The residuals obtained for the one to one reaction with drifting base line was lower than the residuals obtained with bivalent analyte reaction model (Fig. 33 B, C). The parameter values calculated for the one to one reaction with base line drifting appeared reasonable. The binding affinity of the IgG KD (M) was found to be 3,90x10e-6 (Chi^2: 0,583). Surprisingly, the value is about 15-20-fold lower than the scFv measured by Dr. Toleiks in his doctoral work using Biacore 2000, where KA (1/M) is 4,38x10e-6 and KD (M) is 2,28x10e-7.

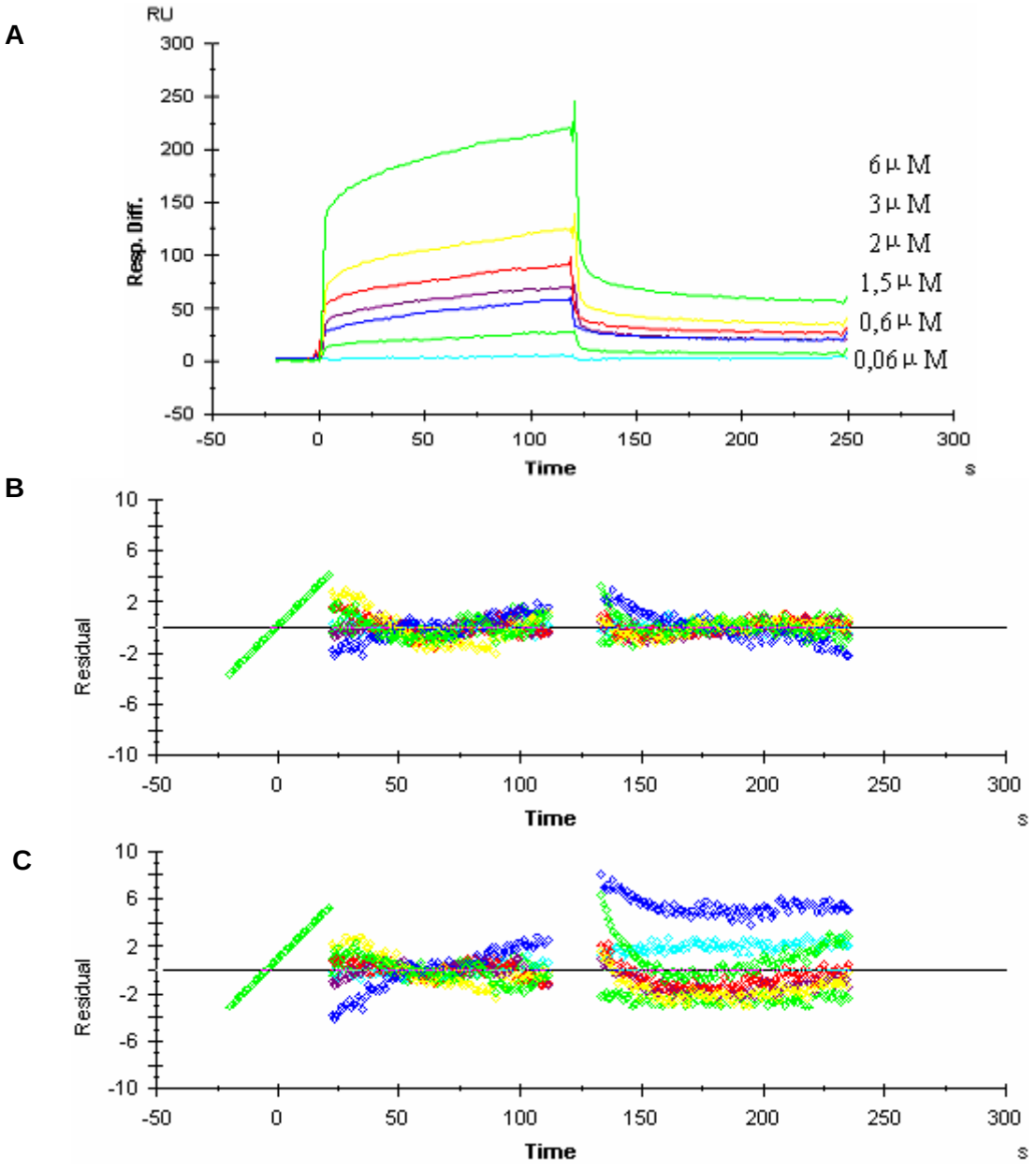

Figure 33 Surface plasmon resonance (SPR) analysis of the IgG antibody on MUC1 peptide. (A)

Response curves obtained during and after injection of IgG on a surface coupled with 16-mer MUC1 glycopeptides. Resdual plots obtained in data analysis using interaction model corresponding to: (B) one to one reaction with drifting baseline; (C) a bivalent analyate.

4 Discussion

IgG is a heterotetrameric glycoprotein with two identical L chains and two identical H chains. To produce IgG in mammalian cells, both H and L chain have to be synthesized in a single cell. The secretion competence, the stability and the rate of synthesis of the two chains are different, but the production levels of IgG are dependent on finally secreted heterotetrameric protein. Therefore, a balanced expression of both chains is essential for high-level production of mature IgG in mammalian cells. To increase IgG expression, numerous studies have been done, including cotransfection of two monocistronic constructs containing H and L chain expression cassettes, fusion of the cells expressing H and L chain respectively (Norderhaug, Johansen et al. 2002), modification of the selection marker (Allison A. Bianchi 2003; Sautter and Enenkel 2005), construction of bicistronic vectors (Jostock, Vanhove et al. 2004) and construction of one vector containing two promoters to drive H and L chain transcription respectively. The commonly used cotransfection of two monocistronic constructs is thought to be an inefficient procedure (Fussenegger, Bailey et al. 1999). The use of one vector with two identical promoters for stable expression bears a certain risk of recombination events. If two different promoters are used in one vector, highly unbalanced expression of both chains may take place. Internal ribosome entry sites (IRES) allow the co-expression of multiple polypeptide chains from the same mRNA. The EMCV IRES element was shown to be least affected by the flanking coding sequences and the mediated translation is accurate using both reticulocyte lysate translation extracts and cultured cells (Borman, Deliat et al. 1994; Borman, Bailly et al. 1995; Borman, Le Mercier et al. 1997; Hennecke, Kwissa et al. 2001). Therefore it seems to be the best choice for driving heterologous gene expression when compared to other picornavirus IRES. However, it was believed that, in most cases, the cistrons downstream of IRES are much less efficiently translated than the cistron following the promoter (Kaufman, Davies et al. 1991; Houdebine and Attal 1999), which limited a broadly use of polycistronic expression vectors for production of oligomeric proteins. In this study, a series of mammalian expression vectors for the production of recombinant IgG antibodies with different expression cassette designs were constructed to assess the influence of the promoter, cistron arrangement as well as the effect of H to L chain ratios on monoclonal antibodies (Mab) production in mammalian cells. The antibody expression levels from different vectors were evaluated in transiently and stably transfected cells. All the vectors constructed could be used to rapidly shuttle phage display derived antibody variable genes.

4.1 The impact of H and L chain on the reporter gene expression

The properly folding and assembly of H and L chain in the endoplasmic reticulum plays important role in the biosynthesis of secretory IgG with full biological activity. It relies on chaperone systems in the ER that monitor and assist in the folding process (Knittler, Dirks et al. 1995; Trombetta and Parodi 2003). To analyze the impact of H or L chain in a bicistronic construct on the expression of the other cistron, a variant of the YFP gene (Venus) was used as reporter to speed up and simplify the evaluation. The Venus variant was shown to be a stable fluorescence marker gene for cell biological use with fast and efficient maturation (Nagai, Ibata et al. 2002).

It shows that the H and L chain did not apparently affect YFP expression from the other cistron in the EMCV IRES containing bicistronic constructs in transiently transfected 293T cells (Fig. 12) . In contrast, in pooled stable CHO-K1 transfectants, the first cistron YFP expression from a setup with L chain as second cistron (pDYIL) gave a two times stronger signal compared to the design with H chain as second cistron (pDYIH) (Fig. 13). One explanation could be that the transcripts from the bicistronic setup pDYIL is shorter than from pDYIH, therefore, the cells transfected with pDYIL have a relative faster recycling of the machinery for transcription and translation than transfected with pDYIH. Therefore pDYIL might be more optimal for reporter gene expression in stably transfected CHO-K1 cells. Another explanation could be that the accumulated H chain is toxic to the cells (Wabl and Steinberg 1982). However, these explanations were not supported by the bicistronic constructs with inverse cistron arrangement in pooled stably transfected CHO-K1 cells. There, at three days after selection, the mean fluorescence intensity yielded from pDLIY was in the same range as from pDHIY. 35 days after selection, the signal from pDLIY is even lower than pDHIY. The toxicity explanation might be excluded since the setup with H chain as first cistron and YFP as second cistron (pDHIY) gave a relative higher H polypeptide intracellular expression level than pDYIH, so that the intracellular accumulation of H chain polypeptide should be higher. However, the YFP signal was not decreased compared to the setup of pDLIY with L chain as first cistron. It might be argued that cap-dependent translation was affected by EMCV IRES mediated downstream cistron expression and that this is related the sequence of the downstream cistron. EMCV mediated H chain translation could exert stronger negative effects to upstream cap-dependent translation than L chian. In contrast to previous reports that the mRNA sequence can negatively affect on IRES mediated translation (Hennecke, Kwissa et al. 2001), the result in this study shows that the EMCV IRES mediated translation was not affected by the mRNA assembly in transiently transfected 293T cells and stably transfected CHO-K1 cells. The setup with H chain as first cistron and L chain as second cistron seems to be more optimal for IgG mammalian expression in a biscistronic construct. If this implication resulted from YFP reporter

gene analysis could be extended to mammalian IgG expression still need further confirmation. The difference between transiently transfected HEK 293T and stably transfected CHO-K1 cells could also due to cellular transacting factors needed for IRES activity. Many transacting factors have been found to be important in modulating IRES activity, however, there was no single protein been identified that is essential for the function of every IRES (Racaniello 2001). It was supposed that certain types of IRES have different requirements for cellular proteins. Different types of cells might provide different transacting factors. These integrative factors might affect YFP reporter gene expression.

The relative translation efficiency of EMCV IRES compared to cap-dependent translation was evaluated in polycistronic vectors with inverse cistron arrangement. In the bicistronic constructs with the YFP reporter gene as first or second cistron, the cap-dependent translated YFP gene expression was about 2-5 times higher than the downstream IRES mediated YFP expression from the same vector with inverse cistron arrangement (Fig. 12, 13). The YFP expression from the 3rd cistron of the tricistronic vector with IgG L and H chian as first and second cistron was as efficient as from the second cistron of a bicistronic vector.

Most IRES mediated bicistronic vectors so far incorporated an IRES downstream of a product and upstream of a selectable marker coding regions or a reporter fluoresence gene (Kaufman, Davies et al. 1991; Davies and Kaufman 1992). It was thought that the downstream gene expression in many cases was shown to be adversely affected by the gene positioned upstream of the IRES. The data in this study suggest that for Mab expression in mammalian cells, the H or the L chain that was positioned at upstream of IRES did not affect much the downstream cistron YFP gene expression in commonly used HEK 293T and CHO-K1 cell lines.

4.2 The impact of different vectors designs on recombinant IgG expression.

To make a commparative analysis of different vector designs on recombinant IgG mammalian expression, a series of monocistronic and bicistronic vectors was constructed (Fig. 14) and evaluated in transiently transfected HEK 293T and CHO-K1 cells. In transient expression, when an equal number of cells were transfected with an equal amount of plasmid DNA, the affection of copy number in single cells on IgG expression levels could be excluded using a large amount of cells so that small probability events should be neglected in the large population. Affection to the results by different transfection efficiencies could be excluded by multiple repeats of the experiment. Therefore, the result from transient transfection should reflect the performance of different vector designs on gene of interest transcription and translation as well as the following polypetide folding and assembly.

In the cotransfection with two monocistronic H chain and L chain expression plasmids (Fig. 15), the EF1-α promoter was shown to be more efficient than the CMV promoter. IgG expression levels were increased when the constructs with EF1-α promoter were used. Enhancement of H chain expression by using the strong EF1-α promoter seems to be more optimal for IgG expression than enhancement of the light chain expression with the strong promoter. The most optimal yield was obtained from cotransfection with two constructs both driven by EF1-α promoter. These may be explained by the fact that the expression of the L chain is more efficient than of the H chain when both H and L chains were driven by an identical promoter. At this situation, the intracellular H chain polypeptide does not saturate the capacity of L chain for IgG folding and assembly. When the EF1-α promoter drove both H and L chain, the total amount of intracellular H and L chain polypeptide is increased. However there may still be excess L chain polypeptide left, being secreted as monomer or homodimer, or being degraded.

The bicistronic expression constructs yielded expression levels in the same range as the cotransfected monocistronic expression constructs (Fig. 15). The setup with L chain as first cistron driven by EF1-α was better by a factor of 2 compared to the design with H chain as first cistron. In the CMV promoter driven bicistronic constructs pDH1 and pDL1, no apparent affection was detected from the different cistron arrangements of H chain and L chain. The translation initiation efficiency of the IRES variant used in these bicistronic constructs is about 3 times lower compared to cap-dependent translation initiation. Therefore, when the cistron arrangement was H-IRES-L, the relative ratio of H and L chain translation efficiencies HC:LC should be around 3:1; when the cistron arrangement was L-IRES-H the relative ratio of H and L chain translation efficiencies HC:LC should be around of 1:3. It was reported that the expression of L chain is about 1,5-2 times more efficient than H chain in transiently transfected cells (Schlatter, Stansfield et al. 2005) and the excess of intracellular L chain is more optimal for IgG mammalian expression (Gonzalez, Andrews et al. 2002; Schlatter, Stansfield et al. 2005). The result in this study shows that bicistronic mammalian expression with an excess of H chain or L chain could give similar IgG yields in transient expression. One possibility could be that the ratio of H and L chain expression from both bicistronic vectors are not in the optimal range. The capacity of L chain driven IgG folding and assembly from transfectants of pDL1 was limited by the expression levels of H chain. In the case of pDH1, the L chain expression levels should be lower than from pDL1. Therefore, the capability of the L chain driven IgG folding and assembly was lowered, however, an excess of H chain peptide in the ER could lead to more efficient usage of L chain. This might cause the cells transfected with the two bicistronic constructs respectively to give IgG yields in the same range, which indicates that H chain might also play an important role on IgG folding and assembly.

One of the most important criteria for successful generation of a recombinant protein from a recombinant cell is to obtain a cell line that maintains stability of production. The stable expression of foreign gene in mammalian cells must be established in the context of the nucleus and is associated with numerous transacting factors. The expression of an integrated gene in either tissue culture or transgenic animals is influenced by the proximity of host heterochromatin, which was conferred to “position effect” of gene expression in mammalian cells (Singh 1994). Stable genes of interest expression must maintain an appropriate status in chromatin in the systems designed for long-term production. These are usually obtained by screening a large amount of clones. In this study, 15 monoclonal stably transfected CHO cell lines were randomly selected, the prevalence of positive clones and antibody expression levels of bicistronic vectors expression are in the same range as monocistronic expression (Fig. 16). However, cotransfection of the two monocistronic in transiently transfected 293T and CHO-K1 cells gave about two times higher expression levels than the bicistronic vectors used (Fig. 15). This indicates that the site of integration plays dominant role on stable recombinant IgG expression. Similar to the results from transient expression, no apparent difference was found between H-IRES-L and L-IRES-H citron arrangements. A previous report showed that for stable expression in CHO cells, expression vectors biased toward low HC:LC polypeptide ratios (<1:2) are likely to generate a greater proportion of cell clones with elevated Mab expression levels in pools of primary transfectants (Schlatter, Stansfield et al. 2005). A high intracellular HC polypeptide concentration could produce ER stress and deleterious effects on cell function which slow down IgG folding and assembly in ER (Lenny and Green 1991; Gonzalez, Andrews et al. 2002). The results in this study might have a possibility that they were derived from clonal variability in transcriptional or translational processing of recombinant genes. Irrespective of the cause, together with the results from transiently transfected HEK 293T and CHO-K1 cells, it was found that bicistronic expression vectors with different cistron arrangement gave the same range of IgG yields. These findings allow the implication that for IgG expression in mammalian cells, when there is an excess of H chain polypeptide, IgG could be produced as efficient as when there is an excess of L chain. It was also reported that the assembly of multimeric protein complexes in the ER is not strictly dependent on the proper folding of individual subunits; rather, assembly can drive the complete folding of protein subunits (Lee, Brewer et al. 1999). Antibody expression and maturation without immunoglobulin L chain is feasible and H chain antibodies that can be secreted independently in some cases (Kirkpatrick, Ganguly et al. 1995; Nguyen, Zou et al. 2003). Therefore, for the design of stable expression vectors with enhanced IgG production, a comparative analysis of the excess of H or L chain should be performed. Further improvement of the expression vectors could help to reveal the underlying mechnism of H and L chain folding and assembly.

The causes of instability of production are varied and the exact molecular mechanisms are unclear. When a new gene element is induced to mediate recombinant protein expression, the affection on the stability should be studied. So far, reports of an affection of IRES elements on stability of recombinant protein production were not found. To test the long-term effect of the IRES element on Mab expression, a stable CHO cell lines were generated and analyzed for expression levels and stability over a period of 300 days (Fig. 17). The stability of IgG expression in CHO cells from a bicistronic vector is in the same range as documentation in a recent review for monocistronic expression (Barnes, Bentley et al. 2003). This indicates that the EMCV IRES is a suitable candidate for stable expression of IgG in CHO cells. It seems that the IRES did not stimulate more repulsion from host cells defense mechanism than other gene elements.

It is known that long term storage, buffer composition and processing conditions can lead to the formation of soluble or insoluble IgG aggregates. The aggregation of IgG could affect the antibody–antigen binding. In analytical gel filtration studies, the recombinant IgG was found to be mainly exists as monomeric. No aggregates were detectable for IgG from transiently transfected HEK293T cells, however, a small fraction of dimeric aggregates were detected for IgG from in stably transfected CHO-K1 cells (Fig. 29). The difference is most likely due to the difference of glycosylation between HEK 293T and CHO-K1 cells; however, a methodological difference during the process of IgG production and the storage of the harvested supernatants cannot be excluded.

4.3 The impact of the relative ratio of H and L chain on IgG transient expression

The ratio of intracellular expression levels of H and L chain polypeptide in the ER is believed to be a crucial factor influencing the rate of folding and assembly (Gonzalez, Andrews et al. 2002). It is important to investigate the optimal ratio of HC:LC in the ER to develope optimal IgG expression vectors. Most studies about the impact of H and L chain ratios on IgG folding and assembly in mammalian cells were performed by cotransfection of two monocistronic H and L chain expression plasmid (Kaloff and Haas 1995; Lee, Brewer et al. 1999; Montano and Morrison 2002; Schlatter, Stansfield et al. 2005). The discovery of internal ribosome entry sites (IRES) provided a new tool for co-expressing multiple polypeptide chains of oligomeric or oligosubunit proteins in polycistronic expression systems. To investigate the optimal ratio of HC:LC in the ER using bicistronic vectors, a series of IRES elements with a continuous range of relative translation efficiencies has to be obtained.

A number of studies have shown the importance of both RNA secondary and tertiary structures in viral cap-independent translation (Jang and Wimmer 1990; Le, Chen et al. 1993; Haller and

Semler 1995; Wang 1995; Hoffman and Palmenberg 1996; Honda, Brown et al. 1996; Witwer, Rauscher et al. 2001). We made a mutational analysis of EMCV IRES, and a series of variants with relative translation efficiencies ranging from 0,03 to 0,6 compared to cap-dependent translation were obtained (Congcong Zhang's master thesis). The IRES variants were used to study the impact of relative the ratio of H to L chain on IgG folding and assembly in bicistronic expression system. It was supposed that the IgG expression levels depend on the H chain expression levels in bicistronic expression vectors with the L chain as first cistron and H chain as second cistron since the IRES mediated cap-independent translation efficiency is lower than the cap-dependent translation efficiency. Promoter strength or local effect was avoided as the L chain and H chain are translated from the same mRNA. It should provide a more accurate method for the evaluation of the optimal ratio of HC:LC than adjustment of the amount of cotransfected H and L chain expression plasmids. The IgG expression levels are presumed to reflect the impact of the H and L chain ratio on IgG folding and maturation. It was found that an optimal IgG production was obtained when an IRES variant with a relative translation efficiency of 50% compared to cap-dependent translation was used (Fig. 27). Therefore, it can be assumed that H chain and L chain translation efficiency was in the range of 1:2. Significantly, the IgG expression levels did not further increase, when a more efficient IRES variant was used. It was concluded that the IgG production reqires intracellular expression levels of HC:LC are in the range of 1:3 to 1:4 as transiently transfected cells synthesize the H chian is 1,5-2 times less efficient than of the L chain (Schlatter, Stansfield et al. 2005). Immunoblot analysis of intracellular H and L chain expression levels showed a similar result (Congcong Zhang's master thesis). It was reported that when the HC: LC polypeptide ratio approaches unity, the Mab assembly time is increased (Gonzalez, Andrews et al. 2002). This could be used to explain that the IgG expression levels were not increased with increasing the relative H chain intracellular expression. In stably transfected CHO cells, a more efficient H chain expression should be needed to get an optimal IgG expression, since the L chain was shown to have a relatively higher intracellular expression in stably transfected cells than in transiently transfected cells (Schlatter, Stansfield et al. 2005). This study has focused on the impact of H chain on IgG production when L chain is in excess. It still needs to be studied what the impact of L chain would be when the H chain is in excess. By using bicistronic vectors with a series of IRES variant with different translation efficiencies, it provides a new method to investigate the IgG production in mammalian cells and to understand the underlying mechanism of IgG folding and assembly.

4.4 The impact of S/MAR elements on IgG expression

It was reported that the use of S/MAR-containing vectors improved transgene expression in a

divers set of cell lines (Agarwal, Austin et al. 1998; Bode, Benham et al. 2000; Kurre, Morris et al. 2003). In this study, the bicistronic expression constructs with one or two S/MAR elements did not increase the IgG expression levels among around 50 randomly selected CHO-K1 clones (Fig. 22). However, the prevalence of positive clones was significantly increased using the construct with two S/MAR elements flanking the expression cassette (Fig. 21). This is partially inconsistent with a previous report where the S/MAR element apparently increased the prevalence of positive clones and the IgG expression levels in 15 randomly selected clones (Zahn-Zabal, Kobr et al. 2001).

The integration copy number of IgG expression cassettes was not compared in this study to see if it was in the same range for the plasmids with or without S/MAR element. This may be one of the reasons that the highest producer resulting from the vector without S/MAR element was much higher compared to all clones obtained with the vectors containing S/MARs. Although, according to recent reports, it seems that the S/MARs do not affect the copy number of integration significantly (Zahn-Zabal, Kobr et al. 2001; Heng, Goetze et al. 2004). The S/MAR enhanced gene expression was directly correlated with the number of transgenes associated with the nuclear matrix but not with the total number of transgenes integrated (Heng, Goetze et al. 2004). Therefore, it may be argued that for the events of single or low copy integration, the expression levels from constructs with S/MAR elements were enhanced, but for the multi-copy integration events, the augmentation induced by S/MARs might be slight if most of integrated expression cassettes are not directly correlated with the S/MAR elements. This might be the case in this study. In addition, an enhancement of expression levels of high producers by S/MAR elements was not reported so far.

To explore an alternative method for IgG expression in mammalian cells and to make a comparative analysis with classic vectors, a supposed S/MAR element mediated episomal vector was constructed. The S/MAR element was placed downstream of a tricistronic expression cassette, encoding an IgG L chain and H chain as well as an YFP reporter protein, upstream of the BGH polyA signal (Fig. 23). The reporter gene expression levels were reduced in both transiently and stably transfected CHO cells compared to the reference vector (Fig. 24, 25 and Tab. 2). This is imaginable since polyadenylation is tightly involved in transcription, splicing and translation etc., the multiple steps process of gene expression (Proudfoot, Furger et al. 2002). When a 2,2kb S/MAR is placed between a transcript and a ploy A signal, at least, the transcription termination could be less efficient and the recycling of the transcription apparatus could be slowed down. Therefore the concentration and the stability of mRNA may be reduced, which leads to lower gene expression levels. Plasmid rescue experiments were not successful

and the H chain constant region could be PCR amplified using genomic DNA as template (Fig. 26). It seems that the tricistronic plasmid with S/AMR was rather integrated than being replicated as an episome, although further experiments need to be done.

In summary, S/MAR elements seem to be willing to help the “poor”, by increasing the prevalence of positive clones but did not give rise to the highest expression levels. When low levels and long-term stable expressions are desired, S/MARs may provide an apparent advantage. The relationship of S/MAR and “elite” producer is not clear although it was recently reported that chicken Lysozyme 5’ MAR is helpful to obtain higher expression levels (Girod, Zahn-Zabal et al. 2005).

4.5 The human anti-MUC1 IgG

Unconjugated antibodies show significant efficacy in the treatment of breast cancer, non-Hodgkin’s lymphoma, and chronic lymphocytic leukemia. The success of antibody drugs like Herceptin and others has stimulated the US NIH to launch an ambitious project to search all alterations of major types of cancer. For a successful use of antibodies for immunotherapy, the choice of target antigen, the immunogenicity of antibodies and the plasma half-life of the antibody have to be considered carefully (White, Weaver et al. 2001). Human MUC1 is a type I transmembrane protein with a mucin-like ectodomain resulting from extensive glycosylation of the variable number tandem repeats (VNTR) (Brayman, Thathiah et al. 2004). Cancer-associated MUC1 is aberrantly overexpressed (10–40 fold) in a variety of cancers. It is incompletely glycosylated and as a result exposes internal sugar units and naked peptide sequences, which are cryptic in the normal mucin molecule. It has been shown to be a useful target for antibodies and cellular immunity, beneficial immune responses can be induced by MUC1 immunization (Gimmi, Morrison et al. 1996; Miles and Taylor-Papadimitriou 1998; von Mensdorff-Pouilly, Verstraeten et al. 2000; Taylor-Papadimitriou, Burchell et al. 2002; Agrawal and Longenecker 2005).

The human anti-MUC1 antibody IIB6 recognizes the tumor associated MUC1 antigen, and was confirmed to specifically bind to the VNTR with the liner epitope “XRPAP”. The MUC1 VNTRs are necessary for an ordered tertiary structure to modulate cell-cell and cell-extracellular matrix (ECM) interactions by steric hindrance of the extracellular domain (Wesseling, van der Valk et al. 1996; Komatsu, Carraway et al. 1997). Except the mechanical function, VNTRs are also important for intercellular adhesion molecule-1 (ICAM-1) recognition (Agrawal, Krantz et al. 1998; Kam, Regimbald et al. 1998), and a specific T cells response directed against an epitope of the human MUC1 VNTRs was found in 1990’s (Spicer, Rowse et al. 1995).

In this study, the phage-derived scFv IIB6 was converted to IgG and produced in mammalian cells. The scFv and IgG specifically bind to breast cancer derived T47D cells. The IgG showed a better binding signal in western blot on cell lysates and in FACS analysis of living T47D cells when an equal molar amount of IgG and scFv antibodies were used (Fig. 31, 32). In the western blot on the cell lysates both, scFv and IgG, showed a smear signal (Fig. 31). The VNT repeats of 20 residues (PDTRPAPGSTAPPAHGVTSA) contain five threonines and serines that are all modified with mucin type O-linked glycans (Hanisch, Uhlenbruck et al. 1989; Hull, Bright et al. 1989; Lloyd, Burchell et al. 1996) and this domain is flanked by imperfect repeats with fewer glycosylation sites. In addition to O-linked glycosylation, MUC1 contains five consensus sites for N-linked glycan addition in a nonrepetitive sequence adjacent to the single transmembrane domain. Therefore, the western blot signal of the aberrant glycosylated tumor associated MUC1 from cancer cells appears to be a characteristic smear. The binding signal of the IIB6 human anti-MUC1 antibody indicates that the antibody binding capacity to the MUC1 antigen was not affected by the glycosylation. It was found that the aberrant intracellular localization of MUC1 in tumor cells correlates with an aggressive tumor and a poor prognosis for the patient. Usually, the highly extended ectodomain inhibit MUC1 internalization (Kinlough, Poland et al. 2004). The aberrant glycosylation could result in an altered endocytic trafficking and lead to subcellular redistribution of MUC1 in tumor cells (Altschuler, Kinlough et al. 2000). This shows that the IIB6 antibody could be a promising candidate for immunotherapy of MUC1 antigen positive cancers. It could be used to prevent the metastasis of tumor cells and to develop targeted immunotoxins.

Surprisingly, the relative MUC1 peptide antigen binding affinity of the IgG was found to be about 20-fold less than that of the IIB6 scFv (Fig. 30). The affection of the IgG by aggregation was excluded after gel filtration analysis, which identified the IgG to be monomer (Fig. 29). The loss of binding affinity could be caused by post-translational modifications of the mammalian expression system, such as glycosylation, which might change the antigen binding properties of the phage display derived scFv. The scFv, which was selected from on *E.Coli* based screening system, might be folded differently from the IgG chains that are folded in the ER of mammalian cells with the cooperation of chaperones. Further, an affection of the linker connecting the V-domains of the scFv on the conformation of the binding site cannot be excluded. To investigate the phenomenon, analysis of mammalian expressed scFv formats of IIB6 would be helpful. In contrast to the peptide recognition, binding of the IgG to native MUC1 on T47D cells was as efficient as or more efficient than binding of the scFv. Probably, the surface of T47D cells has a high density of MUC1 antigen leading to avidity effects, whereas in the peptide ELISA, the coating of the peptide antigen onto the microtitrer plate could be not efficient leading to a low antigen density. Finally, the density of the coated antigen could be too low for bivalent binding.

There are different views toward the effect of the antigen binding affinity on the antitumor efficacy of mAb therapeutics. The use of mAbs with higher relative affinity leads to a higher percentage of of mAb bound to tumor and it was thought to be a distinct therapeutic advantage (Schlom, Eggensperger et al. 1992). The need for a high-affinity antibody is dependent on the density of the target antigen. High-affinity antibodies bind effectively even with a single antigen-antibody interaction, irrespective of the antigen density. In contrast, low-affinity antibodies require the avidity conferred by di- or multi-valent binding for effective attachment, which can only occur if antigen density is above a certain threshold (Zuckier, Berkowitz et al. 2000).

Studies have shown that adjuvant therapy for breast cancer may increase the chance of long-term survival by preventing a recurrence (Hortobagyi 2000). Adjuvant therapy has the goal to kill any cancer cells that may have spread, even if the spread cannot be detected by radiologic or laboratory tests. The use of an appropriate anti-MUC1 antibody might block adhesion between tumor cells and a possible new growing site and thus reduce the metastatic spread of tumor cells. High affinity of the anti-MUC1 IgG is desired in order to arrest the tumor cells in circulation and stop metastases. The human IgG IIB6 could be an alternative therapeutics for breast cancer adjuvant therapy and a potent tool to study the role of MUC1 on breast cancer tumor cells metastasis.

4.6 Outlook

Recombinant protein production in mammalian cells is a complex multistep process including gene transfer, integration, replication, transcription, translation, protein trafficking, polypeptide folding and assembly, secretion, producer screening, host cell growth and subsequent feeding (Fig. 34). Each step plays a crucial role for the final success of protein production. To obtain high-level protein production, an optimal process with a compromise of each step has to be established. The volumetric productivity of mammalian cells cultivated in bioreactors increased significantly over the past 20 years through the improvements in media composition and process control (Wurm 2004). There still is potential to increase the productivity of cells by controlling cell growth (Kaufmann and Fussenegger 2003). Host cell engineering will continue to be the most promising strategy for improvement of recombinant protein production.

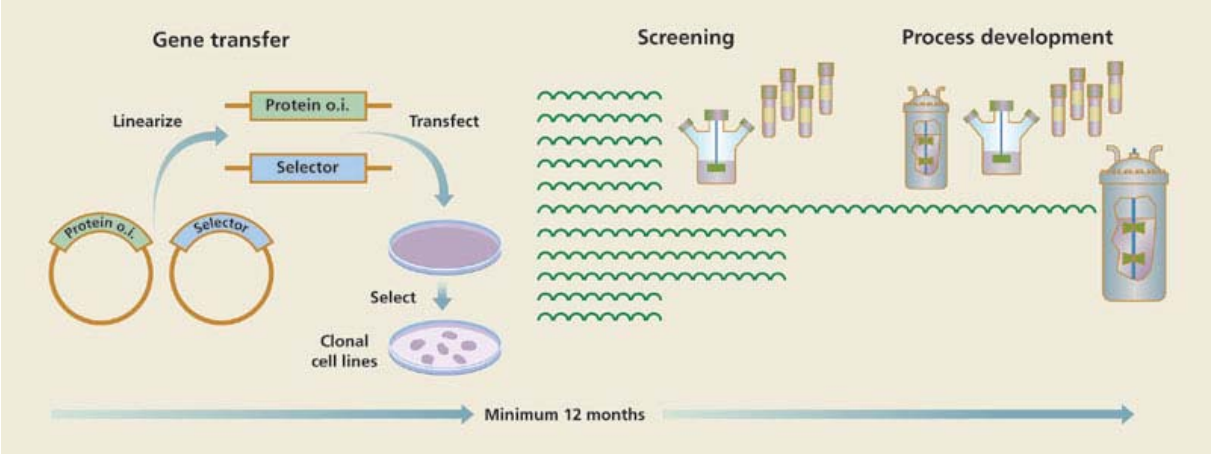

Figure 34 Cell line generation and development for cell culture processes for the generation of recombinant proteins of interest. The wavy lines indicate subcultivations of individual cell lines that are in a screening program to obtain the final producer. Vials indicate banks of cells frozen in liquid nitrogen. Spinner flasks represent scale-down systems for process optimization, and bioreactors represent large-scale production processes. Reproduced from literature (Wurm 2004)

There is little doubt that obtaining a cell line that maintains stability of production is one of the most important criteria for successful generation of a therapeutic protein from a mammalian cell. Stable cell lines were usually obtained by the integration of the gene of interest into the genome of a host cell. The most common method for achieving integration of recombinant genes into a host cell genome is by random insertion into chromosomes. In theory, the integrated genes would be passed onto daughter progeny and keep stable. However, instability of protein production is still a substantial problem for a selected stable integrated cell line. One of the causes of instability of production is the loss of gene of interest from the recombinant host cells' genome, particularly for the CHO expression system (Pallavicini, DeTeresa et al. 1990; Kim SJ, Kim NS et al. 1998; Hammill L, Welles J et al. 2000.). The other causes maybe due to the appearance of nonproducting populations of cells, which often have a growth advantage over production populations, and hence lead to an overall decrease in production (Chuck and Palsson 1992; Bae, Hong et al. 1995). The appearance of nonproducing populations of cells can arise due to loss of gene copies and may also occur as a consequence of problems with transcription and/or subsequent steps of gene expression (Barnes, Bentley et al. 2003). It is generally accepted that the site of integration into the chromosome has dominant effect on the recombinant gene expression in eukaryotic cells (Wilson, Bellen et al. 1990). The position effect can be caused by gene rearrangement or incorporation of recombinant genes into regions with nearby endogenous promoters or enhancers, or areas of heterochromatin (Barnes, Bentley et al. 2003). Modification of the host cells may provide opportunities to increase the stability as well as the expression levels for recombinant protein production. Various DNA elements, including insulators, LCR,

S/MAR and ubiquitous chromatin opening elements (UCOEs) etc, have been discovered, which can modulate the position effect and hence may be important in controlling expression levels and stability of protein production. They mostly function through remodeling the local chromosome structure by enabling the binding of proteins and thus either enhance or inhibit the effect of the surrounding chromatin on specific genes (Agarwal, Austin et al. 1998; Bode, Benham et al. 2000; Kurre, Morris et al. 2003). Using these elements may pave a way to obtain a stable cell line with enhanced stability and high recombinant gene expression levels. However, the underlying mechanisms of the function of these elements are far from clear. More work need to be done to understand and make use of these elements for recombinant gene expression in mammalian cells. A detailed studying of a high producer may help to understand the requirements of high-level stable expression of recombinant genes and the interaction of foreign genes with surrounding genomic regions. With the accelerated advancing in technology, such as whole genome sequencing, genome-scale high-throughput screening, studying the interaction of biological macromolecules in real time and in living cells, new scientific breakthroughs are possible. As we move to the "postgenomic" era, more and more gene products and the way in which they are regulated become well understood. Host cells may be modified as something like a assemble line for protein of interest production. It might include depressing position effect, reducing silencing modification, and enhancement of the recycling of transcription, translation machinery, smoothing the way for polypeptide folding and assembly.

Further promising methods are to improve the gene transfer efficiency or optimize the recombinant gene replication status. The commonly used random integration into chromosome procedure is very inefficient (Gorman and Bullock 2000) and the site of integration, the number of copies integrated, and the level of expression cannot be predicted. The use of episomal vectors might be an alternative method for protein production in eukaryotic cells (Baiker, Maercker et al. 2000; Bode, Fetzer et al. 2001). However, at present the mechanism of nonviral episomal vectors replication is not clear and still far from practical use for recombinant protein production (Jenke, Fetzer et al. 2002; Antequera 2004; Jenke, Stehle et al. 2004; Jackson 2005). One of the most practical methods is the targeted integration of the transgenes into the sites that are thought to be relevant for high expression (Bode, Schlake et al. 2000; Gorman and Bullock 2000). Among these techniques, the recombinase-mediated cassette exchange (RMCE) is a very promising method, which enables a double-reciprocal crossover reaction by mutation of target sequences (Baer and Bode 2001). It is a potent tool for scientific research and a method containing huge commercial value. So far, successful RMCE was mostly reported in ES cell. There are few confirmed reports for the industrial production commonly used CHO, BHK or NSO cells.

Nevertheless, even when the RMCE efficiency is improved for practical use more detailed information is needed to be collected between the successful RMCE and real production.

The H and L chain folding and assembly is a crucial step for IgG production in mammalian cells. It is affected by the ratio of HC:LC intracellular expression levels. Therefore, it is crucial to investigate the optimal ratio of HC:LC for IgG production. Although there are some reports on this topic (Kaloff and Haas 1995; Gonzalez, Andrews et al. 2002; Schlatter, Stansfield et al. 2005), it would be a helpful guideline for IgG production, if a delicate model of HC:LC folding and assembly is established.

5 Materials and methods

5.1 Materials

5.1.1 E.coli strain

XL1-Blue MRF´	Δ(*mcrA*)*183* Δ(*mcrCB-hsdSMR-mrr*)*173* *endA1* *supE44* *thi-1* *recA1* *gyrA96* *relA1* *lac* [F´ *proAB* *lacIqZ*Δ*M15* Tn*10* (Tetr)].	Stratagene, La Jolla, USA
DH5α^{TM}	F$^-$ ϕ80d*lacZ*ΔM15 Δ(*lac*ZYA-*arg*F) U169 *rec*A1 *end*A1 *hsd*R17(r_k^-, m_k^+) *pho*A *sup*E44 λ$^-$ *thi*-1 *gyr*A96 *rel*A1	Invitrogen, La Jolla, USA
K12 GM2163	F$^-$ *dam-13::*Tn *9* *dcm-6* *hsdR2* *leuB6* *his-4* *thi-1* *ara-14* *lacY1* *galK2* *galT22* *xyl-5* *mtl-1* *rpsL136* *tonA31* *tsx-78* *supE44* McrA$^-$ McrB$^-$	NEB, UK

5.1.2 Eukaryotic cells

Cells	Culture medium	Source
CHO-K1	Ham's F12/DMEM + 2mM Glutamine + 10% Foetal Calf Serum (FCS)	ECACC No. 85051005
293T	DMEM + 2 mM L-glutamine +1.5 g/L sodium bicarbonate and 4.5 g/L glucose + 10%FCS	ATCC No: CRL-11268
Jurkat E6.1	RPMI 1640 + 2mM Glutamine + 10% FCS	ECACC No. 88042803
T47D	DMEM + 2mM Glutamine + 10% FCS	ECACC No. 85102201

5.1.3 Chemicals, solvents and enzymes

The commonly used chemicals and solvents were from Fluka (steoheim, Germany), Merck (Darmstadt, Germany), or Carl Roth (Karlsruhe Germany). Enzymes were from NEB, MB

fermantas, Promaga. Monoclonal antibodies, enzyme conjugated antibodies and fluorescence conjugated antibodies were from Sigma (Steinheim, Germany).

5.1.4 Materials for electrophoresis

1 kb and 100 bp DNA ladder	Fermentas, Stuttgart
Ethidium bromide	Roche Diagnostic, Penzberg
Precision plus protein standard, dual color	Bio-Rad, Hercules, CA,USA
Precision plus protein standard, unstained	Bio-Rad, Hercules, CA,USA
Acrylamide solution 30 %	Roth, Karlsruhe
APS	Sigma, Deisenhofen
BCIP	Roth, Karlsruhe
NBT	Roth, Karlsruhe
TEMED	Sigma, Deisenhofen

5.1.5 Materials for cell culture and storage

RPMI 1640	PAA LabGmbH, Parsing Austria
DMEM	PAA LabGmbH, Parsing Austria
DMEM/F12	PAA LabGmbH, Parsing Austria
Trypsin/EDTA	PAA LabGmbH, Parsing Austria
Foetal bovine serum (FCS)	PAA LabGmbH, Parsing Austria
Bacto tryptone	BD, Sparks, USA
Bacto yeast extract	BD, Sparks, USA
DMSO	Roth, Karlsruhe

5.1.6 Equipments

Centrifuge	Biofuge pico Centrifuge 5415 D Centrifuge 5810R Multi fuge 3 S-R Sorvall RC 5 (SS34, GS-3 and SLA3000)	Heraeus-Christ, Eppendorf Eppendorf Heraeus Sorvall
Electroporation apparatus	Gene Pulser II, Pulse Controller	BioRad, Hercules, CA, USA
UV/Visible spectrophotometer	Libra S11 Ultrospec 3100 *pro*	Biochrom, U.K. Amersham Pharmacia

Electrophoresis apparatus	Electrophoresis power supply EPS 601/301	Amersham, Uppsala, Sweden
	Mini protean 3 cell	BioRad, Hercules, CA, USA
	Semi-dry transfer cell	BioRad, Hercules, CA, USA
	Gel dryer model 543	BioRad, Hercules, CA, USA
Protein purification apparatus	Dialysis Tubing	Visking Servapor and Membra-cel
	Äkta prime	Amersham, Uppsala, Sweden
	1mL Protein A column	Amersham, Uppsala, Sweden
	1mL HisTrap HP	Amersham, Uppsala, Sweden
	Superdex 200 HR 10/30	Amersham, Uppsala, Sweden
Mixer	Thermomixer compact	Eppendorf
	Vortex genie 2	Scientific industries, Bohemia N.Y.
	Platform rocker Str6	Bibby stnart, UK
Filter apparatus	Millipore ultrafiltration membranes	Amicon biosepratıons, Molsheim, France
	Cellulose acetate filter: 0,2 µm, 0,45 µm	Sartorius AG, Goettingen
	Whatman filterpaper	Whatman, England
	Arium 611	Sartorius AG, Goettingen
	Reusable bottle top fliter unit	Nalge company
Clean bench	Lamiair HLB 2472	Heraeus
Shaker	Certomat BS-1	B.Braun Biotech international
Squencer	A&B Applied Biosystems, ABI prism 310 collection.	Perkin-Elmer, Applera
FACS	FACScan	Becton Dickinson, San Jose, USA
	FACSCalibur	Becton Dickinson, San Jose, USA
PCR machine	PTC200 peltier thermoral cycler	MJ Research
Freezer	4°C, -20°C and –80°C	Lieberherr, Hera Freeze

5.1.7 Kits for DNA purification and transfection

GFX PCR DNA and gel band purification kit	Amersham, Uppsala, Sweden
GFX micro plasmid prep kit	Amersham, Uppsala, Sweden
Plasmid DNA purification kit	Macherey-Nagel, Germany
Genelute HP plasmid midiprep kit	Sigma-Aldrich, Steinheim
Lipofectamine 2000	Invitrogen, Karlsruhe
HEKFectin	Bio-Rad, Hercules, CA
TransFectin Lipid reagent	Bio-Rad, Hercules, CA

5.1.8 Buffer and solutions

0,5M EDTA (Disodium Ethylene Diamine Tetra-Actate, pH8,0)	Add 181,6 g Na2EDTA.2H2O to 800 mL ddH2O, adjust to pH8,0, make up to 1 litre with ddH2O, sterilized by autoclaving. (Note: EDTA is only soluable in basic pH)
Phosphate Buffered Saline (PBS) pH7,2-7,4	137 mM NaCl, 2,7 mM KCl, 10 mM Na2PO4, 2 mM KH2PO4.
50x TAE buffer	2 M Tris base, 1 M acetate, 100 mM EDTA.
10x non-denaturing Gel running buffer	Dissolve 30,3 g of Tris-base, 144,2 g of glycine in 800 mL ddH2O, adjust the pH to 8,3, make up to 1 litre with ddH2O.
10 x Laemmli Running buffer	Dissolve 30,3 g of Tris-base, 144,2 g of glycine, 10 g of SDS in 800 mL ddH2O, after all the chemicals have dissolved, make up to 1 litre with ddH2O.
5x SDS-PAGE (Hart and Laemmli) sample buffer	0,312 M Tris-HCl pH6,8; 10%SDS; 25% β-mercaptoethnol; 0,05% bromophenol blue.
Staining proteins on Acrylamide (Coomassie Brilliant Blue (CBB))	Dissolve 2,5 g Coomassie Brilliant Blue R250 in 450 mL ddH2O, add 450 mL methanol and 100 mL glacial acid, flirter the solution a Whatman #1 filter paper to remove particulate matter.
Destaining buffer for CBB stained Gels	To 1-liter glass flask, add 250 mL methnol and 70 mL glacial acetic acid, adjust the volume to 1 liter with H2O. Store at room temperature.
BCIP	Dissolve 0,5 g of 5-brmo-4-chloro-3-indolyl phosphate disodium salt in 10 mL of 100% dimethyfomamide, store at 4°C.
Nitroblue Tetrazolium (NBT)	Dissolve 0,5 g of nitroblue tetrazolium chloride in 10 mL 70% dimethylformamide
NBT/BCIP reaction buffer	Add 66 µL of NBT stock and 33 µL of BCIP stock to 10mL alkaline phosphatase buffer. Substrate should be used within 30 min.

Ampicillin (Amp) 100mg/mL	Dissolve 1 g of sodium ampicillin (sodium salt. m.w.=371,40) in sufficient H2O to make a final volume of 10 mL. Dispense to 1 mL aliquots, store at –20°C. Working concentration: 100 µg/mL
Kanamycin (Km) (10-50mg/mL)	Dissolve 100-500 mg kanamycin monosulfate (m.w.=582,60) in sufficient H2O to make a final volume of 10 mL. Divide into 1 mL aliquots and store at –20°C. Working concentration:10-50 µg/mL

5.1.9 Protease inhibitors

Inhibitor	Protease target	Working concentration	Stock solution
Aprotinin	Serine protease	5 µg/mL	1 mg/mL in PBS
Leupeptin	Serine and thiol protease	5 µg/mL	1 mg/mL in H2O
Pepstatin	Acid protease	5 µg/mL	1 mg/mL in methanol
EDTA	metalloprotease	0,5-2 mM	0,5 M in H2O pH8,0
PMSF	Serine protease	1 mM	100 mM in isopropanol

5.1.10 Oligo-nucleotide primers

Jl215-PstI-f1	5’-CATGGCGCAAGTTCAGCTGCAG-3’
Jl215-NheI-r1	5’-GTCCGCTAGCTGAGGATACGGTGACCGTGG-3’
Jl215-SacI-f1	5’-TATCGAGCTCACCCAATCTCCACTCTCC-3’
Jl215-HindIII-r1	5’-GTGCAAGCTTGGTGCCAGCACCGAACGTTAACGG-3’
Jl215-XhoI-f1	5’-GCTCCCTCGAGCAGTCTGGGGCTGAACTGGTGAGG-3’
Jl-bstx1-215kf1	5’-GCATCCACAACCATGGAAACCCCAGCGC-3’
Jl-Xba1-215kr1	5’-AGCTTCTAGAACTAACACTCTC-3’
Jl-Not1-215kr1	5’-ATGGTCTAGAGCGGCCGCTAGAACTAACACTCTCC-3’
Jl-MluI-215kr2	5’-ATGGTCTAGAGGATCCACGCGTCTAACACTCTCCCCTG-3’
Jl-Xba1-hcr2	5’-AGCTTCTAGACTATTTACCCGGGGACAGG-3’
Jlhc-XhoI-f1	5’-CGACCTCGAGCGTCTCCTCAGCTAGC-3’
Jlhc-XbaI-r1	5’-GGCCTCTAGAGGATCCTCATTTACCCGGGGACAGGGAGAGG CTCTTCTGCGTGTAGTGGTTGTGCAGAGC-3’
IIB6-BssH2-f1	5’-CTTGGCGCGCACTCCCAGATGCAGCTGGTACAGTCTGG-3’
IIB6-Nhe1-r1	5’-GTCTAGCTAGCTGAGGCGACGGTGACCAGGG-3’
IIB6-SacI-f1	5’-TATCGAGCTCACGCAGCCACCCTCGGTGTC-3’
IIB6-HindIII-r1	5’-TCCCAAGCTTGGTCCCTCCGCCGAACACCC-3’
LjIIB6-BssH2-f1 (vλ)	5’-GGACAGGCGCGCACTCCCAGTCTGTGCTGACGCAGCCACC-3’

LjIIB6-Xba-r1	5'-CGAGCTTCTAGAACTATGAACATTCTG-3'
Jl-irebamI-f1	5'-TTCCGGATCCGCCCCTCTCCCTCCCCCC-3'
Jl-irexbaI-r1	5'-CCTGTCTAGATCACCATGGTTGTGGCCATATTATCATCGTG-3'
Jl-SVori-SalI-f1	5'-CTGGGTCGACAATTTAACGCGAATTAATTCTGTG-3'
Jl-SVori-EcoR1-r1	5'-CAGCGAATTCAAGGATCTAGGTGAAGATCC-3'
Jl-CMV-Xho1-f1	5'-GTCGCTCGAGAATTCACATTGATTATTGAGTAG-3'
Jl-EF1a-Xho1-f1	5'-GTCGCTCGAGAATTCAAGCTTCGTGAGGCTCC-3'
Jl-polyA-Not1-r1	5'-GGACCGCGGCCGCTCCGCCTCAGAAGCCATAGAGC-3'
Jl-SARw-r20	5'-ACTATTTATAAGGTCACGAC-3'
IIB6-seq-L	5'-TCTGTTCCCGCCCTCCTCTG-3'
Ires-rev-seq1	5'-CTTCGGCCAGTAACGTTAGGG-3'
Jlseq-EF215k1	5'-CTTCCATTTCAGGTGTCGTG-3'
Jlseq-EF215k2	5'-GGATCTGGAACCGATTTCAC-3'
Jlseq-EF215k3	5'-CAGGACAGCAAGGACAGCAC-3'
Jlseq-Hcmv1	5'-CTAACTAGAGAACCCACTGC-3'
Jlseq-Hcmv2	5'-CTCCAAGAGCACCTCTGGGG-3'
Jlseq-Hcmv3	5'-CGTCAGTCTTCCTCTTCCCC-3'
Jlseq-Hcmv4	5'-CCATCTCCAAAGCCAAAGGG-3'
Jl-ireseq1	5'-GGCTCTGCACAACCACTACA-3'
Jl-ireseq2	5'-TAGCGACCCTTTGCAGGCAG-3'

5.1.11 Plasmids

pCMV/myc/ER	Invitrogen, La Jolla, CA
pEF/myc/cyto	Invitrogen, La Jolla, CA
pcDNA4/TO	Invitrogen, La Jolla, CA
pIRES-GFP	Clontech, Palo Alto, CA
pCS-venus	(Nagai, Ibata et al. 2002)
pAc-K-CH3	(Liang, Dübel et al. 2001)
pEPI-1	(Piechaczek, Fetzer et al. 1999)
pOPE-101-215	Dübel et al., 1993
pOPE-101-IIB6	In lab (Toleikis dessertation)

5.2 Methods

5.2.1 Sterilization

All experiment water, liquid solution, medium were autoclaved according to standard procedure

(Sambrook et al., 2001). Heat-sensitive solutions such as antibiotics, glucose were filter-sterilized with 0.20µm filter.

Glassware was sterilized for 3 h at 180°C.

5.2.2 Cell culture and storage

5.2.2.1 E. *coli* culture and storage

Transformed E. *coli* was cultivated overnight on LB plates with appropriate antibiotics at 37°C. Liquid culture was inoculated from a single colony and incubated in LB medium containing appropriate antibiotics at 37°C with 250 rpm overnight shaking. Freshly grown bacterial suspension was adjusted to 15-20% final concentration of sterile glycerol and stored at -80°C.

5.2.2.2 Mammalian cell culture and storage

Mammalian cells were seeded in tissue culture plate in appropriate medium. The cells were incubated at 37°C in a thermostatically-controlled incubator in an atmosphere containing 5 %CO2 and at 96 % humidity. To passage adherent cell lines, the cells were washed with PBS and incubated with trypsine-EDTA until the cells detached from the bottom of the cell culture plate. The cells were pelleted by centrifugation at 1200 rpm for 5 min. The supernatant was discarded and the cells were resuspended in culture medium and seeded at the appropriate density. For long-term storage, the cell lines were harvested as described above, resuspended in 10 % DMSO in relevant culture medium supplement with 20% heat-inactivated FBS for cryo-preservation in 2 mL polypropylene cryo-tubes. To allow a slow and gradual freezing, the tubes were stored at -80°C in a container for 1-2 days, then, the tubes were transferred to liquid nitrogen.

5.2.3 DNA cloning

5.2.3.1 Plasmid DNA preparation from E. coli cells

For minprep plasmid DNA, an alkaline-lysis method (Sambrook & Russel, 2001) or GFX micro prep kit were used according to standard procedure or manufacture instructions. Midipreps plasmid DNA was prepared using the Sigma high performance Midi Plasmid Purification Kit. Plasmid DNA concentration was determined by absorption measurement with 260/280nm in a spectrophotometer in a quartz cuvette or compared the intensity of ethidium bromide stained linerized DNA bands on a 1% agarose gel with the intensity of defined standards.

5.2.3.2 DNA electrophoresis

An agarose gel of 0.8-1.2% was prepared by boiling agarose in 1 x TAE buffer and pouring it into

gel-making models till it cooled down to around 60-70°C. Ethidium bromide was directly added into the gel with final concentration 100 ng/mL. DNA samples were mixed with 6 x DNA loading buffer. DNA samples together with a DNA marker (1 Kb or 100 bp) were separated at 10 V/cm for 30-60 min depending on the DNA molecular weight and the length of the gel in 1 x TAE buffer. The DNA bands separated in the gel were visualizd by 312 nm UV light and pictures were taken with a Gel Jet Imager (INTAS, Goettingen) connected to a video printer.

5.2.3.3 Digestion of DNA by restriction endonucleases

DNA samples (200 ng – 1 µg) were digested by restriction endonucleases using corresponding reaction buffers. Enzyme, DNA, buffer and reaction time varied depending on the specific requirements (generally, 37°C from 1 h to overnight). In the case where it was necessary to treat the same DNA sample with different enzymes, the digestion was carried out first in a buffer with low salt concentration or the buffer compatible to different enzymes.

5.2.3.4 PCR

Polymerase chain reaction (PCR) was accomplished with Taq polymerase (Combizyme), according to manufacturer protocols. Colony PCR was accomplished with RedTaq polymerase (Sigma, steinheim). The oligonucleotide primers were synthesized by MWG Biotech (Ebersberg) or Biomers.net (Ulm, Germany). 0,5 pmol oligonucleotide primer were used in a reaction volume of 50 µL. The PCR reaction was performed at PTC-200 DNA Engine Thermal Cycler (MJ Research). The PCR reaction complex was firstly predenatured at 94°C for 1 min, then followed by the cycle reaction, the reaction condition were as follow: denature for 0,5-1 min, annealing temperature 55-60°C for 0,5-1 min, extension 72°C for 1 min / kb, 30 cycles.

5.2.3.5 DNA isolation from agarose gels

Restricted DNA fragments were separated on 0.8% - 1% argrose gel by electrophoresis. The appropriate DNA bands were cut out under UV light. The DNA purification was carried out using GFX PCR DNA and Gel purification kit according to the supplier’s manual instructions.

5.2.3.6 Precipitation of DNA

2.5 volumes of ethanol and 1/10 volume of 3.0 M NaAc (pH 5.5) were added into the DNA solution, mixed 2-3 times, kept at –20°C for 30 min and centrifuged for 10 min at 12000 rpm. The supernatant was gently discarded and the pellet was washed with 70% ethanol, followed by centrifugation at 12000 rpm for 5 min. The DNA pellet was air dried and dissolved in sterile ddH2O.

5.2.3.7 Dephosphorylation of digested DNA

After the digestion with corresponding restriction enzymes, the vector fragment was dephosphorylated using calf intestine alkaline phosphatase (CIAP) to remove the phosphate group at the 5'-end, which prevent religation of the vector. The reaction mixture was incubated around 30-45 min at 37ºC. Dephosphorylation was only performed when the vector plasmid was digest by only one restriction enzyme or by two enzymes producing compatible end. The dephosphorylation process was omitted, if the two restriction enzymes produced incompatible termini.

5.2.3.8 DNA ligation

DNA ligation was carried out using T4 DNA ligase (Promega) at 16ºC overnight or room temperature for 2-3 hours, in a volume of 10 µL. The concentration of vector and insert DNA was measured on the basis of DNA marker. Around 50ng vector was used in one ligation reaction. The ratio of vector to insert was 1:3 to 1:5 for sticky and blunt end ligation.

5.2.3.9 Transformation of E. coli

Standard procedures of heat shock and electroporation transformation were used (Sambrook et al. 2001). Electroporation was performed with Gene-Pulser(Bio-Rad) using electrocompetent XL1-Blue cells (Stratagene, La Jolla, USA). Heat shock transformation was performed using DH5α (Invitrogen, Leek, Nethelands) chemical competent cells, prepared according to standard procedure (Sambrook et al, 2001).

5.2.4 Plasmid construction

All plasmids were constructed using standard E.coli cloning methods as described (Sambrook et al. 2001) (Fig 10 A, B). pSL1, a monocistronic expression vector for IgG κ chain was constructed based on the vector backbone of pCMV/myc/ER (Invitrogen, La Jolla, CA) through the following modifications. First, a human vκ3 leader sequence and a κ constant region were PCR amplified from pAc-k-CH3 (Liang, Dübel et al. 2001) by using synthetic oligonucleotides, introducing a NcoI restriction site at the 5' terminus, BamHI and XbaI restriction sites at the 3' terminus of the constant region after the stop codon. The NcoI/XbaI fragment with the vκ3 leader sequence and the human κ constant region were then inserted into the NcoI and XbaI sites of pCMV/myc/ER. For the construction of the IgG1 heavy chain expression vector pSH1, a human IgG1 constant region was PCR amplified from pAc-k-CH3 and cloned into pCMV/myc/ER via XhoI and XbaI with a BamHI site introduced at the 3' terminus of the constant region after the stop codon. The variable region genes of a mouse anti-Drosophila RNA polymerase II scFv („215") (Liu, Song et al. 1999) were cloned between BssHII/NheI (VH) and SacI/HindIII (VL) of monocistronic IgG1

expression vectors. The CMV promoter of pSL1 and pSH1 was replaced by the EF1-α promoter, to get the monocistronic expression vectors pSL2 and pSH2. The EF1-α promoter was released as an EcoRI and NcoI fragment from pEF/myc/cyto (Invitrogen, La Jolla, CA).

For the construction of the yellow fluresence protein gene (YFP) expression plasmid pCMV-YFP, a modified YFP (Venus) was released from pCS-venus (Nagai, Ibata et al. 2002) via NcoI and XbaI sites and was cloned into pCMV/myc/ER between the NcoI and XbaI sites. For the construction of the bicistronic expression vectors pDH and pDL, the EMCV-IRES element (nt 260 to nt 848) fragment was PCR amplified from pIRES-GFP (ClonTech, Palo Alto, CA). The BamHI/XbaI fragment of IRES was inserted into pSL and pSH between BamHI and XbaI sites to get pSL-IRES and pSH-IRES plasmids. The two plasmids were digested with NcoI resulting in LC-IRES and HC-IRES fragments. These fragments were ligated to NcoI digested pSH1, pSL1, pSH2, pSL2 and pCMV-YFP respectively, to get bicistronic IgG expression plasmids pDH1, pDL1, pDH2 and pDL2 with HC or LC as first cistron, and CMV or EF1-α as promoter. The bicistronic expression plasmids pDHIY and pDLIY with human/mouse IgG light chian or heavy chain as first cistron and YFP as second cistron were obtained accordingly. The bicistronic expression plasmids with YFP as first cistron were constructed by PCR amplifying IRES-light chain and IRES-heavy chain fragments from pDH1 and pDL1, and insertion into pCMV-YFP via XhoI and XbaI to obtain the bicistronic expression plasmids pDYIH and pDYIL. The tricistronic expression plasmid pTLIY was constructed by using BamHI to prepare the IRES-heavy chain fragment from pDL1, which was inserted into pDLIY at the BamHI site. All the constructions were confirmed by sequencing, the IRES fragment used in this study was a variant with one C deletion between base 270 and 280 and a A345G mutation.

5.2.5 Genomic DNA preparation from mammalian cells

Cells from a confluent 24-, 12- or a 6- well plate were harvested and washed with PBS, 500µl “Modified Bradleys” solution (10 mM Tris/HCl, pH 7.5, 2 mM EDTA, 10 mM NaCl, 0.5 % SDS, 50-100µg/mL Proteinase K) was added to each well. After a short incubation, the viscous solution was transferred in a 1,5 mL Eppendorf tube and incubated at 55°C overnight. The solution was cooled at R.T., slowly 1 mL of 100% ethanol 75 mM NaAc was added and the solution was incubated for 2 hours at R.T. to precipitate the DNA. The DNA was pelleted by centrifugation at R.T. at 5000 rpm for 5 min and the supernatant was discarded carefully. Subsequently the pellet was washed with 0.5 mL 70% ethanol and this solution was kept at R.T. for 30 min followed by centrifugation. Washing was repeated once and the pellet was air-dried. The DNA was resolved in 20-30 µL ddH2O.

5.2.6 Protein samples analysis

5.2.6.1 SDS-Polyacrylamide gel electrophoresis (SDS-PAGE)

The SDS-PAGE gel consisted of a separating gel topped by a stacking gel. The separating gel was casted between the glass plates using Bio-Rad Mini Protean II equipment and overlayed by isopropanol. After gel polymerisation, the isopropnol was removed and the gel chamber was filled with stacking gel and a comb was inserted. The protein samples were diluted to appropriate concentrations, mixed with 5 x Laemmli sample buffer (for non-reducing gel, using sample buffer without beta-mercaptoethanol) heated at 95ºC for 5-10 min and the samples were loaded onto the gel. Run gels under constant current, 20 mA per mini Gel, at room temperature in 1xSDS-PAGE running buffer.

Table 3 Components for preparation of SDS-PAGE

	Stacking Gels	Separating Gels		
	4%	6,%	10%	12%
Distilled H_2O	1,0 mL	2.1 mL	1,6 mL	1,3 mL
1.5 M Tris-HCl, pH 8.8		1 mL	1 mL	1 mL
0.5 M Tris-HCl, pH 6.8	0,20 mL			
10% (w/v) SDS	15 µL	40 µL	40 µL	40 µL
Acrylamide/Bis-acrylamide (30%/0.8% w/v)	0.26 mL	0,8 mL	1.3 mL	1,6 mL
10% (w/v) APS	15 µL	40 µL	40 µL	40 µL
TEMED	2 µL	2 µL	2 µL	2 µL
Total monomer	1,5 mL	4 mL	4 mL	4 mL

5.2.6.2 Coomassie blue staining

The gel was placed in at least 10-15 volumes of Coomasie Blue staining solution for 1-2 hours. The dye solution was rocked gently to distribute evenly over the gel. At the end of the staining, the gels were washed with several changes of water. The gels were moved into a solution of 7% acetic acid for at least 1 hour. If the background is still deeply stained, the gel was moved to fresh 7% acetic acid as often as necessary. The gels were placed into containers filled with 7% acetic acid as a final fixative and were photographed or scanned for analysis.

5.2.6.3 Preparation of Cell extracts

The cells were washed with pre chilled PBS, centrifuged at 1200 rpm for 5 min and lysed with 200 µL lysis buffer (10 mM Tris pH 7.6, 150 mM NaCl 5 mM EDTA, 1% Nonidet P-40, Protease

inhibitors were added before using, 1 mM PMSF, Aprotinin 5 µg/mL, Leupeptin 5 µg/mL, Pepstatin 5 µg/mL), incubated on ice for 30 min and centrifuged at 4°C12000 rpm for 10 min. The supernatant was collected into a fresh 1,5 mLeppendorf centrifuge tube and stored at –20°C, the pellet was discarded.

5.2.6.4 Western-blot

SDS-PAGE separated protein samples were transferred to a PVDF membrane through a Bio-Rad semi-dry transfer cell, under stable volt 20v (0,75mA per mini Gel) for 45 min. The membrane was blocked with 2% skim milk powder-PBS R.T. for 30 min. After washing with PBS, the membrane was incubated in 2% skim milk powder-PBS with appropriate diluted primary antibody R.T. for 1-2 hours. After washing with PBS-T for 3x5 min, the membrane was incubated with appropriate diluted AP conjugated secondary antibody at R.T. for 1-2 hours. After 3x5 min washing with PBS-T, the membrane was briefly rinsed with distilled water and developed in BCIP/NBT solution for about 20min.

5.2.6.5 Sample preparation for protein N-terminal sequencing

The purified IgG protein samples were diluted to about 100-200 µg/mL, 5 x Laemmli sample buffer was added and heated at 95ºC for 5-10 min and 10 µL of the samples (about 1-2µg protein) were separated on 10% SDS-PAGE under a constant current of 20 mA per mini gel for 50min. The gel was rinsed briefly in blotting buffer to wash away excess Tris/glycine/SDS electrophoresis buffer (TGS). Then, the separated protein samples were transferred to PVDF membrane through a semi-dry transfer cell using freshly prepared transfer buffer for 30-45 min. After blotting, the gel was subsequently stained with Coomassie Blue to check the effectiveness of transfer. The membrane was briefly washed with Milli-Q water and stained with Coomassie Blue till the blot appeared clearly. The membrane was rinsed with Milli-Q water to remove excess stain and dried. The desired bands were excised and stored in a microcentrifuge tube at -20°C for sequence analysis.

5.2.7 Transient transfection

HEK 293T cells were cultured in Dulbecco's Modified Eagle Medium (DMEM) high glucose (4,5 g/L), 8% fetal calf serum (FCS) 1% antibiotics. CHO-K1 cells were cultivated in DMEM/Ham F12 supplemented with 8% fetal calf serum (FCS). Cells were grown in 6-well or 24-well flat bottom tissue culture plate (Greiner bio-one Corp.). The transfection of plasmids was performed using the HEKFectin for HEK 293T and the Lipofectamine 2000 reagents in OPTIMEM1 medium according to manual instruction. 48 hours after transfection, antibody expression levels in the supernatant were measured by ELISA, reporter florescence gene expression levels were

measured by direct readout of the fluorescence protein intensity by TECAN GENios and/or FACS.

5.2.8 Establishment of stable cell lines

5.2.8.1 Titrating G418 (Kill Curves)

CHO-K1 culture medium was prepared in 24-well plate, 0,5 mL/well, containing G418 in 0, 500, 1000, 1500, 2000, 2500 µg/mL respectively in triplicate. CHO-K1 cells were split to the 24-well plate at about 50000 cells/well in 0,5 mL medium. The final concentration of G418 was 0, 250, 500, 750, 1000 and 1250 µg/mL respectively. The cells were incubated at 37°C, 5% CO2 and cell growth was observed everyday till the cells were dead.

5.2.8.2 Cell counting using Hemacytometer

The cells were tripsinized and pipetted up and down for several times to make cells in single cell suspension. A 100µl aliquot was mixed with an equal amount of Trypan Blue. The cover lip was placed squarely above the grid of the hemacytometer with a good stick. A small amount of the cells and trypan blue mixture about 15-20 µL was added to each side of the grid, so that it flows under the covers lip to cover the grid. The cell counter was watched under the microscope and the cells were counted in the area upon the grid. The total volume above the grid is 0.0001 mL. The blue cells are dead ones, and the bright whiter coloured cells are alive. The total number of cells alive and the total number of cells dead were counted in each of the two grids. The cell density and total cell amount were calculated.

5.2.8.3 Screening of stably transfected CHO-K1 clone

Cells were seeded in 6-well plates at 500000 cells per well and allowed to attach overnight. The gene of interest was transfected using lipfectamine 2000 according to the manufacturer's instructions. The supernatant was harvested from each transfected well 48 hours after transfection, pre-warmed medium containing G418 500 µg/mL was added. Mock-transfected cells were set as control. Antibody concentration in the harvested supernatant from transfected cells was measured using ELISA to determine if the transfection was successful. Cell growth was observed every 2-3 days and fresh medium with selection drug was changed when it was necessary. When the cells in the control wells were all dead, the transfected cells were trypsized and counted using a hemacytometer. Cells were diluted to 10,000 cells/mL. 96-well plates were prepared with 100 µL fresh medium each well containing 500 µg/mL G418. The cells were dispensed to the wells of the first line (8 wells), 100 µL per well, about 1000cells per well. A two-time serial dilution was made in the same row from line 1 to 3. Then 1 mL cell solution was diluted into 9 mL fresh medium, the cells density would be about 1000 cells/mL. 0,3 mL of the

diluted cells solution, about 300 cells, was diluted into 30 mL pre-warmed medium containing 500 µg/mL G418 and dispensed into the three 96-well plates at 100 µL/well. In the end, there would be one cell in 200 µL medium per well. Cell growth was observed, when the medium in the first three lines was changed to yellow, the antibody concentration in the supernatant of the first 3 lines was measured to monitor protein expression. Tiny colonies could be found in the other wells, and the wells with only one small colony were marked. About 50-60 mono-colonies could usually be found in all the three plates. Cell growth was observed, when the wells containing colonies turned to yellow (about at day 21), culture supernatants were harvested and antibody concentration was measured using ELISA to screen for positive clones.

5.2.9 Analysis of the expression levels of YFP reporter gene

5.2.9.1 Measurement of fluorescence expression using the TECAN GENios

The expression of yellow florescence protein (YFP) was screened using a TECAN GENios at excitation wavelength 485 nm, emission wavelength 535nm, number of flashes 3, lag time 0 µs, integration time 20 µs. Multiple reads 12x12 for 6-well plate and 5x5 for 24-well plates was performed with the same gain value set in one measurement. Cells transfected with only Lipofectamine 2000 reagents were set as background control in every plate.

5.2.9.2 Flow cytometry

For analysis of the expression YFP in mammalian cells, all experiments were analyzed using a fluorescence activated cell sorter (FACS) analyzer (FACS, Becton Dickinson, San Jose, CA). Excitation wavelength was 488 nm and a 530/30 nm bandpass emission filter was used. Forward and side scatter was used to establish a collection gate through which dead cells and debris were excluded. Between 10000 and 50000 events were collected using list-mode format for each experiment. Data were acquired and analyzed using CellQuest^{TM} Pro or with WinMDI 2.8.

5.2.10 Affinity chromatography purification of IgG1

About 1 L of culture medium was collected from one antibody expressing CHO-K1 clone or from transiently transfected HEK 293T cells. IIB6 human anti-MUC1 IgG1 was purified on a 1-mL HiTrap Protein-A-Sepharose column (Amersham, Uppsula, Sweden). The column was equilibrated with 20 CV (column volumes) washing buffer, (20 mM sodium phosphate, pH7,0) which had been filtered (0.20 µm). The filtered samples were loaded on the column at a flow rate of 1 mL/min. The column was washed with washing buffer thoroughly. The antibodies were then eluted with 12,5 mM citric acid, pH2,7, 1 mL fractions were collected into tubes containing 50 µL 1M Tris-HCl pH8,0. Relevant fractions were pooled after checking by SDS-PAGE and dialyzed against PBS using dialysis cassettes.

5.2.11 Determination of protein concentration

5.2.11.1 Human IgG capture sandwich ELISA

Falcon 96-well microtiter plates were coated with 100 µL goat anti-human IgG polyvalent antibody (Sigma) (1 µg/well) in 50 mM NaHCO3, pH 9,6 and incubated at 4°C overnight. 100 µL FCS was added for blocking at 37°C for 1 hour. The plate was washed with PBS-T for 3 times. A standard antibody dilution series was prepared in triplicates at 100 µL per well. 100 µL supernatants of transfected cells at different dilutions in PBS-FCS were loaded into the microtiter plate in triplcates. Incubated at 37°C for 1 hour. After washing 3 times with PBS-T, 100 µL horseradish peroxidase conjugated goat anti-human IgG γ chain specific antibody (Sigma, 1:10.000 in 50%FCS-PBS) was added and Incubated at 37°C for 1 hour. After washing 3 times with PBS-T, 100 µL TMB peroxidase substrates (Dimethylformamide and hydrogen peroxide) was added and developed at R.T. for about 30 min (time course depends on colour developing). The reaction was stopped by adding 100 µL 1N H2SO4. Absorbance at 450 nm (reference 620 nm) was read with Sunrise TECAN ELISA reader. For each well, the mean absorbance of the buffer wells was subtracted from the mean absorbance of the sample wells to calculate a net absorbance value. A standard curve was produced using dilutions of the IgG preparation with known concentration.

5.2.11.2 Bradford Assay

The TECAN GENios machine was turned on to allow the bulb to warm up (approx. 10 min. before use). 5x Bradford Reagent (BioRad) was diluted 4:1 with water. Protein standards were prepared in triplicate (10 µL per well) and plated in a 96-well microtitre plate. Column 1 was left as blank, plating was started from column 2. The samples was prepared in triplicates (10 µL per well), samples should be in the range of the standard curve (0-1 mg/mL for BSA). Samples were diluted serially. 200 µL of diluted Bradford reagent was added to each well and incubated for 5 minutes. The O.D. was read under excitation light through a 595 nm filter. Standard curve was graphed and the samples concentration was determined according to the standards.

5.2.12 Analytical gel filtration

Size exclusion chromatography was done on a calibrated Superdex 200 10/300 GL column (Amersham, Uppsala Sweden) with an ÄKTA Prime system (Amersham, Uppsala Sweden) at a flow rate of 1 mL/min in PBS at pH 7.2. A LMW gel filtration calibration kit (Amersham, Uppsala Sweden) was used to calibrate the column according to supplier's instructions. The apparent molecular mass of IgG was estimated relative to the calibration proteins. 250 µL of purified IgG was injected.

5.2.13 IgG characterization

5.2.13.1 Peptide ELISA

Nunc Maxi microtiter plates were coated with 100 µL streptavidin 2 µg/mL in 0.05 M carbonate buffer (pH 9.6) per well and incubated at 4°C overnight. The plate was blocked with 2% BSA/PBS at room temperature for 1 hour. 100 µL of the biotinylated peptide solutions into the plate was dispensed into the plate and incubated at 4°C overnight (alternatively, peptide can also be diluted in coating buffer and coated to Nunc Maxi microtiter plates directly without pre-coated streptavidin). After washing 3 times with PBS-T, 100 µL of the samples (appropriately diluted in blocking buffer) was added to each well of the plate containing the captured peptides. It was incubated at R.T. for 1-2 hrs. After washing 3 times, secondary antibody was added in appropriately dilution, incubate at R.T. for 1-2 hours. After washing 3 times, horseradish peroxidase conjugated detection antibody was added (appropriately diluted in blocking buffer) and incubated at R.T. 1-1,5 hours. The plate was washed 3 times with PBS-T. 100 µL TMB peroxidase substrates (Dimethylformamide and hydrogen peroxide) were added and developed at R.T. for about 30 min (depending on color developing). The reaction was stopped by adding 100 µL1N H2SO4. Absorbance at 450 nm (reference 620 nm) was read with Sunrise TECAN ELISA reader. For each well, the mean absorbance of the background wells was subtracted from the mean absorbance of the wells coated with peptide to calculate a net absorbance value.

5.2.13.2 FACS analysis of IIB6 IgG binding to cells

T47D cells were gently scraped from a 10 cm petri dish and collected to a 15 mL falcon centrifuge tube. Jurkat cells were used as negative control. Cells were washed one time with staining buffer (1xPBS/BSA1%, 5 mM EDTA) and centrifuged at 1200 rpm for 5 min at 4°C. The cell pellet was resuspended with staining buffer and aliquoted at 10^5 cells in 100µL washing buffer to each tube. Purified IgG, scFv at different dilutions in 1x PBS/BSA 1% were added and incubated on ice for 30 min. The cells were washed with 10 mL staining buffer 2-3 times and spun down at 4°C at 1200 rpm for 5 minutes, supernatant was discarded gently. The secondary antibodies at appropriate dilution were added and incubated on ice for 30 min. After washing 2-3 times, the cells were stained with fluorescence-conjugated antibody at appropriate dilution, incubated on ice for 30 mins. After washing 2-3 times, the cell pellet was resuspended in 400 µL staining buffer and kept on ice, till FACS analysis. For live/dead discrimination, propidium iodide (PI) solution was added.

5.2.13.3 Surface plasmon resonance

The binding affinity analysis of IIB6 IgG to the synthetic MUC1 peptide was performed using

surface plasmon resonance (BIAcore X). Binding curves and kinetic parameters were obtained as follows: the MUC1 16-mer biotin conjugated (NH2-APDT(GalNAC)RPAPGSTAPPAC-COOH) was captured by flowing (20 ng/mL, at 30 µL/min for 2 min) them over a streptavidin chip. 120 µg/mL BSA was injected to block the unspecific binding (flow rate 30 µl/min for 2 min). Subsequently, IIB6 IgG was injected (0,06−6 µM, flow rate 30 µL/min for 1.5 min, dissociate about 5 min). The MUC1 peptide surface was regenerated by pulse injection of 0,5% SDS before each injection of IgG samples. The curves were analysed with a global fit 1:1 binding algorithm with drifting baseline.

6 Abbreviations

6.1 General abbreviations

°C	Degree centigrade
µg	Microgramm
µL	Microliter
µM	Micromolar
A	Adenine
AA	Amino acid
Ab	Antibody
Amp	Ampicillin
AP	Alkaline phosphatase
APS	Ammonium-persulphate
AT CC	American Type Culture Collection
ATP	Adenosin-triphosphate
BCIP	5-Brom-4-Chlor-3-Indolylphosphate-p-Toluidinsa
BE	Boundary element
BHK	Baby Hamster Kidney
bp	Base pair
BSA	Bovine serum albumin
C	Cytosine
cDNA	Complementary DNA
CDR	Complementary determining region
CHO	Chinese hamster ovary
Cre	Causes recombination (Cre-Recombinase)
DMEM	Dulbecco’s modified Eagle Medium
DMSO	Dimethyl sulphoxide
DNA	Deoxy-ribonucleic acid
dNTP	Desoxyribonukleosidtriphosphat
DTT	Dithiothreitol
E. coli	*Escherichia coli*
EDTA	Ethylendiamine-tetra-acetic acid
EF1-α	Elongation factor 1-a

ELISA	Enzyme-Linked Immunosorbent Assay
ES	Embryonic Stem cell
F	Wild type FRT site
F3	Mutated FRT Site
Fab	antigenbindendes Fragment
FACS	Fluorescence Activated Cell Sorting
FBS	Fetal bovine serum
Fc	Crystallizable fragment
FITC	Fluorescein isothiocyanate
Flp	Flippase recombinase
Flpe	Enhanced flippase recombinase
FR	Framework region
FRT	Flippase recombinase recognition target sequence
g	Gramm
G	Guanine
G418	Aminoglycoside-2'-deoxystreptine (Gentamycin-derivative)
Ganc	ganciclovir
GFP	Green Fluorescent Protein
h	Hour
HAMA	Human anti-mouse antibody
hCMV	Human cytomegalovirus
HRP	Horseradish peroxidase
hygtk	Hygromycin and thymidine kinase fusion gene
Ig	Immunoglobulin
IRES	Internal ribosome entry site
kbp	1000 base pairs
kDa	Kilo-Dalton
kV	Kilovolt
LB	Luria Bertani
LCR	Locus control region
loxP	Locus of crossing over of P1 (target sequence for the Cre recombinase)
M	Molar
mA	Milliampere
mAb	monoclonal Antibody
MAR	Matrix attachment region

mg	Milligramm
min	Minute
mL	Milliliter
mM	Millimolar
mRNA	Messenger RNA
MUC1	Mucin 1
NBT	p-Nitrotetrazoliumbluechloride
NC	Negative control
neo	Neomycin-phosphotransferase gene
nm	Nanometer
NP40	Nonidet P40
nt	Nucleotide
ori	origin of replication
PAGE	Polyacrylamide gel electrophoresis
PBS	Phosphate buffered saline
PBS-T	Phosphate buffered saline-tween
PCR	Polymerase chain reaction
POD	Peroxidase
RNA	Ribonucleic acid
rpm	Rotations per minute
RT	Room temperature
S/MAR	Scaffold/matrix attach region
SAR	scaffold attachment region
scFv	Single chain variable fragment
SDS	Sodium dodecyl sulfate
SRP	Surface plasmon resonance
SV40	Simian Virus 40
T	Thymine
TAE	Tris-Acetat-EDTA-buffer
TE	Tris-EDTA-buffer
TEMED	N, N, N´, N´-Tetramethylendiamine
Tk	thymidine kinase
Tris	Tris-(hydroxymethyl)-aminomethan
U	Unit
UCOEs	Ubiquitous chromatin opening elements

v/v	Volume percent
VH	Variable region of antibody heavy chain
VL	Variable region of antibody light chain
VNTR	Variable number of tandem repeats
YFP	Yellow Fluorescent Protein

6.2 Amino acid

Nonpolar		
Ala	A	Alanine
Leu	L	Leucine
Val	V	Valine
Ile	I	Isoleucine
Pro	P	Proline
Met	M	Methionine
Phe	F	Phenylalanine
Trp	W	Tryptophan
Polar, uncharged		
Gly	G	Glycine
Ser	S	Serine
Thr	T	Threonine
Asn	N	Asparagine
Gln	Q	Glutamine
Acidic		
Asp	D	Aspartic acid
Glu	E	Glutamic acid
Cys	C	Cysteine
Tyr	Y	Tyrosine
Basic		
Lys	K	Lysine
Arg	R	Arginine
His	H	Histidine

7 Literature

Acres, B., V. Apostolopoulos, et al. (1999). "MUC1-specific immune responses in human MUC1 transgenic mice immunized with various human MUC1 vaccines." Cancer Immunology, Immunotherapy **48**(10): 588-594.

Agarwal, M., W. T. Austin, et al. (1998). "Scaffold Attachment Region-Mediated Enhancement of Retroviral Vector Expression in Primary T Cells." J. Virol. **72**(5): 3720.

Agrawal, B., M. J. Krantz, et al. (1998). "Cancer-associated MUC1 mucin inhibits human T-cell proliferation, which is reversible by IL-2." **4**(1): 43-49.

Agrawal, B. and B. M. Longenecker (2005). "MUC1 mucin-mediated regulation of human T cells." Int. Immunol. **17**(4): 391-399.

Allison A. Bianchi, J. T. M. (2003). "High-level expression of full-length antibodies using trans-complementing expression vectors." Biotechnology and Bioengineering **84**(4): 439-444.

Antequera, F. (2004). "Genomic specification and epigenetic regulation of eukaryotic DNA replication origins." EMBO J. **23**(22): 4365-4370.

Apostolopoulos, V., C. Osinski, et al. (1998). "MUC1 cross-reactive Gal[alpha](l,3)Gal antibodies in humans switch immune responses from cellular to humoral." **4**(3): 315-320.

Araki, K., M. Araki, et al. (2002). "Site-directed integration of the cre gene mediated by Cre recombinase using a combination of mutant lox sites." Nucl. Acids Res. **30**(19): e103-.

Auboeuf, D., D. H. Dowhan, et al. (2005). "A Subset of Nuclear Receptor Coregulators Act as Coupling Proteins during Synthesis and Maturation of RNA Transcripts." Mol. Cell. Biol. **25**(13): 5307-5316.

Back, S. H., Y. K. Kim, et al. (2002). "Translation of polioviral mRNA is inhibited by cleavage of polypyrimidine tract-binding proteins executed by polioviral 3C(pro)." J Virol **76**(5): 2529-42.

Bae, S., H. Hong, et al. (1995). "Stability of transfectomas producing chimeric antibody against the pre-S2 surface antigen of hepatitis B virus during a long-term culture." Biotechnol Bioeng **47**: 243-251.

Baer, A. and J. Bode (2001). "Coping with kinetic and thermodynamic barriers: RMCE, an efficient strategy for the targeted integration of transgenes." Current Opinion in Biotechnology **12**(5): 473-480.

Baer, A. and J. Bode (2001). "Coping with kinetic and thermodynamic barriers: RMCE, an efficient strategy for the targeted integration of transgenes." Curr Opin Biotechnol . **12**:

473–480.

Baiker, A., C. Maercker, et al. (2000). "Mitotic stability of an episomal vector containing a human scaffold/matrix-attached region is provided by association with nuclear matrix." Nature Cell Biology **3**: 181-184.

Barnes, L. M., C. M. Bentley, et al. (2003). "Stability of protein production from recombinant mammalian cells." Biotechnology and Bioengineering **81**(6): 631-639.

Bergman, L., E. Harris, et al. (1981). "Glycosylation causes an apparent block in translation of immunoglobulin heavy chain." J. Biol. Chem. **256**(2): 701-706.

Berruti, A., M. Tampellini, et al. (1994). "Prognostic value in predicting overall survival of two mucinous markers: CA 15-3 and CA 125 in breast cancer patients at first relapse of disease." European Journal of Cancer **30**(14): 2082-2084.

Blyn, L. B., K. M. Swiderek, et al. (1996). "Poly(rC) binding protein 2 binds to stem-loop IV of the poliovirus RNA 5' noncoding region: Identification by automated liquid chromatography-tandem mass spectrometry." PNAS **93**(20): 11115-11120.

Bode, J., C. Benham, et al. (2000). "Transcriptional augmentation: modulation of gene expression by scaffold:matrix-attached regions (S/MAR elements)." Crit. Rev. Eukaryot. Gene Exp. . **10,**: 73–90.

Bode, J., C. P. Fetzer, et al. (2001). "The hitchhiking principle: Optimizing episomal vectors for use in gene therapy and biotechnology." Int J Gene Ther Mol Biol **6**: 33-46.

Bode, J., S. Goetze, et al. (2003). "From DNA structure to gene expression: mediators of nuclear compartmentalization and dynamics." Chromosome Research **11**(5): 435-445.

Bode, J., T. Schlake, et al. (2000). "The transgeneticist's toolbox: Novel methods for the targeted modification of eukaryotic genomes." Biol Chem . **381**: 801–813.

Bode, J., T. Schlake, et al. (1995). "Scaffold/matrix-attached regions: Structural properties creating transcriptionally active loci." Int. Rev. Cytol. **162**: 389-454.

Bode, J., M. Stengert-Iber, et al. (1996). "Scaffold/matrix-attached regions: Topological switches with multiple regulatory functions." Crit. Rev. Eukaryot. Gene Expr. **6**: 115-138.

Borman, A., J. Bailly, et al. (1995). "Picornavirus internal ribosome entry segments: comparison of translation efficiency and the requirements for optimal internal initiation of translation in vitro." Nucl. Acids Res. **23**(18): 3656-3663.

Borman, A., F. Deliat, et al. (1994). "Sequences within the poliovirus internal ribosome entry segment control viral RNA synthesis." EMBO J. **13**(13): 3149-3157.

Borman, A., P. Le Mercier, et al. (1997). "Comparison of picornaviral IRES-driven internal

initiation of translation in cultured cells of different origins." Nucl. Acids Res. **25**(5): 925-932.

Boussadia, O., M. Niepmann, et al. (2003). "Unr is required in vivo for efficient initiation of translation from the internal ribosome entry sites of both rhinovirus and poliovirus." J Virol **77**(6): 3353-9.

Brayman, M., A. Thathiah, et al. (2004). "MUC1: A multifunctional cell surface component of reproductive tissue epithelia." Reproductive Biology and Endocrinology **2**(1): 4.

Brossart, P., K. S. Heinrich, et al. (1999). "Identification of HLA-A2-Restricted T-Cell Epitopes Derived From the MUC1 Tumor Antigen for Broadly Applicable Vaccine Therapies." Blood **93**(12): 4309-4317.

Byrd, K. and V. G. Corces (2003). "Visualization of chromatin domains created by the gypsy insulator of Drosophila." J. Cell Biol. **162**(4): 565-574.

Chen, Y. C. and D. J. Hunter (2005). "Molecular Epidemiology of Cancer." CA Cancer J Clin **55**(1): 45-54.

Chuck, A. S. and B. O. Palsson (1992). "Population balance between producing and nonproducing hybridoma clones is very sensitive to serum level, state of inoculum, and medium composition." Biotechnol Bioeng **39**: 354-360.

Clark, A. T., M. E. M. Robertson, et al. (2003). "Conserved Nucleotides within the J Domain of the Encephalomyocarditis Virus Internal Ribosome Entry Site Are Required for Activity and for Interaction with eIF4G." J. Virol. **77**(23): 12441-12449.

Clarke, C., S. Glaser, et al. (2002). "Breast cancer incidence and mortality trends in an affluent population: Marin County, California, USA, 1990-1999." Breast Cancer Res **4**(6): R13.

Craig, A. W., Y. V. Svitkin, et al. (1997). "The La autoantigen contains a dimerization domain that is essential for enhancing translation." Mol Cell Biol **17**(1): 163-9.

Crittenden, S. L., E. R. Troemel, et al. (1994). "GLP-1 is localized to the mitotic region of the C. elegans germ line." Development **120**: 2901.

Davies, M. and R. Kaufman (1992). "The sequence context of the initiation codon in the encephalomyocarditis virus leader modulates efficiency of internal translation initiation." J. Virol. **66**(4): 1924-1932.

Duke, G., M. Hoffman, et al. (1992). "Sequence and structural elements that contribute to efficient encephalomyocarditis virus RNA translation." J. Virol. **66**(3): 1602-1609.

Dul, J. and Y. Argon (1990). "A Single Amino Acid Substitution in the Variable Region of the Light Chain Specifically Blocks Immunoglobulin Secretion." PNAS **87**(20): 8135-8139.

Dul, J. L., S. Aviel, et al. (1996). " Ig light chains are secreted predominantly as monomers." J. Immunol. **157**: 2969-2975.

Feng, Y.-Q., J. Seibler, et al. (1999). "Site-specific chromosomal integration in mammalian cells: highly efficient CRE recombinase-mediated cassette exchange." Journal of Molecular Biology **292**(4): 779-785.

Fong, Y. W. and Q. Zhou (2001). "Stimulatory effect of splicing factors on transcriptional elongation." **414**(6866): 929-933.

Fukushige, S. and B. Sauer (1992). "Genomic Targeting with a Positive-Selection lox Integration Vector Allows Highly Reproducible Gene Expression in Mammalian Cells." PNAS **89**(17): 7905-7909.

Fussenegger, M., J. E. Bailey, et al. (1999). "Genetic optimization of recombinant glycoprotein production by mammalian cells." Trends in Biotechnology **17**(1): 35-42.

Gendler, S. J. and A. P. Spicer (1995). "Epithelial Mucin Genes." Annual Review of Physiology **57**(1): 607-634.

Gimmi, C. D., B. W. Morrison, et al. (1996). "Breast cancer-associated antigen, DF3/MUC1, induces apoptosis of activated human T cells." **2**(12): 1367-1370.

Girod, P.-A., M. Zahn-Zabal, et al. (2005). "Use of the chicken lysozyme 5' matrix attachment region to generate high producer CHO cell lines." Biotechnology and Bioengineering **91**(1): 1-11.

Gonzalez, R., B. A. Andrews, et al. (2002). " Kinetic model of BiP- and PDI-mediated protein folding and assembly." J. Theor. Biol. **214**: 529-537.

Gorman, C. and C. Bullock (2000). "Site-specific gene targeting for gene expression in eukaryotes." Current Opinion in Biotechnology **11**(5): 455-460.

Gosert, R., K. H. Chang, et al. (2000). "Transient expression of cellular polypyrimidine-tract binding protein stimulates cap-independent translation directed by both picornaviral and flaviviral internal ribosome entry sites In vivo." Mol Cell Biol **20**(5): 1583-95.

Gray, N. K. and M. Wickens (1998). "Control of translation initiation in animals." Annual Review of Cell and Developmental Biology **14**(1): 399-458.

Hahm, B., Y. K. Kim, et al. (1998). "Heterogeneous nuclear ribonucleoprotein L interacts with the 3' border of the internal ribosomal entry site of hepatitis C virus." J Virol **72**(11): 8782-8.

Haller, A. A. and B. L. Semler (1995). "Stem-loop structure synergy in binding cellular proteins to the 5´ noncoding region of poliovirus RNA." Virology **206**: 923-934.

Hammill L, Welles J, et al. (2000.). " The gel microdrop secretion assay: Identification of a low

productivity subpopulation arising during the production of human antibody in CHO cells." Cytotechnology **34**: 27–37.

Hammond, C. and A. Helenius (1995). "Quality control in the secretory pathway." Current Opinion in Cell Biology **7**(4): 523-529.

Hannam-Harris, A. C. and J. L. Smith (1981). "Free immunoglobulin light chain synthesis by human foetal liver and cord blood lymphocytes." Immunology **43**: 417-423.

Harris, J. R., M. Lippman, et al. (1992). "Breast cancer." N. Engl. J. Med. **327**(3): 19-28.

Hart, C. M. and U. K. Laemmli (1998). "Facilitation of chromatin dynamics by SARs." Current Opinion in Genetics & Development **8**(5): 519-525.

Hart, C. M. and U. K. Laemmli (1998). "Facilitation of chromatin dynamics by SARs." Curr Opin Genet Dev. **8**(5): 519-25.

Hellen, C. U., T. V. Pestova, et al. (1994). "The cellular polypeptide p57 (pyrimidine tract-binding protein) binds to multiple sites in the poliovirus 5' nontranslated region." J Virol **68**(2): 941-50.

Heng, H. H. Q., S. Goetze, et al. (2004). "Chromatin loops are selectively anchored using scaffold/matrix-attachment regions." J Cell Sci **117**(7): 999-1008.

Hennecke, M., M. Kwissa, et al. (2001). "Composition and arrangement of genes define the strength of IRES-driven translation in bicistronic mRNAs." Nucl. Acids Res. **29**(16): 3327-3334.

Hoffman, M. and A. Palmenberg (1995). "Mutational analysis of the J-K stem-loop region of the encephalomyocarditis virus IRES." J. Virol. **69**(7): 4399-4406.

Hoffman, M. A. and A. C. Palmenberg (1996). "Revertant analysis of J-K mutations in the EMCV IRES detects an altered leader protein." J. Virol. **70**: 6425-6430.

Honda, M., E. A. Brown, et al. (1996). "Stability of a stem-loop involving the initiator AUG controls the efficiency of internal initiation of translation on hepatitis C virus RNA." RNA **2**: 955-968.

Hopper, J. E. and E. Papagiannes (1986). "Evidence by radioimmunoassay that mitogen-activated human blood mononuclear cells secrete significant amounts of light chain Ig unassociated with heavy chain." Cell. Immunol. **101**: 122-131.

Houdebine, L. M. and J. Attal (1999). "Internal ribosome entry sites (IRESs): reality and use." Transgenic Research **8**(3): 157-177.

Hunt, S. L., J. J. Hsuan, et al. (1999). "unr, a cellular cytoplasmic RNA-binding protein with five cold-shock domains, is required for internal initiation of translation of human rhinovirus

RNA." Genes Dev **13**(4): 437-48.

Hunt, S. L. and R. J. Jackson (1999). "Polypyrimidine-tract binding protein (PTB) is necessary, but not sufficient, for efficient internal initiation of translation of human rhinovirus-2 RNA." Rna **5**(3): 344-59.

Hurtley, S., D. Bole, et al. (1989). "Interactions of misfolded influenza virus hemagglutinin with binding protein (BiP)." J. Cell Biol. **108**(6): 2117-2126.

Hust, M. and S. Dübel (2004). "Mating antibody phage display with proteomics." Trends in Biotechnology **22**(1): 8-14.

Izumi, R. E., S. Das, et al. (2004). "A peptide from autoantigen La blocks poliovirus and hepatitis C virus cap-independent translation and reveals a single tyrosine critical for La RNA binding and translation stimulation." J Virol **78**(7): 3763-76.

Jackson, D. (2005). "Understanding nuclear organization: when information becomes knowledge: Workshop on Nuclear Organization." EMBO Reports **6**(3): 213-217.

Jackson, D. A. (1997). "Chromatin domains and nuclear compartments: establishing sites of gene expression in eukaryotic nuclei." Molecular Biology Reports **24**(3): 209-220.

Jang, S., H. Krausslich, et al. (1988). " A segment of the 5' nontranslated region of encephalomyocarditis virus RNA directs internal entry of ribosomes during in vitro translation." J Virol **62**: 2636.

Jang, S. K. and E. Wimmer (1990). " Cap-independent translation of encephalomyocarditis virus RNA: structural elements of the internal ribosomal entry site and involvement of a cellular 57 kD RNA-binding protein." Genes Dev. **4**: 1560-1572.

Jenke, A. C. W., I. M. Stehle, et al. (2004). "Nuclear scaffold/matrix attached region modules linked to a transcription unit are sufficient for replication and maintenance of a mammalian episome." PNAS **101**(31): 11322-11327.

Jenke, B. H. C., C. P. Fetzer, et al. (2002). "An episomally replicating vector binds to the nuclear matrix protein SAF-A in vivo." EMBO Reports **3**(4): 349-354.

Jostock, T., M. Vanhove, et al. (2004). "Rapid generation of functional human IgG antibodies derived from Fab-on-phage display libraries." Journal of Immunological Methods **289**(1-2): 65-80.

Kaloff, C. R. and I. G. Haas (1995). "Coordination of immunoglobulin chain folding and immunoglobulin chain assembly is essential for the formation of functional IgG." Immunity **2**(6): 629-637.

Kam, J., L. Regimbald, et al. (1998). "MUC1 synthetic peptide inhibition of intercellular adhesion molecule-1 and MUC1 binding requires six tandem repeats." Cancer Res **58**(23): 5577-5581.

Kaminski, A., S. L. Hunt, et al. (1995). "Direct evidence that polypyrimidine tract binding protein (PTB) is essential for internal initiation of translation of encephalomyocarditis virus RNA." Rna **1**(9): 924-38.

Kaminski, A. and R. J. Jackson (1998). "The polypyrimidine tract binding protein (PTB) requirement for internal initiation of translation of cardiovirus RNAs is conditional rather than absolute." Rna **4**(6): 626-38.

Kaufman, R., M. Davies, et al. (1991). "Improved vectors for stable expression of foreign genes in mammalian cells by use of the untranslated leader sequence from EMC virus." Nucl. Acids Res. **19**(16): 4485-4490.

Kaufmann, H. and M. Fussenegger (2003). Metabolic engineering of mammalian cells for higher protein yield. Gene Transfer and Expression in Mammalian Cells. Amsterdam, Elsevier Science**:** 457-569.

Kim, J. H., K. Y. Paek, et al. (2003). "Heterogeneous nuclear ribonucleoprotein C modulates translation of c-myc mRNA in a cell cycle phase-dependent manner." Mol Cell Biol **23**(2): 708-20.

Kim SJ, Kim NS, et al. (1998). " Characterization of chimeric antibody producing CHO cells in the course of dihydrofolate reductase-mediated gene amplification and their stability in the absence of selective pressure." Biotechnol Bioeng **58**: 73-84.

Kirkpatrick, R. B., S. Ganguly, et al. (1995). "Heavy chain dimers as well as complete antibodies are efficiently formed and secreted from Drosophila via a BiP-mediated pathway." J. Biol. Chem. **270**(34): 19800-19805.

Kirsch, M., M. Zaman, et al. (2005). "Parameters affecting the display of antibodies on phage." Journal of Immunological Methods **301**(1-2): 173-185.

Knittler, M., S. Dirks, et al. (1995). "Molecular Chaperones Involved in Protein Degradation in the Endoplasmic Reticulum: Quantitative Interaction of the Heat Shock Cognate Protein BiP with Partially Folded Immunoglobulin Light Chains that are Degraded in the Endoplasmic Reticulum." PNAS **92**(5): 1764-1768.

Knittler, M. and I. Haas (1992). "Interaction of BiP with newly synthesized immunoglobulin light chain molecules: cycles of sequential binding and release." EMBO J. **11**(4): 1573-1581.

Kolupaeva, V. G., C. U. Hellen, et al. (1996). "Structural analysis of the interaction of the pyrimidine tract-binding protein with the internal ribosomal entry site of encephalomyocarditis virus and foot-and-mouth disease virus RNAs." Rna **2**(12): 1199-212.

Komatsu, M., C. A. C. Carraway, et al. (1997). "Reversible Disruption of Cell-Matrix and Cell-Cell Interactions by Overexpression of Sialomucin Complex." J. Biol. Chem. **272**(52): 33245-33254.

Kozak, M. (1980). "Evaluation of the "scanning model" for initiation of protein synthesis in eukaryotes." Cell **22**: 7-8.

Kozak, M. (1986). "Point mutations define a sequence flanking the AUG initiator codon that modulates translation by eukaryotic ribosomes." Cell **44**(22): 283-92.

Kozak, M. (1987). "At least six nucleotides preceding the AUG initiator codon enhance translation in mammalian cells." J Mol Biol. **196**(4): 947-50.

Kozak, M. (1989). "The scanning model for translation: an update." J. Cell Biol. **108**(2): 229-241.

Kozak, M. (1990). "Downstream Secondary Structure Facilitates Recognition of Initiator Codons by Eukaryotic Ribosomes." PNAS **87**(21): 8301-8305.

Kozak, M. (1997). "Recognition of AUG and alternative initiator codons is augmented by G in position +4 but is not generally affected by the nucleotides in positions +5 and +6." EMBO J. **16**(9): 2482-2492.

Kozak, M. (2002). "Pushing the limits of the scanning mechanism for initiation of translation." Gene **299**(1-2): 1-34.

Kozak, M. and E. Neufeld (2003). "Not every polymorphism close to the AUG codon can be explained by invoking context effects on initiation of translation." Blood **101**(3): 1202-.

Kurre, P., J. Morris, et al. (2003). "Scaffold attachment region–containing retrovirus vectors improve long-term proviral expression after transplantation of GFP-modified CD34+ baboon repopulating cells." Blood **102**: 3117-3119.

Laden, F. and D. J. Hunter (1998). "Environmental risk factors and female breast cancer." Annual Review of Public Health **19**(1): 101-123.

Le, S., J. Chen, et al. (1993). "Conserved tertiary structural elements in the 5' nontranslated region of cardiovirus, aphthovirus and hepatitis A virus RNAs." Nucl. Acids Res. **21**(10): 2445-2451.

Lee, Y.-K., J. W. Brewer, et al. (1999). "BiP and Immunoglobulin Light Chain Cooperate to Control the Folding of Heavy Chain and Ensure the Fidelity of Immunoglobulin Assembly." Mol. Biol. Cell **10**(7): 2209-2219.

Leitzgen, K., M. R. Knittler, et al. (1997). "Assembly of Immunoglobulin Light Chains as a Prerequisite for Secretion." J. Biol. Chem. **272**(5): 3117-3123.

Lenny, N. and M. Green (1991). "Regulation of endoplasmic reticulum stress proteins in COS cells transfected with immunoglobulin μ heavy chain cDNA." J. Biol. Chem. **266**: 20532-20537.

Li, Y., H. Kuwahara, et al. (2001). "The c-Src Tyrosine Kinase Regulates Signaling of the Human

DF3/MUC1 Carcinoma-associated Antigen with GSK3beta and beta -Catenin." J. Biol. Chem. **276**(9): 6061-6064.

Liang, M., S. Dübel, et al. (2001). "Baculovirus expression cassette vectors for rapid production of complete human IgG from phage display selected antibody fragments." Journal of Immunological Methods **247**(1-2): 119-130.

Lilie, H., R. Rudolph, et al. (1995). "Association of Antibody Chains at Different Stages of Folding: Prolyl Isomerization Occurs after Formation of Quaternary Structure." Journal of Molecular Biology **248**(1): 190-201.

Lillehoj, E. P., B. T. Kim, et al. (2002). "Identification of Pseudomonas aeruginosa flagellin as an adhesin for Muc1 mucin." Am J Physiol Lung Cell Mol Physiol **282**(4): L751-756.

Liu, Z., D. Song, et al. (1999). "Fine mapping of the antigen-antibody interaction of scFv215, a recombinant antibody inhibiting RNA polymerase II from *Drosophila melanogaster*." Journal of Molecular Recognition **12**(2): 103-111.

Madigan, M., R. Ziegler, et al. (1995). "Proportion of breast cancer cases in the United States explained by well-established risk factors." J Natl Cancer Inst **87**(22): 1681-1685.

Martin, T. M., G. D. Wiens, et al. (1998). "Inefficient Assembly and Intracellular Accumulation of Antibodies with Mutations in VH CDR2." J Immunol **160**(12): 5963-5970.

Martinez-Salas, E., J. Saiz, et al. (1993). "A single nucleotide substitution in the internal ribosome entry site of foot-and-mouth disease virus leads to enhanced cap-independent translation in vivo." J. Virol. **67**(7): 3748-3755.

Mathews, M. B., N. Sonenberg, et al. (2000.). Origins and principles of translational control. Translational Control of Gene Expression. N. Sonenberg, Hershey, J.W.B., Mathews, M.B. NewYork, Cold Spring Harbor Laboratory Press**:** 1-31.

Meerovitch, K., Y. V. Svitkin, et al. (1993). "La autoantigen enhances and corrects aberrant translation of poliovirus RNA in reticulocyte lysate." J Virol **67**(7): 3798-807.

Mehren, M. v., G. P. Adams, et al. (2003). "Monoclonal antibody therapy for cancer." Annual Review of Medicine **54**(1): 343-369.

Melnick, J. and J. L. A. Dul, Y. (1994). "Sequential interaction of the chaperones BiP and GRP94 with immunoglobulin chains in the endoplasmic reticulum." Nature **370**: 373-375.

Mielke, C., Y. Kohwi, et al. (1990). "Hierarchical binding of DNA fragments derived from scaffold-attached regions: correlation of properties in vitro and function in vivo." Biochemistry **29**(32): 7475.

Miles, D. and J. Taylor-Papadimitriou (1998). "Mucin based breast cancer vaccines." Expert Opinion on Investigational Drugs **7**(11): 1865-1877.

Montano, R. F. and S. L. Morrison (2002). "Influence of the Isotype of the Light Chain on the Properties of IgG." J Immunol **168**(1): 224-231.

Morrison, S. and M. Scharff (1975). "Heavy chain-producing variants of a mouse myeloma cell line." J Immunol **114**(2): 655-659.

Nagai, T., K. Ibata, et al. (2002). "A variant of yellow fluorescent protein with fast and efficient maturation for cell-biological applications." Nat Biotech **20**(1): 87-90.

Namciu, S. J. and R. E. K. Fournier (2004). "Human Matrix Attachment Regions Are Necessary for the Establishment but Not the Maintenance of Transgene Insulation in Drosophila melanogaster." Mol. Cell. Biol. **24**(23): 10236-10245.

Narlikar, G. J., H.-Y. Fan, et al. (2002). "Cooperation between Complexes that Regulate Chromatin Structure and Transcription." Cell **108**(4): 475-487.

Nguyen, V. K., X. Zou, et al. (2003). "Heavy-chain only antibodies derived from dromedary are secreted and displayed by moused B cells." Immunology **109**: 93-101.

Nickerson, J. (2001). "Experimental observations of a nuclear matrix." J Cell Sci **114**(3): 463-474.

Norderhaug, L., F.-E. Johansen, et al. (2002). "Balanced expression of single subunits in a multisubunit protein, achieved by cell fusion of individual transfectants." Eur J Biochem **269**(13): 3205-3210.

O´Gorman, S., D. Fox, et al. (1991). "Recombinase-mediated gene activation and site-specific integration in mammalian cells." Science **251**: 1351-1355.

Ohlmann, T., M. Rau, et al. (1995). "Proteolytic cleavage of initiation factor eIF-4 gamma in the reticulocyte lysate inhibits translation of capped mRNAs but enhances that of uncapped mRNAs." Nucl. Acids Res. **23**(3): 334-340.

Oi, V. T., S. L. Morrison, et al. (1983). "Immunoglobulin Gene Expression in Transformed Lymphoid Cells." PNAS **80**(3): 825-829.

Orphanides, G. and D. Reinberg (2002). "A Unified Theory of Gene Expression." Cell **108**(4): 439-451.

Pallavicini, M., P. DeTeresa, et al. (1990). "Effects of methotrexate on transfected DNA stability in mammalian cells." Mol Cell Biol **10**: 401-404.

Pandey, P., S. Kharbanda, et al. (1995). "Association of the DF3/MUC1 breast cancer antigen with Grb2 and the Sos/Ras exchange protein." Cancer Res **55**(18): 4000-4003.

Parkin, D. M., F. Bray, et al. (2005). "Global Cancer Statistics, 2002." CA Cancer J Clin **55**(2): 74-108.

Peto, R., J. Boreham, et al. (2000). "UK and USA breast cancer deaths down 25% in year 2000 at ages 20-69 years." The Lancet **355**(9217): 1822.

Piechaczek, C., C. Fetzer, et al. (1999). "A vector based on the SV40 origin of replication and chromosomal S/MARs replicates episomally in CHO cells." Nucl. Acids Res. **27**(2): 426-428.

Proudfoot, N. J., A. Furger, et al. (2002). "Integrating mRNA Processing with Transcription." Cell **108**(4): 501-512.

Racaniello, V. R. (2001). Picornaviridae: The Viruses and Their Replication. Fields Virology. Howley, Lippincott Williams & Wilkins.

Rahman, N. and M. R. Stratton (1998). "The genetics of breast cancer susceptibilty." Annual Review of Genetics **32**(1): 95-121.

Rahn, J. J., Q. Shen, et al. (2004). "MUC1 Initiates a Calcium Signal after Ligation by Intercellular Adhesion Molecule-1." J. Biol. Chem. **279**(28): 29386-29390.

Reddy, P., A. Sparvoli, et al. (1996). "Formation of reversible disulfide bonds with the protein matrix of the endoplasmic reticulum correlates with the retention of unassembled Ig light chains." EMBO J. **15**(9): 2077-2085.

Reed, R. and E. Hurt (2002). "A Conserved mRNA Export Machinery Coupled to pre-mRNA Splicing." Cell **108**(4): 523-531.

Sautter, K. and B. Enenkel (2005). "Selection of high-producing CHO cells using NPT selection marker with reduced enzyme activity." Biotechnology and Bioengineering **89**(5): 530-538.

Schlatter, S., S. H. Stansfield, et al. (2005). "On the optimal ratio of heavy to light chain genes for efficient recombinant antibody production by CHO cells." Biotechnol. Prog. **21**(1): 122-133.

Schmiedl, A., F. Breitling, et al. (2000). "Effects of unpaired cysteines on yield, solubility and activity of different recombinant antibody constructs expressed in E. coli." Journal of Immunological Methods **242**(1-2): 101-114.

Schroeder, J. A., M. C. Thompson, et al. (2001). "Transgenic MUC1 Interacts with Epidermal Growth Factor Receptor and Correlates with Mitogen-activated Protein Kinase Activation in the Mouse Mammary Gland." J. Biol. Chem. **276**(16): 13057-13064.

Seibler, J., D. Schubeler, et al. (1998). "DNA Cassette Exchange in ES Cells Mediated by FLP Recombinase: An Efficient Strategy for Repeated Modification of Tagged Loci by Marker-Free Constructs." Biochemistry **37**(18): 6229-6234.

Shapiro, A. L., M. D. Scharff, et al. (1966). "Synthesis of excess light chains of gamma globulin by rabbit lymph node cells." Nature **211**: 243-245.

Singh, P. (1994). "Molecular mechanisms of cellular determination: their relation to chromatin structure and parental imprinting." J Cell Sci **107**(10): 2653-2668.

Skvortsov, V. T. and A. E. Gurvich (1968). "Relative rates of synthesis of immunoglobulins and light chains in rabbit spleen cells during secondary response." Nature **218**: 377-378.

Sonenshein, G., M. Siekevitz, et al. (1978). "Control of immunoglobulin secretion in the murine plasmacytoma line MOPC 315." J. Exp. Med. **148**(1): 301-312.

Spicer, A. P., G. J. Rowse, et al. (1995). "Delayed Mammary Tumor Progression in Muc-1 Null Mice." J. Biol. Chem. **270**(50): 30093-30101.

Taylor-Papadimitriou, J., J. M. Burchell, et al. (2002). "MUC1 and the Immunobiology of Cancer." Journal of Mammary Gland Biology and Neoplasia **7**(2): 209-221.

Toleiks, L. (2003). "Recombinante Antikörper gegen tumorassoziertes MUC1." Inaugural Dissertation.

Trombetta, E. S. and A. J. Parodi (2003). "Quality control and protein folding in the secretory pathway." Annu. Rev. Cell Dev. Biol. **19**(1): 649-676.

Vimal, D., M. Khullar, et al. (2000). "Intestinal mucins: the binding sites forsalmonella typhimurium." Molecular and Cellular Biochemistry **204**(1 - 2): 107-117.

von Mensdorff-Pouilly, S., A. A. Verstraeten, et al. (2000). "Survival in Early Breast Cancer Patients Is Favorably Influenced by a Natural Humoral Immune Response to Polymorphic Epithelial Mucin." J Clin Oncol **18**(3): 574-.

Wabl, M. and C. Steinberg (1982). "A Theory of Allelic and Isotypic Exclusion for Immunoglobulin Genes." PNAS **79**(22): 6976-6978.

Walsh, M. D., S. M. Luckie, et al. (2000). "Heterogeneity of MUC1 expression by human breast carcinoma cell lines in vivo and in vitro." Breast Cancer Research and Treatment **58**: 255-266.

Wang, C. e. a. (1995). "An RNA pseudoknot is an essential structural element of the internal ribosome entry site located within the hepatitis C virus 5´ non-coding region." RNA **1**: 526-537.

Wesseling, J., S. van der Valk, et al. (1996). "A mechanism for inhibition of E-cadherin-mediated cell-cell adhesion by the membrane-associated mucin episialin/MUC1." Mol. Biol. Cell **7**(4): 565-577.

West, A. G., M. Gaszner, et al. (2002). "Insulators: many functions, many mechanisms." Genes Dev. **16**(3): 271-288.

White, C. A., R. L. Weaver, et al. (2001). "Antibody targeted immunotherapy for treatment of

malignancy." Annu. Rev. Med. **52**: 125.

Wilson, C., H. J. Bellen, et al. (1990). "Position effects on eukaryotic gene expression." Annu Rev Cell Biol **6**: 679-714.

Witwer, C., S. Rauscher, et al. (2001). "Conserved RNA secondary structures in Picornaviridae genomes." Nucl. Acids Res. **29**(24): 5079-5089.

Wu, G. E., N. Hozumi, et al. (1983). "Secretion of a lambda2 immunoglobulin chain is prevented by a single amino acid substitution in its variable region." Cell **33**(1): 77-83.

Wurm, F. M. (2004). "Production of recombinant protein therapeutics in cultivated mammalian cells." **22**(11): 1393-1398.

Yamamoto, M., A. Bharti, et al. (1997). "Interaction of the DF3/MUC1 Breast Carcinoma-associated Antigen and beta -Catenin in Cell Adhesion." J. Biol. Chem. **272**(19): 12492-12494.

Zahn-Zabal, M., M. Kobr, et al. (2001). "Development of stable cell lines for production or regulated expression using matrix attachment regions." Journal of Biotechnology **87**: 29-42.

Zhu, J., M. L. Musco, et al. (1999). "Three-color flow cytometry analysis of tricistronic expression of eBFP, eGFP, and eYFP using EMCV-IRES linkages." Cytometry **37**(1): 51-59.

8 Acknowledgements

First of all, I would like to express my deeply appreciation to my tutor Mr. Professor Dr. Stefan Dübel for the opportunity he gave me to be a Ph.D. student at Institute of Biochemistry and Biotechnology, T.U. Braunschweig. I am delighted about this opportunity for studying, working and living in Braunschweig, Germany. It will benefit me in the whole life. Sincerely thanks are not only for the know-how I got but also for his support, trust, and understanding.

I am particularly indebted to Mr. Professor Dr. Jürgen Bode, the Leader of Epigenetic Regulation Mechanisms, Gesellschaft für Biotechnologische Forschung mbH (GBF), for his kindly help and generous support during in the past three years. His help let me further understanding of the mechanism underlying eukaryotic gene expression.

I can't thank the people at my lab enough, beginning with my supervisor Dr. Thomas Jostock, for the discussion of experiment and carefully correction of my writings, he kept organizing everything well on the way; Dr. Michael Hust, from the beginning of my stay in Braunschweig, he went together with me to the different administration office to fill many kinds of forms, he never lost his patience, furnished the lab, organized the experiments, his energy never flagged; my colleagues Christian Menzel, Thomas Schirrmann, Doris Meier, Martina Kirsch, Nina Strebe, Bernd Voedisch, Aymen El-Ghezal, Wolfgang Graßl, and Saskia Helmsing, Laila Al-Halabi, Holger Thie, Eva Jordan, Hasan Cicek, Torsten Meyer, Andrea Walzog, I enjoy working together with them and the exchange of views towards science and life with them. Thank all of them; I got more than what I could say!

I want to thank my colleagues Rolf Heckmann, Andrea Holtkamp, Olof Palme, Adelheid Langner, Bettina Sandner, George S. Comanescu, with them, our large research group become more active, warm and colorful.

I owe thanks to Dr. André Oumard, Mr. Junhua Qiao, Frau Astrid Hans and Dr. Peter Müller, from GBF, Germany. They gave me very kindly support on construction of stable cell line by using recombinase mediated cassette exchange and FACS analysis of transfected cells as well as the discussions about eukaryotic gene expression.

I am deeply indebted Mr. Professor Dr. Siegmund Lang, Frau Margret Hesse and Mr. PD Dr. Udo Rau, from daily life to the normal research work, to computer network, their kind helps smooth the

obstacles I might meet.

I owe a debt to Mr. Congcong Zhang, his excellent job during his master project gave much help to my research.

My work was helped greatly by Dr. Lars Toleiks, the human anti-MUC1 antibody he isolated during his Ph.D. studying broaden the area of my work.

I appreciate Professor Mifang Liang from Institute of Viral Disease Control and Prevention, China CDC, for her recommendation and her support and help before and present.

Finally, I want to thank all my family members, for the encouragement and patience; for the joy and meaning of life they bring me. No matter what happened to me, success or failure, happy or unhappy, they are always there, I can always find a room to recharge!

Thanks all the people I have mentioned or not mentioned, with them all, I could always go ahead step by step more confidently! Thanks!

9 Curriculum Vitae

Personal information
Given name: Jiandong,
Surname: Li
Place of birth: China
Nationality: Chinese

Education
1990-1995, Bachelor of Medicine, Tongji Medical College, Huazhong University of Science and Technology, China
1999-2002, Masters degree in Immunology, Institute of Virology, Chinese Academy of Preventive Medicine
2003---present, Ph.D. candidate, Institute of Biochemistry and Biotechnology, T.U. Braunschweig Germany,

Work experience
1996-1999, Research assistant, Chinese Academy of Preventive Medicine, Acute infectious diseases control and prevention.

Publications
Jiandong Li, Doris Meier, Stefan Dübel and Thomas Jostock. (2005) A comparative study of different vector designs for mammalian expression of recombinant IgG antibodies (poster). 4th International Congress on Recombinant Antibodies, Hilton Berlin, Germany.

Lars Toleikis, Jiandong Li, Doris Meier, Thomas Jostock and Stefan Dübel. (2005) A human antibody for targeting adenocarcinomas (poster). 4th International Congress on Recombinant Antibodies, Hilton Berlin, Germany.

Wang Tao, Zhang quanfu, Li Chuan, Liu Qinzhi, Li Jiandong, Liang Mifang, Li Dexin. Analysis of the Liner and Conformational Epitopes of Hantaan virus N Protein Chinese J. Virol. 2005 21 (3)161-167

Wang Tao, Li Jiandong, Li Chuan Liang Mifang, Construction and stable expression intracellular Antibody to Hantavirus Glycoproteins, Chinese J. Exp. Clin. Virol. 2003 17 (2):106-112

LI Jian-dong, Wang Tao, Ji Yan, LIANG Mi-fang. Construction and expression single chain antibody (scFv) to Hantaanvirus N protein. Chinese J. Virol.2002, 19(4) 154-160

Wu Guizhen, Zhang Jing, Li Jiandong, et al, Analysis of Chinese Cholera Epidemic Situation in 1999. Chin. J. Epidemiology, 2000 21(s1)(1-6)

CAO hui-lin, DAI su-ling, JIA zhi-yuan, LI Jian-dong, et al, Investigation on Etiology of Viral Hepatitis in Six Flood stricken provinces of China in 1998. Chin. J. Vaccines and

Immunization 1999, 5 (5): 254-257

Wu Guizhen, Li Jiandong, et al: Analysis of Chinese Cholera Epidemic Situation in 1998. Chin. J. Epidemiology, 1999, 20(s1): 1-7

Datum:.....

.....

(Unterschrift)